



**Pacific Northwest**  
NATIONAL LABORATORY

*Proudly Operated by Battelle Since 1965*

# The Infrared Spectroscopy of Equilibrium Mixtures of Vapor-Phase Water and Hydrogen Fluoride

**April 2017**

TA Blake  
CS Brauer

CJ Thompson

## DISCLAIMER

This report was prepared as an account of work sponsored by an agency of the United States Government. Neither the United States Government nor any agency thereof, nor Battelle Memorial Institute, nor any of their employees, makes **any warranty, express or implied, or assumes any legal liability or responsibility for the accuracy, completeness, or usefulness of any information, apparatus, product, or process disclosed, or represents that its use would not infringe privately owned rights.** Reference herein to any specific commercial product, process, or service by trade name, trademark, manufacturer, or otherwise does not necessarily constitute or imply its endorsement, recommendation, or favoring by the United States Government or any agency thereof, or Battelle Memorial Institute. The views and opinions of authors expressed herein do not necessarily state or reflect those of the United States Government or any agency thereof.

PACIFIC NORTHWEST NATIONAL LABORATORY  
*operated by*  
BATTELLE  
*for the*  
UNITED STATES DEPARTMENT OF ENERGY  
*under Contract DE-AC05-76RL01830*

Printed in the United States of America

Available to DOE and DOE contractors from  
the Office of Scientific and Technical Information,  
P.O. Box 62, Oak Ridge, TN 37831-0062

[www.osti.gov](http://www.osti.gov)

ph: (865) 576-8401

fox: (865) 576-5728

email: [reports@osti.gov](mailto:reports@osti.gov)

Available to the public from the National Technical Information Service  
5301 Shawnee Rd., Alexandria, VA 22312

ph: (800) 553-NTIS (6847)

or (703) 605-6000

email: [info@ntis.gov](mailto:info@ntis.gov)

Online ordering: <http://www.ntis.gov>

# **The Infrared Spectroscopy of Equilibrium Mixtures of Vapor- Phase Water and Hydrogen Fluoride**

TA Blake  
CS Brauer

CJ Thompson

April 2017

Prepared for  
the U.S. Department of Energy  
under Contract DE-AC05-76RL01830

Pacific Northwest National Laboratory  
Richland, Washington 99352

## Abstract

Hydrogen fluoride readily associates with water vapor in the air to form the H<sub>2</sub>O-HF complex, which has optical absorption properties that are different from those of unassociated hydrogen fluoride. Consequently, to accurately quantify the total amount of hydrogen fluoride coming from an industrial stack or vent, for example, requires that the complexed amount of hydrogen fluoride be accounted for. To do this, the equilibrium constant for the association reaction is needed. Using statistical mechanical methods, Adebayo and coworkers [Adebayo SLA, AC Legon and DJ Millen. 1991. *J. Chem. Soc. Faraday Trans.* 87:443-447.] made an estimate of this equilibrium constant based on measured and estimated spectroscopic values for the complex. This value is  $K_{eq} = 84(18)$  but has never been confirmed experimentally. In the research described herein, we have measured the equilibrium constant for the formation of H<sub>2</sub>O-HF by monitoring the decrease in the infrared absorption features of water vapor and hydrogen fluoride in mixtures of these two vapors in a temperature-regulated cell. Our experimental values for  $K_{eq}$  at 25 °C, based on the diminution of the water vapor and HF transitions, are 77(46) and 51(24), respectively. The decay of the spectral features continues long after (hours) the two vapors are mixed in the gas cell. This suggests that other reactions (the growth of a film of hydrofluoric acid, perhaps) are taking place. While the experimental results agree reasonably well with the calculated equilibrium value of Adebayo et al., further improvements in experimental and analysis techniques are needed to reduce the uncertainties in the experimental results.

## Summary

Hydrogen fluoride readily associates with water vapor in air to form the H<sub>2</sub>O-HF complex, which has optical absorption properties that are different from those of unassociated hydrogen fluoride. Consequently, to accurately quantify the total amount of hydrogen fluoride coming from an industrial stack or vent, for example, requires that the complexed amount of hydrogen fluoride be accounted for. Alvarez and Spry considered this phenomenon when designing a hydrogen fluoride monitoring system for petroleum refineries [Alvarez MS and DB Spry. 2013. US Patent No. 8,614,096 B2]. To accurately quantify HF in the presence of water vapor, the equilibrium constant for the association reaction is needed. Using statistical mechanical methods, Adebayo and coworkers [Adebayo SLA, AC Legon and DJ Millen. 1991. *J. Chem. Soc. Faraday Trans.* 87:443-447] made an estimate of this equilibrium constant based on measured and estimated spectroscopic values for the complex. This value is  $K_{eq} = 84(18)$ , but it has never been confirmed experimentally.

In this work, we measured the equilibrium constant for the formation of H<sub>2</sub>O-HF by monitoring the decrease in the infrared absorption features of water vapor and hydrogen fluoride in mixtures of these two vapors in a temperature-regulated cell. A vacuum bench Fourier transform spectrometer operated with an instrument resolution of 0.112 cm<sup>-1</sup> was used to record the spectra. For most of the data sets, spectra were recorded approximately every eleven minutes for 10-14 hours. Hydrogen fluoride sample pressures ranged from 0.5 to 4 Torr, and the water vapor sample pressures ranged from 1 to 4 Torr. The cell was pressurized to approximately one atmosphere by adding dry nitrogen. Fourteen data sets were recorded at 25 °C, one was measured at 10 °C, and one was obtained at 40 °C.

Decreases in several water and hydrogen fluoride rotational-vibrational lines were utilized to estimate the H<sub>2</sub>O-HF equilibrium constant. Four water transitions were used: two in the  $\nu_3$  band, 3837.8 cm<sup>-1</sup> (001 – 000; 4<sub>04</sub> – 3<sub>03</sub>) and 38161.1 cm<sup>-1</sup> (001 – 000; 3<sub>13</sub> – 2<sub>12</sub>), and two in the  $\nu_2$  band, 1695.9 cm<sup>-1</sup> (010 – 000; 5<sub>05</sub> – 4<sub>14</sub>) and 1717.4 cm<sup>-1</sup> (010 – 000; 6<sub>16</sub> – 5<sub>05</sub>). The intensities of these transitions rapidly decreased in the first thirty minutes after the vapors were mixed, and then the signals slowly decayed for the remainder of each experiment (ten to fourteen hours). A double exponential decay equation fit the data very well. Regardless of the initial water vapor pressure, the decay curves of the four water transitions ran parallel to one another in most cases until the measurements were stopped. Three hydrogen fluoride fundamental ( $\nu = 1 - 0$ ) R-branch transitions, R(5) at 4174.0 cm<sup>-1</sup>, R(6) at 4203.3 cm<sup>-1</sup>, and R(7) at 4230.7 cm<sup>-1</sup> were also monitored. With the exception of the early decay of the R(5) transition, the decay curves of these three transitions fit well to straight lines. Interestingly, the three decay curves for HF are not parallel to one another. The R(5) decay rate is approximately three times that of the R(6), which is three times that of the R(7). The source of these differences in HF decay is unknown.

Though small, the decays of the spectral features continued long after (hours) the two vapors were mixed in the gas cell. At the cell pressures used here, individual sites on the cell walls would be occupied by molecules and reach equilibrium in a fraction of a second (Langmuir adsorption). To explain the much longer decay, there may be a slow buildup of a hydrofluoric acid film on the gas cell wall that the water and HF vapors slowly dissolve into. Since the calculation of the equilibrium constant requires determining the decrease in water and HF partial pressures from their initial values, and because this decrease is constantly changing, it was decided to calculate the equilibrium constant at each data point on each decay curve from hour one to hour ten for all the data sets. The equilibrium constants for the water decay curves were averaged separately from those of the hydrogen fluoride decay curves. Our experimental values for  $K_{eq}$  at 25 °C based on the diminution of the water vapor and HF transitions are 77(46) and 51(24), respectively. While the experimental results at 25 °C agree reasonably well with the

calculated equilibrium value of Adebayo et al., further improvements in experimental and analysis techniques are needed to reduce the uncertainties in the experimental results. We also recorded one set of spectra at 10 °C and then another series at 40 °C. From the 10 °C series we found  $K_{eq} = 44(27)$  from the HF transitions and  $K_{eq} = 63(22)$  from the water transitions. For the 40 °C series, we found  $K_{eq} = 27(15)$  from the HF transitions and  $K_{eq} = 21(6)$  from the water transitions. The general trend is consistent with expectations: the 10 °C measurement should give a larger  $K_{eq}$  value than that of 40 °C, but the measured 10 °C  $K_{eq}$  value is nowhere close to the predicted value of 191 based on calculated thermodynamic values. The 40 °C  $K_{eq}$  measured values are closer to the predicted values with a smaller standard deviation.

## **Acknowledgments**

The authors would like to thank the U.S. Department of Energy, National Nuclear Security Administration, Office of Defense Nuclear Nonproliferation (DNN, NA-22), and Drs. Victoria Franques and Steven Sharpe for their support and interest in this research. The authors also would like to thank Dr. Bruce Kay of the Pacific Northwest National Laboratory for fruitful discussions regarding the results.

## Acronyms and Abbreviations

ACGIH	American Conference of Governmental Industrial Hygienists
ASCII	American Standard Code for Information Interchange
B	b-axis molecular rotational constant
°C	temperature, Celsius unit
C#	C-sharp programming language
$\chi^2$	chi-squared, goodness of fit parameter
$\text{cm}^{-1}$	wavenumber (1/wavelength (cm))
cm	centimeter
D	diffusion coefficient
$D_0$	bond dissociation energy
FTIR	Fourier transform infrared
FWHM	full width at half maximum, a linewidth parameter
G	Gibbs free energy
H	enthalpy
HF	hydrogen fluoride
$(\text{HF})_n$	hydrogen fluoride cluster, $n = 1, 2, 3, \dots$
$\text{H}_2\text{O}$	water
$\text{H}_2\text{O-HF}$	water-hydrogen fluoride cluster
$(\text{H}_2\text{O})_n$	water cluster, $n = 1, 2, 3, \dots$
IR	infrared
$K_{\text{eq}}(T)$	equilibrium constant at temperature, T.
K	temperature, Kelvin unit
$\log_{10}$	base-10 logarithm
$\text{M}\Omega$	megaOhm, unit of electrical resistance
m	meter
$\text{N}_2$	nitrogen
$\nu_i$	$i^{\text{th}}$ harmonic vibrational mode
NWIR	Northwest Infrared
P	partial pressure in atmospheres
P(J)	P-branch transition for ground state rotational constant J, $J - 1 \leftarrow J$
ppm	parts per million
PTFE	polytetrafluoroethylene
Q(J)	Q-branch transition for ground state rotational constant J, $J \leftarrow J$
R	gas constant
R(J)	R-branch transition for ground state rotational constant J, $J + 1 \leftarrow J$
S	entropy
$\sigma$	standard deviation
T	temperature
$\tau_i$	$i^{\text{th}}$ 1/e decay constant
TLV-C	threshold limit value-ceiling
TLV-TWA	threshold limit value-time weighted average
Torr	unit of pressure, 1 Torr = 1/760 atmosphere
v	vibrational quantum number

# Contents

Abstract .....	iii
Summary .....	v
Acknowledgments.....	vii
Acronyms and Abbreviations .....	ix
1.0 Introduction .....	1.1
2.0 Experimental.....	2.1
3.0 Results .....	3.1
3.1 Hydrogen Fluoride and Water Vapor Calibration Measurements.....	3.1
3.2 Hydrogen Fluoride and Water Mixture Measurements.....	3.5
4.0 Discussion.....	4.1
5.0 References .....	5.1
Appendix A Pacific Northwest National Laboratory Hydrogen Fluoride First Aid, Handling, and Monitoring .....	A.1
Appendix B MATLAB Codes for Data Handling and Processing .....	B.1
Appendix C HF and Water Vapor Decay Curve Plots .....	C.1
Appendix D Fit Parameters for HF and Water Vapor Decay Curves.....	D.1

## Figures

<b>Figure 1.1</b>	Calculated percentage of uncomplexed hydrogen fluoride in water vapor at 25 °C....	1.3
<b>Figure 1.2</b>	Calculated vapor pressures of hydrogen fluoride in water vapor at 25 °C.....	1.3
<b>Figure 1.3</b>	Calculated vapor pressures of hydrogen fluoride and H <sub>2</sub> O-HF at 25 °C.....	1.4
<b>Figure 1.4</b>	Infrared spectrum of the $\nu_1$ (HF) stretch band of H <sub>2</sub> O-HF .....	1.5
<b>Figure 2.1</b>	Experimental layout for water vapor and hydrogen fluoride infrared absorption measurements .....	2.2
<b>Figure 3.1</b>	Infrared spectrum of the fundamental band of hydrogen fluoride.....	3.1
<b>Figure 3.2</b>	Hydrogen fluoride calibration data.....	3.3
<b>Figure 3.3</b>	Water vapor calibration data.....	3.4
<b>Figure 3.4</b>	Phase diagram for water and hydrogen fluoride vapors at 25 °C.....	3.6
<b>Figure 3.5</b>	Infrared spectrum (3500 – 4500 cm <sup>-1</sup> ) of a water vapor and hydrogen fluoride mixture.....	3.8
<b>Figure 3.6</b>	Infrared spectrum (1200 – 2100 cm <sup>-1</sup> ) of a water vapor and hydrogen fluoride mixture.....	3.9
<b>Figure 3.7</b>	Decay curves for water and hydrogen fluoride absorption features for data taken August 31, 2016 .....	3.10
<b>Figure 3.8</b>	Decay curves for hydrogen fluoride absorption features for data taken August 19, 2016 .....	3.11
<b>Figure 3.9</b>	Decay curves for water vapor absorption features for data taken August 19, 2016 .....	3.12
<b>Figure 3.10</b>	Decay curves for hydrogen fluoride absorption features for data taken September 1, 2016 .....	3.14
<b>Figure 3.11</b>	Decay curves for water vapor absorption features for data taken September 1, 2016 .....	3.14
<b>Figure 3.12</b>	Infrared spectrum of the $\nu_1$ (HF) stretching band of H <sub>2</sub> O-HF from data taken July 27, 2016.....	3.15

## Tables

<b>Table 1.1</b>	Initial and equilibrium state stoichiometry for the water-HF reaction given in Eq. 1 ...	1.2
<b>Table 3.1</b>	Ro-vibrational transition line centers of the hydrogen fluoride fundamental mode .....	3.1
<b>Table 3.2</b>	Hydrogen fluoride sample pressures for gas-phase calibration measurements .....	3.2
<b>Table 3.3</b>	Hydrogen fluoride sample pressures for repeat gas-phase calibration measurements...	3.3
<b>Table 3.4</b>	Water sample pressures for gas-phase calibration measurements .....	3.4
<b>Table 3.5</b>	Sample pressures and temperatures used for determining water-HF equilibrium constant.....	3.7
<b>Table 3.6</b>	Slope and intercept values for linear fit of HF decay curves .....	3.12
<b>Table 3.7</b>	Decay constants $\tau_1$ and $\tau_2$ for double exponential decay fits of H <sub>2</sub> O decay curves .....	3.13

# 1.0 Introduction

Hydrogen fluoride (HF) is an important effluent associated with many industrial chemical processes.<sup>1-28</sup> As such, numerous methods have been devised for detecting and monitoring this gas either remotely or using a point sensor.<sup>29-36</sup> Many of these sensor methods rely on optical absorption spectroscopy, cueing off of a fundamental or first overtone ro-vibrational transition to quantify the concentration of HF. Since hydrogen fluoride is highly electronegative, it readily forms a hydrogen-bonded dimer with water, H<sub>2</sub>O–HF, which unlike most other van der Waals or hydrogen bonded molecular clusters, can exist at atmospheric temperatures and pressures.<sup>37-52</sup> In fact, under most atmospheric temperature and relative humidity conditions, a substantial fraction of the HF molecules can be “tied up” in H<sub>2</sub>O–HF. Thus, without accounting for H<sub>2</sub>O–HF, optical absorption spectroscopy methods could significantly underestimate total HF concentrations.<sup>24</sup>

We report here our results for measuring the temperature dependent equilibrium constant,  $K_{eq}(T)$ , for the reaction



$$K_{eq}(T) = \frac{P(\text{H}_2\text{O}-\text{HF})}{P(\text{H}_2\text{O})P(\text{HF})} \quad (2)$$

where  $P(\text{HF})$ , for example, is the equilibrium partial pressure of HF in atmospheres referenced to a standard state of 1 atmosphere pressure at temperature,  $T$ .  $K_{eq}$  is, therefore, unitless.<sup>53, 54</sup>

To determine the accurate total hydrogen fluoride burden in the atmosphere from optical spectroscopic measurements of HF ro-vibrational transitions, the partial pressure of H<sub>2</sub>O–HF in the atmosphere must be considered. If we express the total amount of HF in an atmospheric sensing scenario as

$$P(\text{HF})_{\text{total}} = P(\text{HF}) + P(\text{H}_2\text{O}-\text{HF}), \quad (3)$$

where  $P(\text{HF})$  is the partial pressure of HF monomer as measured with our sensor, and from the expression of the temperature-dependent equilibrium constant for the reaction  $\text{HF} + \text{H}_2\text{O} \leftrightarrow \text{H}_2\text{O}-\text{HF}$ , Eq. (2), we can write

$$P(\text{H}_2\text{O}-\text{HF}) = K_{eq}(T) P(\text{H}_2\text{O})P(\text{HF}) \quad (4)$$

and, substituting into the above expression gives<sup>24, 53, 54</sup>

$$P(\text{HF})_{\text{total}} = [P(\text{HF}) + K(T) P(\text{H}_2\text{O})P(\text{HF})](1 \text{ atm}) = [(1 + K(T) P(\text{H}_2\text{O})) P(\text{HF})](1 \text{ atm}). \quad (5)$$

If  $K_{eq}(T)$  is known, if  $P(\text{HF})$  can be measured in the field, if the relative humidity can be measured, which gives  $P(\text{H}_2\text{O})$ , and if the temperature is known, then the total burden of HF,  $P(\text{HF})_{\text{total}}$ , in the sensing scenario can be calculated. Depending on temperature and humidity conditions, more than half of the HF in air can be bound up as [H<sub>2</sub>O–HF]. This estimate assumes that chemical equilibrium has been established, and would not apply, for example, in the immediate aftermath of a sudden release of a large quantity of hydrogen fluoride.<sup>55-60</sup>

Hydrogen fluoride is used in the petrochemical industry as an alkylation catalyst in the production of high-octane gasoline and also for the dehydrogenation of alkanes to produce olefins.<sup>22, 24, 61, 62</sup> Because monitoring hydrogen fluoride levels in and around refineries is an important safety concern, oil

companies have invested in air monitoring equipment, typically using infrared tunable diode lasers (TDL) for detecting and quantifying HF levels in the air.<sup>24, 33</sup> Since these laser systems base their quantification on individual HF monomer transitions, the sequestration of HF in H<sub>2</sub>O–HF is a concern to engineers responsible for calibrating, operating, and interpreting the data from these sensors, particularly in climates where high humidity is common.

In 2013, Alvarez and Spry of ExxonMobil Research and Engineering Company were granted a United States patent (Patent No. US 8,614,096 B2)<sup>24</sup> in which methods are described for calibration of TDL sensors, and correcting for the presence of H<sub>2</sub>O–HF in the atmosphere to give a total HF burden in the tested air sample.

The equilibrium constant,  $K_{eq}(T)$ , for the reaction  $HF + H_2O \leftrightarrow H_2O-HF$  can be calculated from the standard expression

$$K_{eq}(T) = \exp\left(\frac{-\Delta G}{RT}\right) \quad (6)$$

where  $\Delta G$  is the Gibbs free energy,  $R$  is the gas constant, and  $T$  is the temperature in Kelvin. The free energy is given by  $\Delta G = \Delta H - T\Delta S$  (standard molar quantities), and for the cluster formation reaction, the values of  $\Delta H$  and  $\Delta S$  have not been determined directly by experiment; however, Adebayo and coworkers have estimated these values using statistical mechanical calculations and incomplete spectroscopic data.<sup>46</sup> The vibrational spectrum of H<sub>2</sub>O–HF has not been completely measured and few of the anharmonicity constants are known; consequently, Adebayo et al.<sup>46</sup> used a rigid-rotor-harmonic oscillator approximation for calculating the energies and partition functions. Also, Legon and coworkers made microwave absolute intensity measurements to estimate  $D_0 = 34.3$  kJ/mole,<sup>45</sup> which is used to calculate the standard enthalpy,  $\Delta H$ . They calculated  $\Delta H = -39.1(3)$  kJ/mole and  $\Delta S = -0.09442$  (no error given) kJ/(mole K) at 298.15 K. Combining these values in Eq. 6 gives  $K(298.15 \text{ K}) = 83(11)$ . The uncertainty is dominated by the uncertainty in the enthalpy (see Tables 3 and 6 in Adebayo et al.<sup>46</sup>). Using the same numbers Adebayo et al. report this value as 84(18).

Given  $K_{eq}$  and initial partial pressures of HF and water vapor in units of atmospheres ( $a$  and  $b$  in **Table 1.1** below), we can calculate the equilibrium vapor pressures of these constituents and of the complex H<sub>2</sub>O–HF by choosing the physically realistic root of the resulting quadratic equation.<sup>53</sup>

**Table 1.1** Initial and equilibrium state stoichiometry for the water-HF reaction given in Eq. 1.

	HF	H <sub>2</sub> O	H <sub>2</sub> O–HF
<b>Initial</b>	$a$	$b$	$0$
<b>Change</b>	$-x$	$-x$	$+x$
<b>Equilibrium</b>	$a - x$	$b - x$	$+x$

$$K_{eq}(T) = \frac{x}{(a-x)(b-x)} \quad (7)$$

As an example, we have used Eq. 7 and  $K_{eq} = 83$  to calculate a series of equilibrium vapor pressures for HF, H<sub>2</sub>O and H<sub>2</sub>O–HF assuming an initial pressure of HF of 1.00 Torr (0.00132 atm), relative humidities

from 0 to 100% (0.12 to 23.71 Torr water vapor), and a temperature of 25.0 °C. The results are shown in **Figures 1.1 – 1.3**. As can be seen in **Figure 1.1**, at 90% relative humidity and 25 °C, only about 30% of the initial partial pressure of HF remains uncomplexed with water, and because of the small initial partial pressure of HF, the impact on the partial pressure of water vapor is marginal (see **Figures 1.1** and **1.2**).

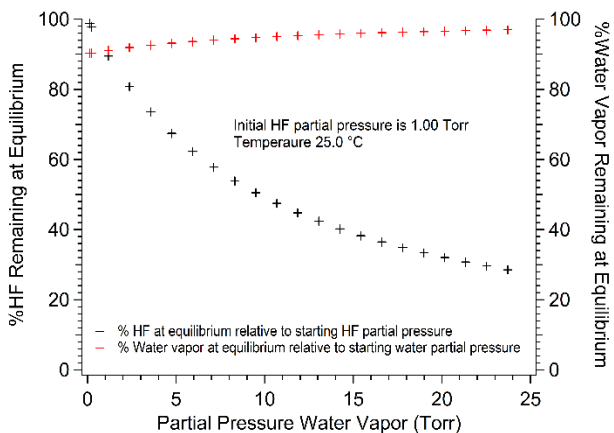


**Figure 1.1** The calculated percentage of uncomplexed HF in equilibrium with water vapor as a function of water vapor pressure. The initial vapor pressure of HF is 1.00 Torr, the temperature is 25.0 °C, and  $K_{eq}$  is 83. The percentage of remaining water vapor is also shown.

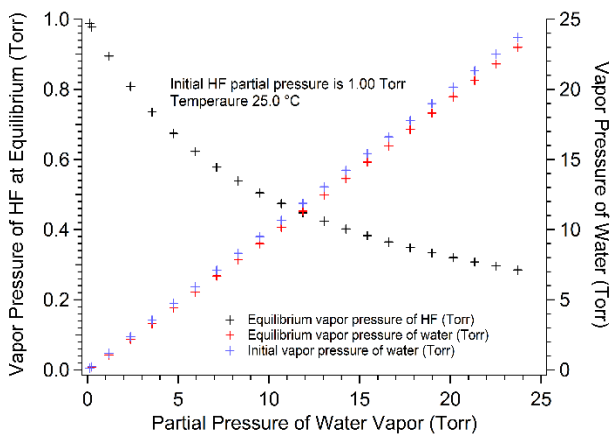


**Figure 1.2** The calculated vapor pressures of HF and water vapor at equilibrium, in Torr, as a function of the partial pressure of water. The initial pressure of water vapor is also shown. The same conditions as those shown in **Figure 1.1** apply.

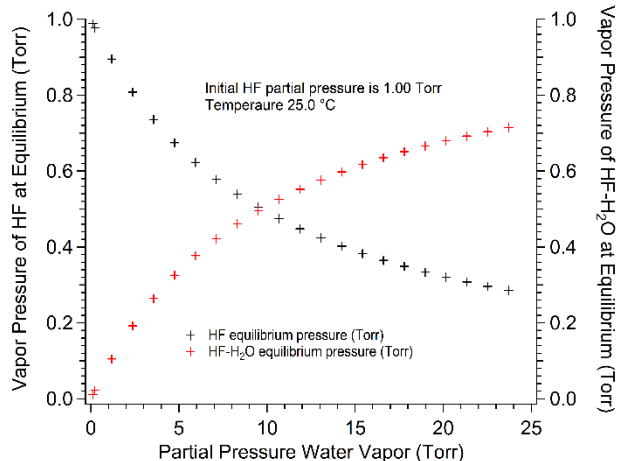


**Figure 1.3** The calculated vapor pressures of HF and H<sub>2</sub>O-HF at equilibrium, in Torr, as a function of the partial pressure of water. The same conditions as those shown in **Figure 1.1** apply.

The calculated partial pressure of H<sub>2</sub>O-HF, in Torr, as a function of the partial pressure of water vapor is shown in **Figure 1.3** for the conditions discussed above.

As the example shows, the amount of HF complexed with water can be considerable, and the calculation of the H<sub>2</sub>O-HF concentration is important for accurate  $P(\text{HF})_{\text{total}}$  retrievals.<sup>24</sup> Given the importance of  $K_{\text{eq}}(T)$  in the above calculation, and its current unvetted estimation, we have attempted to make accurate, quantitative measurements of  $K_{\text{eq}}(T)$  over a small range of temperatures and HF and water vapor partial pressures.

Assuming the standard molar thermodynamic quantities for H<sub>2</sub>O-HF,  $\Delta H$  and  $\Delta S$  have a weak temperature dependence from 10 °C to 40 °C, we calculate  $K_{\text{eq}}$  to be 191 at 283.15 K and 39 at 313.15 K. These values are reasonable in light of LeChatelier's principle: the H<sub>2</sub>O-HF formation reaction is exothermic ( $\Delta H = -39.1$  kJ/mole) and increasing the temperature would favor reactants and decreasing the temperature would favor the products.<sup>46, 53, 54</sup>

Another objective of this research was to measure the spectroscopic signature of the H<sub>2</sub>O-HF vibrational HF stretching mode,  $\nu_1$ ,  $\nu = 1 \leftarrow 0$  at 3608  $\text{cm}^{-1}$ . The red shift between the HF monomer fundamental mode and the HF stretch in the cluster is about 350  $\text{cm}^{-1}$ . The data for this objective were a direct consequence of the measurements to attain  $K_{\text{eq}}(T)$ . The results of this objective would not be useful for remote sensing retrievals since the 2.8  $\mu\text{m}$  region is opaque over sizeable distances in the atmosphere, but it would be useful for researchers using point sensors to measure HF in air.

Early research by Thomas,<sup>37</sup> and more recent measurements by Bulychev et al.,<sup>50, 51</sup> have measured the  $\nu_1$  HF stretching band of the H<sub>2</sub>O-HF cluster and attempted to model its shape through empirical or non-empirical calculation methods. Thomas used a dispersion instrument to record his spectra, and though he did not state his instrument resolution, it was certainly greater than 1  $\text{cm}^{-1}$ . Bulychev et al. used FTIR instruments in their work with resolutions of 0.2, 0.05, and 0.02  $\text{cm}^{-1}$ . At room temperature and Torr-levels of water vapor and HF, the rotational structure of the  $\nu_1(\text{HF})$  band, despite the cluster's 0.24  $\text{cm}^{-1}$   $B$  rotational constant value, remained unresolvable: the density of hot bands is too high to see individual ro-vibrational lines, though their spectra show several Q-branches emerging from the unresolved mass. See **Figure 1.4**.

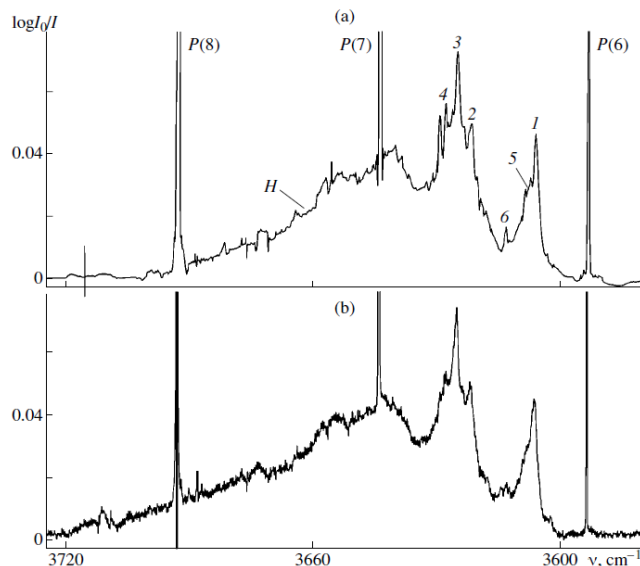


**Figure 1.4** This figure is from Bulychev et al.<sup>50</sup> Traces (a) and (b) are of the  $\nu_1(\text{HF})$  stretch band of the  $\text{H}_2\text{O}\text{--}\text{HF}$  complex at  $3608\text{ cm}^{-1}$  after the water lines have been subtracted from the spectrum. The upper (a) trace is the  $0.2\text{ cm}^{-1}$  resolution spectrum of a 20 cm long cell at 293 K with initial partial pressures of 18 Torr and 10 Torr for water and HF, respectively. The lower (b) trace is the  $0.02\text{ cm}^{-1}$  resolution spectrum of a 20 cm long cell at 293 K with initial partial pressures of 14 Torr and 8 Torr for water and HF, respectively.

Because the presence of HF alters the line shapes of water's infrared ro-vibrational transitions, Bulychev et al.<sup>50, 51</sup> had to use an iterative procedure to fit Gaussian and Lorentz line shapes to each of the five hundred  $\nu_1$ ,  $\nu_3$  and  $2\nu_2$  water transitions that are in the vicinity of the  $\nu_1(\text{HF})$  cluster mode. Once the water lines were properly fit and subtracted, they could observe a "clean" view of the  $\nu_1(\text{HF})$  cluster band region. Under their experimental conditions (20 cm pathlength, 293 K, water partial pressures up to the saturation value at 293 K,  $10 < P(\text{HF}) < 40$  Torr and total pressure no greater than 40 Torr) Bulychev et al.<sup>50, 51</sup> also observed an  $(\text{HF})_2$  band near the P(2) monomer transition at  $3878\text{ cm}^{-1}$ .

The  $\nu_1(\text{HF})$  band would not be observable in open-path scenarios – the  $2.8\text{ }\mu\text{m}$  region would be opaque – but we found it useful to monitor the intensity of this band in our proposed laboratory measurements, since it served as a useful check of the consistency of equilibrium monomer intensity measurements. A quantitative measure of the  $\nu_1(\text{HF})$  cluster band intensity as a function of temperature may be useful for those making point sensor measurements, assuming the sensor has sufficient bandwidth to cover the region.

## 2.0 Experimental

Our experimental approach for measuring  $K_{eq}(T)$  was to introduce measured partial pressures of HF and H<sub>2</sub>O vapors into a small gas cell that has calcium fluoride windows on either end and is jacketed in such a way that the cell's temperature can be regulated by water flowing through the jacket from a temperature-stabilized circulating bath. Dry nitrogen would be added to the gas cell to bring the total pressure to approximately one atmosphere. Once the gases were mixed, we would monitor the change in the absorbances of several HF fundamental and water vapor  $\nu_2$  ro-vibrational transitions over some period of time using a Fourier transform infrared (FTIR) spectrometer with an instrumental resolution of 0.112 cm<sup>-1</sup>. We assumed that after some brief period (minutes) of mixing and reacting, the intensities of the HF and water ro-vibrational transitions would decrease and then stabilize. From these measurements and initial partial pressures, we could determine the percent decrease and equilibrium pressures of the reactants. The equilibrium constant,  $K_{eq}(T)$ , could then be calculated using Eq. 7 above. Additionally, by changing the temperature of the circulating bath we could change the temperature of the gas cell, and determine  $K_{eq}$  at several temperatures.

A Bruker model 66V vacuum bench FTIR was used for these measurements. Details concerning the use of this spectrometer for these types of measurements are given by Sharpe et al.<sup>63</sup> The gas cell is hard plumbed into the sample compartment with ¼" stainless steel tubing that exits the sample compartment through a welded bulkhead connection to tubing outside the spectrometer. A pneumatic valve inside the sample compartment can be opened to let gas into the cell or used to evacuate the cell, and the valve can be closed to seal off the cell from the external gas line. In this way, the cell does not need to be removed from the spectrometer to be filled or evacuated. The gas cell is gold-coated inside and out, is 20 cm long, has an interior diameter of 4.72 cm, and has a volume of 350 mL. Calcium fluoride windows (ISP Optics CF-WW-50-6, 50.8 mm diameter, 6 mm thick, with 30' wedge) are sealed to the ends of the cell with Viton O-rings.

A schematic of the gas handling system is shown in **Figure 2.1**. Two separate gas manifolds were used: one for metering anhydrous HF into the gas cell and the other for preparing H<sub>2</sub>O vapor/nitrogen mixtures and introducing these into the gas cell. Both manifolds are made of gold-coated stainless steel, each has a 2" diffusion pump backed by a mechanical vacuum pump that allows the manifold to be pumped from atmosphere to below  $1 \times 10^{-5}$  Torr, and each has a set of 1, 10, and 1000 Torr capacitance manometers (MKS Baratrons models 690A 01TRA (1 Torr), 690A 11TRA, (10 Torr) and 690A 13TRA, (1000 Torr) with model 270 power supply and 274 reader). The measurement resolution of the manometers is  $1 \times 10^{-6}$  of the full scale and the accuracy is 0.08% of the reading. ¼" tubing lines from the two gas manifolds and the gas cell meet at a four-way cross. The fourth tubing line leads to a third diffusion pump/mechanical pump pair. See **Figure 2.1**.

A stainless-steel finger with a volume of about 50 mL was connected to the water/nitrogen gas manifold. The finger was filled with about 20 mL of 18 MΩ Millipore water. Each day a measurement was run the water in the finger was put through two liquid nitrogen temperature freeze/pump/thaw cycles. The nitrogen used was ultrapure grade that was passed through a copper coil in a dewar of liquid nitrogen to remove any additional water vapor, carbon dioxide, or carbon monoxide before entering the gas manifold through a 1" diameter pneumatic gate valve. A needle valve placed in the gas line before the copper coil was used to meter the nitrogen into the manifold. The water vapor/nitrogen manifold is heated to ~ 60 °C with heat tape to prevent water vapor and organics from sticking to its inner surface.

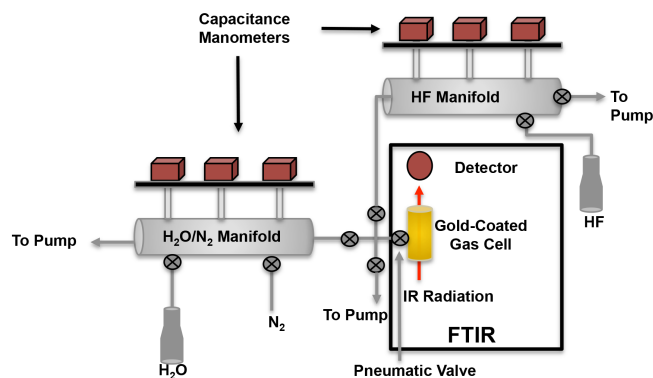


**Figure 2.1** Schematic of the connections between the gas manifolds and the gas cell in the FTIR is shown. The pneumatic valve on the gas cell is not shown.

The anhydrous hydrogen fluoride was purchased from Matheson (G1534160, UHP/99.99%, 1.59 kg/size 4 cylinder). This supply cylinder was housed in a sprinklered, ventilated gas cabinet in a service corridor behind the laboratory. The cylinder was connected to a cross purge regulator system (Matheson part/model #SEQNEWSP1/PAN-9300-66-0) in the gas cabinet that allowed the gas line and regulator be purged with dry nitrogen. From the cross purge in the gas cabinet a 1/4" stainless steel tube led into the laboratory to another ventilated cabinet. All joints in this gas line were welded. In the latter cabinet, the welded HF gas line terminated at a bellows valve that acted as an emergency shut off valve. 1/4" stainless tubing line led from this valve to the HF gas manifold (see **Figure 2.1**). A 50 mL stainless steel gas cylinder with welded bellows valve (Swagelok part # SS-4BRW-WY4) and needle valve (Swagelok part # SS-4BMRW-VCR) was attached to the gas manifold via a 1/4" VCR fitting. The HF manifold is filled with about 500 Torr of the anhydrous HF, the manifold was sealed off, and then the HF was condensed into the 50 mL gas cylinder. This was done twice during the course of the experiments described here. From the 50 mL cylinder HF could be metered out to the gas cell in the spectrometer. Before each experiment, the HF in the 50 mL cylinder was put through two liquid nitrogen temperature freeze/pump/thaw cycles. The HF gas manifold and 1/4" stainless steel line leading to the infrared cell were heated to 55 °C using heat tape.

Anhydrous hydrogen fluoride presents a considerable hazard in the laboratory, and safety considerations will be presented here.<sup>64-66</sup> See Appendix A for further details. For most experiments, less than a Torr-liter was used, and when a measurement was finished, the gas was exhausted through a small diffusion pump and mechanical pump. Alumina bead traps were installed in the fore lines of the mechanical pumps. The exhaust from the pumps goes out through the lab's exhaust ventilation system.

There is no inexpensive, reliable, continuous air monitoring system for hydrogen fluoride. The odor threshold for hydrogen fluoride is 0.03 ppm. The odor is strong, pungent and irritating. Symptoms of HF exposure include irritation of the eyes, skin, nose, and throat, eye and skin burns, rhinitis, bronchitis, pulmonary edema (fluid buildup in the lungs), and bone damage. The American Conference of Governmental Industrial Hygienists (ACGIH) Threshold Limit Value-Time Weighted Average (TLV-TWA) for HF is 0.5 ppm. The ACGIH Threshold Limit Values-Ceiling. (TLV-C) is 2.0 ppm. Personnel shall not be exposed to concentrations above this ceiling under any circumstance.<sup>64, 65</sup>

Real-time exposure monitoring for HF gas was required during the initial startup of the HF gas and FTIR system, and this was done using a Drager Accuro hand-operated bellows pump with HF-sensitive colorimetric detection tubes (Drager #8103251, 0.5 to 90 ppm HF sensitivity range, twenty draws on the

hand pump). Several sampling measurements were made prior to startup to establish backgrounds, and sampling was performed several times over the course of the several months that the experiments were being performed. Sampling was to be performed when modification or repair of the experimental system with the potential for release of more than trace quantities of HF gas was a possibility.

During normal operations and in the absence of real-time HF monitoring, HF odor detection or the presence of a white fog (caused by HF aerosols in the air) would be the cues to alert personnel to a hydrogen fluoride leak (“see and flee”). The presence of HF odor or a white HF aerosol cloud was NOT expected and was NOT within the work scope. Upon sensing the odor or seeing the cloud, the lab space was to be immediately evacuated and the single point of contact called. If possible, and if it was safe to do so, the valve on the hydrogen fluoride cylinder in the cabinet in the Service Corridor was to be closed.

Tubes of calcium gluconate gel were kept near the hydrogen fluoride gas handling manifold in the laboratory and near the gas cabinet in the service corridor behind the laboratory. The gluconate is for skin contact only. Local first responders have calcium gluconate nebulizers for respiratory contact and calcium gluconate eye washes. A sheet with HF skin contact first aid measures was placed near the work area and in the vicinity of the calcium gluconate gel supplies.

## 3.0 Results

### 3.1 Hydrogen Fluoride and Water Vapor Calibration Measurements

To begin, we wanted to determine how well we could quantitatively measure the partial pressures of HF and water vapor, separately, in the gas cell using infrared spectroscopy. To do this we made a series of measurements where aliquots of HF or H<sub>2</sub>O vapor, of 1 Torr or less, were metered into the gas cell, noting the pressure reading on the 1 Torr capacitance manometer, and then back filling the cell with dry nitrogen so that the total pressure in the cell was about 760 Torr, as measured on the 1000 Torr capacitance manometer. After the spectrum of the gas mixture was recorded it was ratioed to an empty cell background spectrum, converted to log<sub>10</sub> absorbance, and then scaled to ppm•m units using the factor  $\{(analyte\ pressure)/total\ pressure\} \times (1 \times 10^{-6}) \times 0.1996\}^{-1}$ . Using this scaling factor allows us to compare the integrated intensities of each measured spectrum directly to the quantitative Northwest Infrared database spectrum.<sup>63</sup>

**Table 3.1** Ro-vibrational transition line centers of the hydrogen fluoride fundamental mode.<sup>67</sup>

Assignment	Line Center (cm <sup>-1</sup> )	Assignment	Line Center (cm <sup>-1</sup> )
R(0)	4000.99	P(1)	3290.31
R(1)	4038.96	P(2)	3877.71
R(2)	4075.29	P(3)	3833.66
R(3)	4109.94	P(4)	3788.23
R(4)	4142.85	P(5)	3741.46
R(5)	4173.98	P(6)	3693.41
R(6)	4203.30	P(7)	3644.14
R(7)	4230.76	P(8)	3593.71
R(8)	4256.32	P(9)	3542.16
R(9)	4279.96	P(10)	3489.56
R(10)	4301.64	P(11)	3435.96
R(11)	4321.32		

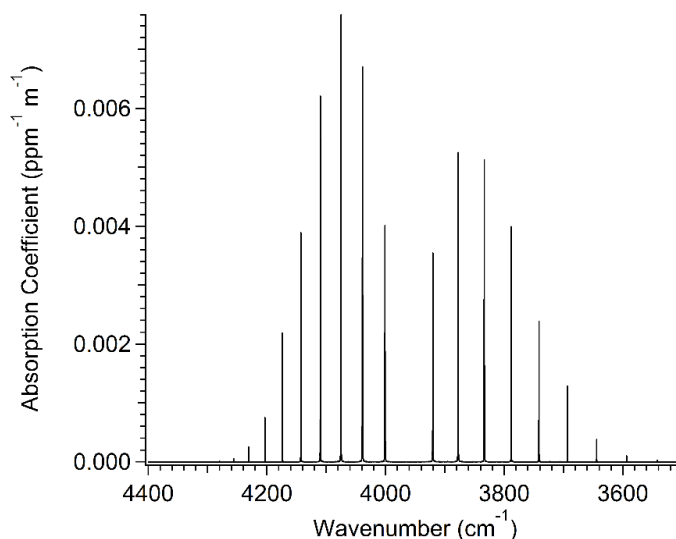


**Figure 3.1** Infrared spectrum of the fundamental band of hydrogen fluoride from the Northwest Infrared spectral database.<sup>63</sup> The ordinate axis is the log<sub>10</sub> absorption coefficient in units of ppm<sup>-1</sup> m<sup>-1</sup>.

The fundamental vibrational mode spectrum for hydrogen fluoride is shown in **Figure 3.1** and the assignment of the ro-vibrational diatomic transitions of that spectrum are given in **Table 3.1**.<sup>67</sup> The Doppler-broadened transitions for HF in this wavenumber region are approximately 0.011 cm<sup>-1</sup> full width at half maximum (FWHM). With an instrument resolution of 0.112 cm<sup>-1</sup> the Doppler-broadened transitions would be severely under-sampled. By adding approximately one atmosphere of nitrogen to the gas cell the transitions are broadened out to approximately 0.20 cm<sup>-1</sup> FWHM.<sup>63, 67</sup>

We made spectroscopic measurements of HF-in-nitrogen mixtures with HF pressures ranging from 0.06 to 1 Torr; these data are shown in **Table 3.2**.

**Table 3.2** Hydrogen fluoride calibration table giving the capacitance manometer reading of the HF sample pressure placed in the gas cell and the sample pressure as determined by integrating the R-branch side of the HF fundamental band (4285 – 3985 cm<sup>-1</sup>) and calculating the pressure from the NWIR database. After filling the cell with the HF sample, the cell was backfilled with enough nitrogen to bring the total pressure in the cell to approximately 760 Torr. All pressures in Torr. Repeat entries in the HF pressure (manometer) column represent two spectral measurements of the same gas fill of the cell.

Date	HF Pressure (Manometer)	HF Pressure (Spectrum)	% Difference <sup>1</sup>
2016-26-04	0.06150	0.07180	15.5
2016-25-04	0.14248	0.14580	1.30
2016-25-04	0.14248	0.13582	4.79
2016-26-04	0.20634	0.22609	9.13
2016-26-04	0.42493	0.43275	1.82
2016-26-04	0.42493	0.41052	3.45
2016-25-04	0.52292	0.53006	1.36
2016-25-04	0.52292	0.49343	5.80
2016-27-04	0.60130	0.60216	0.143
2016-29-04	0.60050	0.64139	6.59
2016-27-04	0.70570	0.68317	3.24
2016-29-04	0.70206	0.70839	0.898
2016-27-04	0.80220	0.79386	1.04
2016-27-04	0.80220	0.73242	9.09
2016-29-04	0.82027	0.82440	0.502
2016-27-04	0.90362	0.92728	2.58
2016-27-04	0.90362	0.93237	3.13
2016-27-04	1.03157	1.03601	0.429
2016-27-04	1.03157	1.02539	0.601

<sup>1</sup> Percent difference given by  $\{|V_1 - V_2|/(V_1 + V_2)/2\} \times 100\%$ .

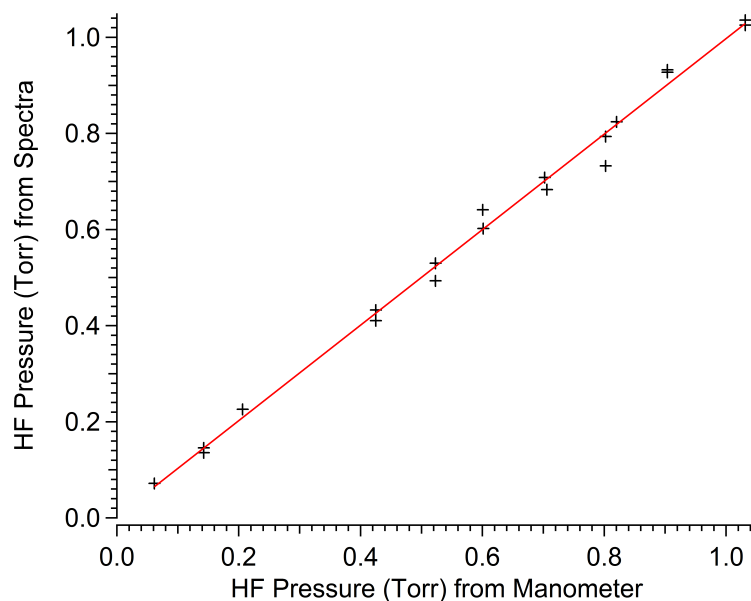


**Figure 3.2** The pressure data given in **Table 3.2** are shown (markers) and fit to a straight line (red trace).

**Figure 3.2** shows a plot of the HF sample pressure as measured using the capacitance manometer on the abscissa against the sample pressure as determined from the integrated spectra. The slope of the line is 0.9937(0.0192) and the intercept is 0.0038(0.0128),  $1\sigma$  deviations are shown in parentheses. The average percent difference between the capacitance manometer pressure reading and the sample pressure determined from the recorded spectrum is 3.76% with a  $1\sigma$  standard deviation of 3.99%. The capacitance manometer set used for measuring the HF samples pressures was calibrated by MKS during January 2016.

We also made seven repetitive measurements with hydrogen fluoride sample pressures of approximately 0.60 Torr pressurized to one atmosphere with nitrogen. The results are shown in **Table 3.3**.

**Table 3.3** Hydrogen fluoride calibration table for repeat measurements with nominal 0.60 Torr HF sample pressure. The table gives the capacitance manometer reading of the HF sample pressure placed in the gas cell and the sample pressure as determined by integrating the R-branch side of the HF fundamental band and calculating the pressure from the NWIR database. After filling the cell with the HF sample, the cell was backfilled with enough nitrogen to bring the total pressure in the cell to approximately 760 Torr. All pressures in Torr.

HF pressure (manometer)	HF pressure (spectrum)	% Difference <sup>1</sup>
0.60200	0.5572	7.73
0.60235	0.5559	8.02
0.60253	0.5595	7.41
0.60338	0.5573	7.94
0.60350	0.5587	7.71
0.60673	0.5687	6.47
0.60708	0.5590	8.25

<sup>1</sup> Percent difference given by  $\{|V_1 - V_2|/(V_1 + V_2)/2\} \times 100\%$ .

The average of the relative errors for the repeat HF measurements is 7.65% with a standard deviation of 0.583%.

We can apply a similar analysis for the water transitions. Water vapor samples were introduced into the cell and the pressure was measured using the 1 Torr capacitance manometer. The cell was then pressurized with nitrogen to a total pressure of 760 Torr and spectra were recorded. For the water measurements, the OH stretch ( $4000 - 3390 \text{ cm}^{-1}$ ) and HOH bend regions ( $2115 - 1250 \text{ cm}^{-1}$ ) were integrated and the sample pressures calculated by comparison with the NWIR Database  $25 \text{ }^\circ\text{C}$  water spectrum. The water vapor manometer pressures and the calculated  $\text{H}_2\text{O}$  vapor pressures are shown in **Table 3.4**. A plot of the estimate of the water partial pressure (in Torr) from the spectral measurement vs. the manometer pressure measurement is shown in **Figure 3.3**.

**Table 3.4** Water calibration table giving the capacitance manometer reading of the water sample pressure placed in the gas cell and the sample pressure as determined by integrating the water OH stretch and HOH bend fundamental bands ( $4000 - 3390 \text{ cm}^{-1}$ ;  $2115 - 1250 \text{ cm}^{-1}$ ) and calculating the pressure from the NWIR database. After filling the cell with the water sample, the cell is backfilled with enough nitrogen to bring the total pressure in the cell to approximately 760 Torr. All pressures in Torr.

<b>H<sub>2</sub>O pressure (manometer)</b>	<b>H<sub>2</sub>O pressure (spectrum)</b>	<b>% Difference<sup>1</sup></b>
0.0624	0.08614	31.96
0.0981	0.1248	23.96
0.1590	0.1630	2.503
0.5500	0.5471	0.5287
1.1252	1.120	0.4811

<sup>1</sup> Percent difference given by  $\{|V_1 - V_2|/(V_1 + V_2)/2\} \times 100\%$ .

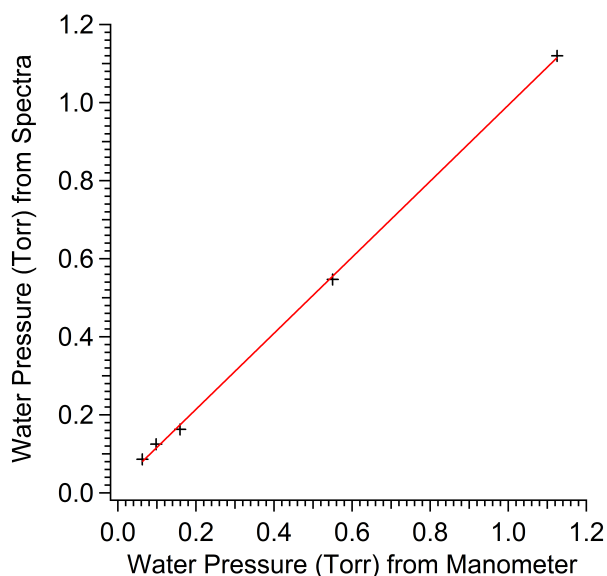


**Figure 3.3** The pressure data given in **Table 3.4** are shown (markers) and fit to a straight line (red trace).

The slope of the fit line in **Figure 3.3** is  $0.9737(0.0119)$  and the intercept is  $0.01973(0.0067)$ ;  $1\sigma$  deviations are shown in parentheses.

## 3.2 Hydrogen Fluoride and Water Mixture Measurements

To determine the equilibrium constant for the reaction given in Eq. 1, we introduced a controlled amount of anhydrous hydrogen fluoride into the gas cell and then added a prepared mixture of water vapor and nitrogen to the cell. The initial gas quantities were precisely measured by the capacitance manometers. We then used infrared spectroscopy to monitor the decrease of a select number of HF and H<sub>2</sub>O rovibrational absorbance lines for an extended period of time (up to fourteen hours).

One difficulty we encountered was preparing homogeneous mixtures of water vapor and nitrogen in the gas manifold. As we stated above, if we put a quantitative amount of water vapor in the gas cell and then added nitrogen, we obtained good quantitative agreement between our spectra and the NWIR database. If, however, we made a mixture in the gas manifold and then expanded this into the gas cell, the measured spectrum showed a water vapor spectrum of only a few percent of the expected amount. If after making the water vapor and nitrogen mixture in the gas manifold, we waited an hour for mixing and then flowed the mixture into the gas cell, the measured spectrum was about 73% of the expected amount of water vapor. If we waited two hours for mixing in the manifold, we observed about 75% of the expected amount of water vapor, and if we left the water/nitrogen mixture in the manifold overnight, we observed about 85% of the expected amount. The mixtures were prepared accounting for the expansion ratio between the gas manifold and the gas cell. Using a simple diffusion analysis to calculate the mixing time for water vapor in nitrogen ( $D = 30 \times 10^{-6} \text{ m}^2/\text{sec}$ ) gives a mixing time of approximately 2 hours.<sup>68, 69</sup> A more realistic estimate of the mixing time would require a counter diffusion analysis of unequal amounts of gas pressures.<sup>70-74</sup> Such an analysis is beyond the scope of this study.

To keep the preparation time reasonable, we developed a procedure for preparing the gases for each gas mixture measurement. With some trial and error, we determined, for example, that to put 1 Torr of water vapor into the gas cell we would meter 1.65 Torr of water vapor into the manifold, add 874 Torr of nitrogen to the manifold, and wait one hour for mixing. When this mixture was expanded into the gas cell the partial pressure of the water vapor in the cell, as determined by infrared absorption spectroscopy referenced to the infrared database, was approximately 1 Torr. For a typical HF/water mixture measurement, the desired amount of anhydrous hydrogen fluoride was metered into the cell from its manifold thirty minutes before the water vapor/nitrogen mixture was expanded into the cell. Once introduced into the cell, the pressure of the HF begins to drop and the thirty-minute period is used to allow the pressure to stabilize. Hydrogen fluoride is extremely hygroscopic and reacts with any water sorbed onto the walls of its manifold, the gas line connecting the manifold to the cell, the cell walls, and the cell windows. Hydrogen fluoride also may have reacted with the Viton O-rings sealing the windows to the cell.

Another consideration for this experiment is the possible condensation of water/hydrogen fluoride vapor phase mixtures onto a surface. We wanted to work in a water vapor/hydrogen fluoride partial pressure regime where such condensation on the gas cell walls was not likely to happen. Helms and Deal<sup>75</sup> studied the mechanisms for water/HF vapor phase etching of silicon dioxide on silicon wafers. They discovered that a film of water on a surface at a particular temperature was necessary to begin condensing HF out of the vapor phase and begin the etching process. Using their own measurements and data found in the literature,<sup>76-78</sup> they developed the partial pressure diagram shown in **Figure 3.4** that delineates regions where a water/HF film will or will not grow on a surface. The surface temperature for the diagram in **Figure 3.4** is assumed to be 25 °C. To minimize condensation on the gas cell walls or windows, we selected water vapor and hydrogen fluoride vapor pressure combinations in the “no condensation” region of **Figure 3.4** to measure the equilibrium constant of Eq. 1. Despite working in this regime, we found that if the gas cell was heated to 45 °C and pumped on with a diffusion pump overnight, the pressure of the anhydrous hydrogen fluoride took longer to stabilize when it came time to fill the cell with the aliquot of

HF for a measurement. If we did not heat the cell and pump on it overnight, but rather pumped on the cell for a few hours at 25 °C, we found that small HF and water spectral features would grow in when the “evacuated” cell was isolated from the vacuum pump. Most of the water/HF measurements we made by evacuating the cell of the contents from the previous experiment for a few hours at 25 °C before adding the HF and water/nitrogen samples.

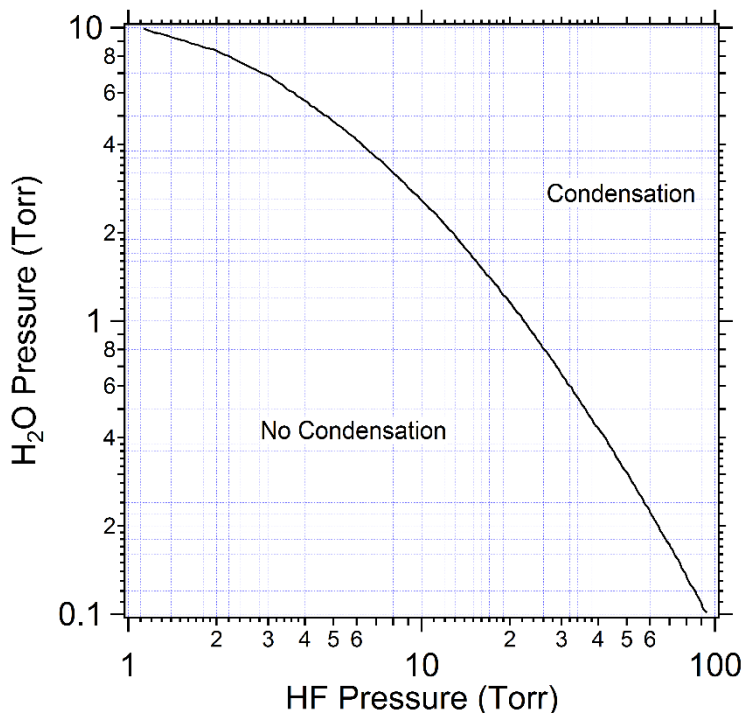


**Figure 3.4** A phase diagram for water and hydrogen fluoride vapors at 25.0 °C. The diagram shows regions where films of water/hydrogen fluoride will (condensation) and will not (no condensation) grow on surfaces at 25.0 °C. The diagram is from the work of Helms and Deal.<sup>75</sup>

The water and HF partial pressures used for determining the equilibrium constant are given in **Table 3.5**. Most of these measurements were made with the gas cell stabilized to 25.0 °C; one measurement was made at 10 °C, and another was made at 40 °C. Also, for most of the measurements, data were recorded by co-adding 256 scans per spectrum using a 60 kHz scanner velocity. Under these recording parameters, spectra are spaced approximately 10.8 minutes apart. To provide a finer time step, a few spectra were recorded by co-adding 25 spectra with a 60 kHz scanner velocity. This resulted in spectra that were spaced approximately 1.2 minutes apart. Spectra were recorded for approximately 10 to 14 hours after the vapors were mixed. The liquid nitrogen hold time of the MCT detector dewar is approximately 12 hours.

A typical daily schedule for conducting an H<sub>2</sub>O–HF equilibrium experiment was as follows. Preparation of the cell began in the early afternoon by pumping out the cell and collecting background spectra of the evacuated cell. In late afternoon, the water vapor and nitrogen mixture was made in the manifold, and anhydrous hydrogen fluoride was put into the gas cell thirty minutes after the water/nitrogen mixture was prepared. The water/nitrogen mixture was added to the gas cell after sixty minutes of mixing in the manifold, the total pressure was noted, the pneumatic valve was closed, and spectral recording was started between 4:00 and 5:00 PM. The MCT detector dewar was topped off with liquid N<sub>2</sub> between 8:00 and 10:00 PM. The Bruker OPUS software repeat measurement function was used to collect spectra overnight.

**Table 3.5** Hydrogen fluoride and water vapor pressures, total pressures with nitrogen ballast gas, and gas cell temperatures for the measurements used to determine the equilibrium constant for the reaction given in Eq. 1.

Date	Temperature (°C)	P(HF) (Torr)	P(H <sub>2</sub> O) (Torr)	Total Press (Torr)
8/8/2016 <sup>a</sup>	25.0	0.4833	0.9882	760.76
8/5/2016 <sup>a</sup>	25.0	0.57748	2.4605	761.11
7/21/2016 <sup>a</sup>	25.0	1.034	0.9935	756.82
8/19/2016 <sup>a</sup>	25.0	0.9723	0.9931	760.16
8/29/2016 <sup>b</sup>	25.0	1.06	1.0498	761.61
8/4/2016 <sup>a</sup>	25.0	1.012	2.4126	760.62
8/22/2016 <sup>a</sup>	25.0	1.01198	2.4128	758.29
8/23/2016 <sup>a</sup>	25.0	1.01487	2.4222	759.32
8/17/2016 <sup>a</sup>	25.0	1.0066	3.9371	761.69
8/25/2016 <sup>a</sup>	25.0	2.0147	2.4233	760.91
8/18/2016 <sup>a</sup>	25.0	2.0218	3.9374	763.18
9/1/2016 <sup>c</sup>	25.0	2.0175	3.9358	761.95
8/26/2016 <sup>a</sup>	25.0	4.0102	3.9385	759.89
8/31/2016 <sup>c</sup>	25.0	4.0114	3.9381	760.12
9/9/2016 <sup>c</sup>	10.0	4.0066	3.9117	758.72
9/7/2016 <sup>c</sup>	40.0	4.0015	3.9609	766.79

- 256 co-added scans per spectrum for all spectra recorded after mixing; 60 kHz scanner velocity; 10.8 minutes between spectra.
- 25 co-added scans per spectrum for first hour after mixing; 60 kHz scanner velocity; 2.8 minutes between spectra (with extra delay compared to c). Water spectra show increase in water vapor pressure.
- 25 co-added scans per spectrum for first twenty minutes after mixing; 60 kHz scanner velocity; 1.2 minutes between spectra.

To process the spectral data, the spectra, which were encoded in an OPUS binary format, were converted to ASCII format using a custom C# program that utilizes the Bruker OPUS-controller library. The spectra were then imported into MATLAB. Selecting one of the background spectra recorded just prior to the mixture spectra, absorbance spectra ( $-\log_{10}$ ) were calculated and slight adjustments were made to these spectra so that their baselines were aligned and, on average, passed through zero absorbance. These manipulations were performed using MATLAB scripts (Appendix B).

To track the progress of the reaction (see Eq. 1), we measured the peak areas of three hydrogen fluoride fundamental ( $v = 1 - 0$ ) R-branch transitions: R(5) at  $4174.0 \text{ cm}^{-1}$ , R(6) at  $4203.3 \text{ cm}^{-1}$ , and R(7) at  $4230.7 \text{ cm}^{-1}$ , and four water transitions: two in the  $\nu_3$  band,  $3837.8 \text{ cm}^{-1}$  ( $001 - 000$ ;  $4_{04} - 3_{03}$ ) and  $38161.1 \text{ cm}^{-1}$  ( $001 - 000$ ;  $3_{13} - 2_{12}$ ), and two in the  $\nu_2$  band,  $1695.9 \text{ cm}^{-1}$  ( $010 - 000$ ;  $5_{05} 4_{14}$ ) and  $1717.4 \text{ cm}^{-1}$  ( $010 - 000$ ;  $6_{16} - 5_{05}$ ). As an example, these transitions are marked on **Figures 3.5** and **3.6**. The spectrum in these figures is of 4.0114 Torr HF and 3.9381 Torr H<sub>2</sub>O pressurized to 760.12 Torr with dry nitrogen. The spectrum was recorded on August 31, 2016, approximately 60 minutes after mixing in the gas cell. At all HF partial pressures, the R(6) and R(7) transitions remain unsaturated. For P(HF) with nominal pressures 0.5, and 1 Torr the R(5) transition is unsaturated, but it is saturated for the P(HF) = 2 and 4 Torr mixtures. The water transitions remain unsaturated for all water vapor pressures used here. The areas of these transitions over the duration of each measurement set given in **Table 3.5** are tabulated in an Excel file that is available upon request. A 10% transmitting spectral transition has a  $-\log_{10}$  absorbance of 1, and a 1% transmitting spectral transition has a  $-\log_{10}$  absorbance of 2.

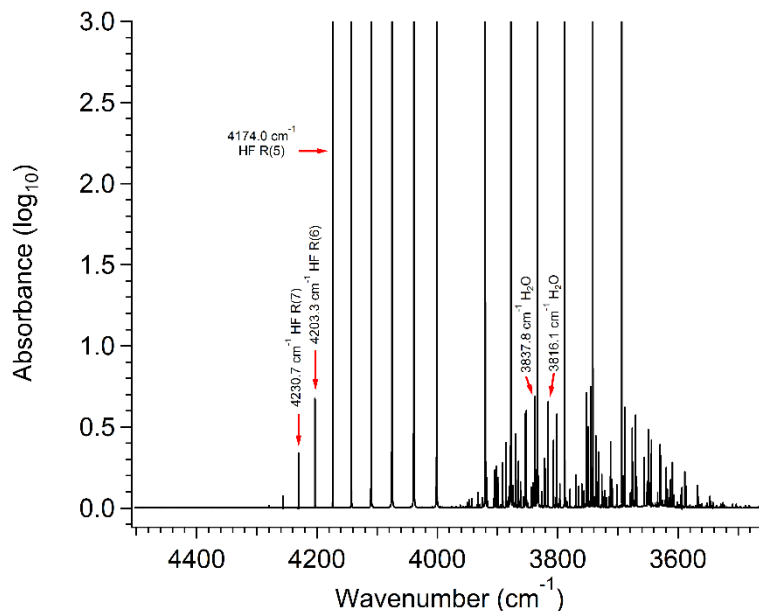


**Figure 3.5** A portion of the infrared absorption spectrum of a mixture of 4.0114 Torr HF and 3.9381 Torr of water vapor. The HF fundamental and water  $\nu_1$  region is shown. The total pressure of the mixture is brought to 760.12 Torr with dry nitrogen. The spectrum was recorded on August 31, 2016 approximately sixty minutes after mixing. The gas cell was thermostatted at 25.0 °C.

In an idealized reaction, the water and hydrogen fluoride would mix, react, and reach an equilibrium mixture in the static gas cell, and the partial pressures of water, HF, and  $\text{H}_2\text{O-HF}$  would remain constant. Instead, we found that the partial pressures of all three components continuously decreased over time. **Figure 3.7** shows the decrease of the integrated peak areas for the two unsaturated HF transitions and the four water transitions for the measurement made on August 31, 2016 (see **Figures 3.5** and **3.6**). For this data, set the four water transitions are observed to decrease rapidly during the first hour after mixing and then follow a slower decay for the duration of the measurement. The two HF transitions follow a linear decay for the entire measurement. The decay curves for each of the select water and HF transitions for the measurement conditions tabulated in **Table 3.4** are shown in Appendix C.

Given the initial partial pressures of the water vapor and anhydrous hydrogen fluoride, we can calculate the “equilibrium” partial pressures of these vapors and that of the  $\text{H}_2\text{O-HF}$  complex using the information from the tabulated spectral decay data. From those values, we can then calculate the equilibrium constant for the reaction (Eq. 1) using Eq. 7, remembering that the partial pressures must be expressed in atmospheres. A  $K_{\text{eq}}$  value has been calculated for each transition that is not saturated or shows an increase in partial pressure for each time step from one hour after mixing to ten hours after mixing, in each 25 °C measurement set listed in **Table 3.5**. This gives a range of  $K_{\text{eq}}$  values using the HF transitions and for the  $\text{H}_2\text{O}$  transitions. Averaging the thirty-seven  $K_{\text{eq}}$  values calculated from the HF transitions gives  $K_{\text{eq}} = 51(24)$ , where the value in parenthesis is one standard deviation, and averaging the forty-eight  $K_{\text{eq}}$  values calculated from the  $\text{H}_2\text{O}$  transitions gives  $K_{\text{eq}} = 77(46)$ . Adebayo and coworkers<sup>46</sup> calculated  $K_{\text{eq}}(25\text{ °C}) = 84(18)$ .

The large variation in the  $K_{\text{eq}}$  values determined from the spectroscopic decay data points to a systematic error in our experimental technique. The persistent decay of the partial pressures of the water, HF and  $\text{H}_2\text{O-HF}$  in the cell suggests that there is a slow accretion of these constituents onto the walls and windows of the cell, perhaps the buildup of a film of hydrofluoric acid on the cell walls. We had a gas cell

constructed with the same dimensions as the gold-coated cell and had the interior surface of this new cell coated with Teflon (PTFE) (Continental Coating Corp., Tualatin, OR). With this new cell, we made several water/HF gas mixture measurements with the hope that the vapors would not stick to the walls of the cell. The results using this cell, however, were far worse than those obtained with the gold-coated cell. The Teflon seemed to be very porous to both HF and water. The vapors decayed more rapidly in the closed cell after mixing and the cell required longer to evacuate residual vapors at the end of a measurement. Results from this Teflon-coated cell are not discussed further in this report.

Returning to the data recorded using the gold-coated cell, there are some exceptions to the aforementioned decay patterns in the data set. For example, on August 5, 2016, the water partial pressure leveled off about six hours after mixing and the HF partial pressure continued to decrease. This was also the case for data recorded on August 4, 2016, though here the water vapor pressure increased slightly over time. On July 21, 2016, the HF partial pressure declined linearly, but the water partial pressure increased linearly. This was the case for data recorded on August 29, 2016. On August 25, 2016, the partial pressure of HF declined as measured by the R(6) and R(7) transitions; the R(5) transition shows an increase in HF partial pressure during the second hour followed by a decrease and leveling off of the integrated signal. The water partial pressure leveled off after about hour six for this measurement. A similar increase in the HF signal for the R(5) transition was observed for the data recorded on August 18, 2016 and also on September 1, 2016 (see the plots in Appendix C). The aberrations in the R(5) integrated intensities in these cases can be attributed to the saturation of the transition at these HF partial pressures.

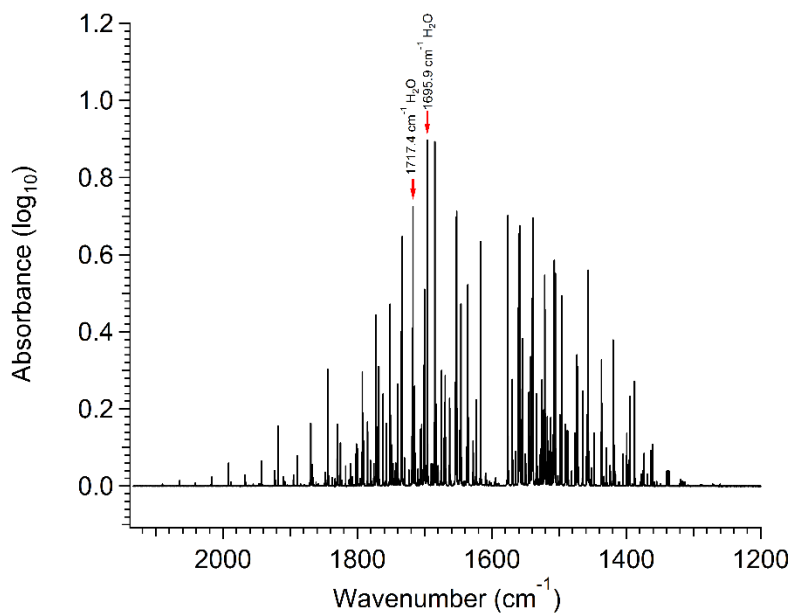


**Figure 3.6** A portion of the infrared absorption spectrum of a mixture of 4.0114 Torr HF and 3.9381 Torr of water vapor. The water  $\nu_2$  region is shown. The total pressure of the mixture is brought to 760.12 Torr with dry nitrogen. The spectrum was recorded on August 31, 2016, approximately sixty minutes after mixing. The gas cell was thermostatted at 25.0 °C.

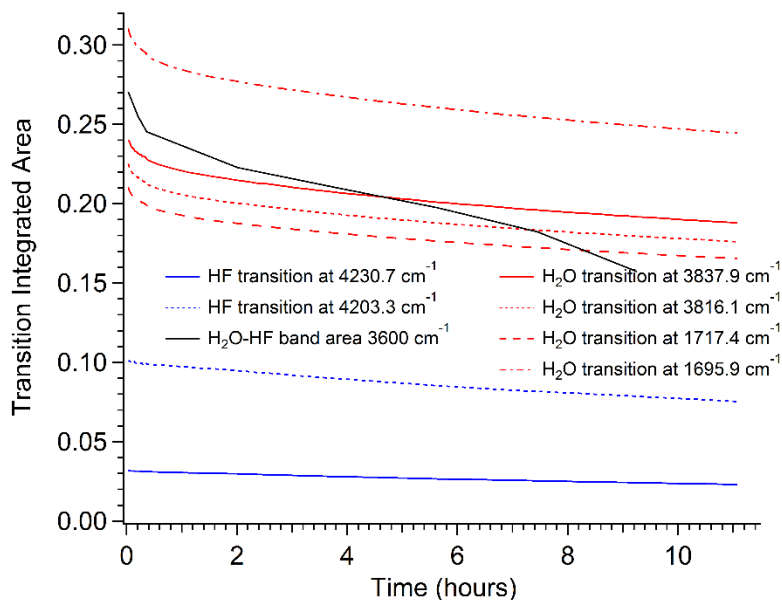


**Figure 3.7** The decay curves for the integrated areas of the two unsaturated HF transitions R(6) and R(7), and the four water transitions are shown. The integrated areas are assumed to be directly proportional to the partial pressures of the chemical components in the gas cell. The curves are for the data set recorded August 31, 2016. The decay of the H<sub>2</sub>O–HF complex is also shown.

The trends in the decay of the HF and water vapor partial pressures can be seen in further detail by examining **Figures 3.8 and 3.9**. These data were recorded on August 19, 2016. The starting HF pressure was 0.9723 Torr, the water pressure was 0.9931 Torr, and the total pressure with nitrogen was 760.16 Torr. The peak areas of the three HF transitions as a function of time after the start of the experiment are represented as “x” markers in **Figure 3.8**. The spacing between these markers is about 10.8 minutes. Each decay curve was fit to a line with a slope and intercept;  $\chi^2$  is used as a measure of the goodness of fit, and one-standard deviation uncertainties for the fit parameters are given in parentheses. The slope of the R(5) decay is  $-9.1(3) \times 10^{-4}$  /hour, the R(6) slope is  $-2.94(7) \times 10^{-4}$  /hour and the R(7) slope is  $-8.7(2) \times 10^{-5}$  /hour. The ratio of the slopes of R(5) to R(6) for this data set is 3.1, the ratio of the slopes of R(6) to R(7) is 3.4, and the ratio of the slopes of R(5) to R(7) is 10.5. As the partial pressure of HF is increased in the initial mixture for these experiments, the absolute value of the slope increases, and this increase is independent of the amount of water vapor partial pressure. Despite the changes in the HF slope values for the different HF partial pressures used for these experiments, the ratios of the slopes as described above remain the same. See **Table 3.6** and Appendix D for the slopes of the decay curves as measured from the HF R(5), R(6) and R(7) transitions.

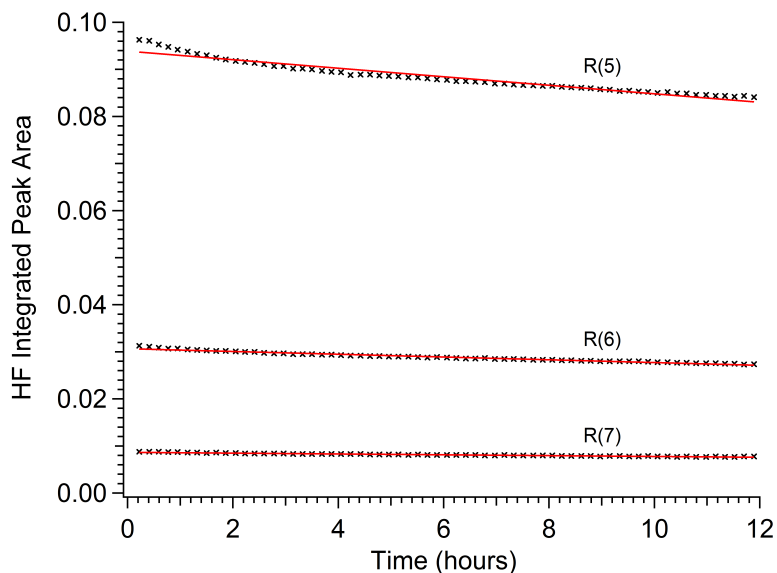


**Figure 3.8** The decay curves for the three HF transitions monitored for the data set recorded on August 19, 2016 are shown. The initial partial pressure of HF was 0.9723 Torr, the water pressure was 0.9931 Torr, and the total pressure with nitrogen was 760.16 Torr. The measured peak areas are designated by “x” markers and a linear fit to each decay curve is shown as a red trace.

The water vapor decay curves for the four water transitions monitored for the August 19, 2016 data set are shown in **Figure 3.9**. Again, the individual peak areas are designated by “x” markers, and these are plotted as a function of time since the start of the experiment. The data were fit to the double exponential decay equation given in Eq. 8.

$$y = y_0 + A_1 \left\{ \frac{-(x-x_0)}{\tau_1} \right\} + A_2 \left\{ \frac{-(x-x_0)}{\tau_2} \right\} \quad (8)$$

The fit parameters for the water decay curves using Eq. 8 are given in Appendix D for the data sets given in **Table 3.5**. The tau values, which give the 1/e decay constants in units of hours, are summarized in **Table 3.7**. For a given data set, the  $\tau_1$  are close in value as are the  $\tau_2$ ; that is, the tau values do not have any discernable dependence on the transitions from which they are fit. The average  $\tau_1$  value is 0.451 hours and the average  $\tau_2$  value is 5.77 hours.<sup>1</sup> There does not appear to be any dependence for the tau values on either the water partial pressure or the HF partial pressure.

<sup>1</sup> The fit of the data for August 18, 2016 gives the larger value for  $\tau_1$  and the smaller value for  $\tau_2$ . These values have been swapped for the purpose of calculating the average tau values.

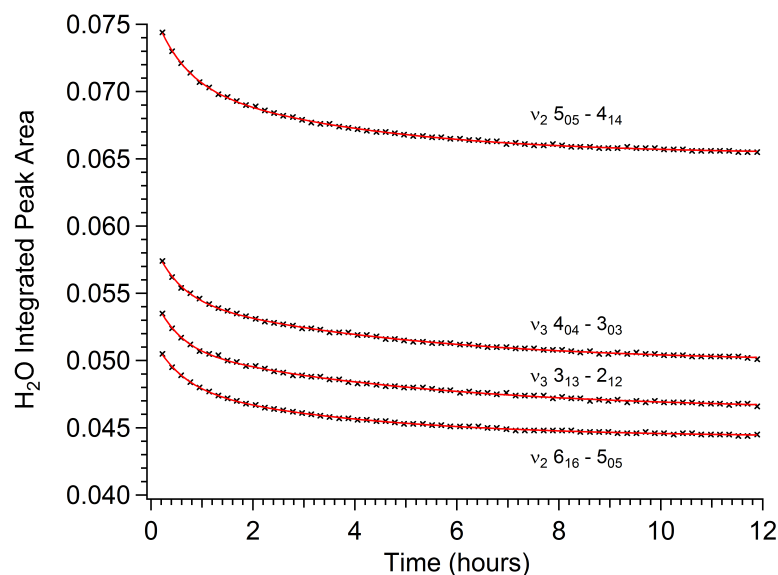


**Figure 3.9** The decay curves for the four water vapor ro-vibrational transitions monitored for the data set recorded on August 19, 2016 are shown. The initial partial pressure of HF was 0.9723 Torr, the water pressure was 0.9931 Torr, and the total pressure with nitrogen was 760.16 Torr. The measured peak areas are designated by “x” markers and a double exponential fit to each decay curve is shown as a red trace.

**Table 3.6** Slope and intercept values for linear fit of HF decay curves (Appendices C and D).

Date	Temp. (°C)	P(HF) (Torr)	HF 4230.7 cm <sup>-1</sup>		HF 4203.3 cm <sup>-1</sup>		HF 4174.0 cm <sup>-1</sup>	
			Slope	Intercept	Slope	Intercept	Slope	Intercept
8/8/2016	25.0	0.4833	-5.2264E-05	4.1688E-03	-1.8168E-04	1.5302E-02	-5.4971E-04	4.5524E-02
8/5/2016	25.0	0.57748	-6.9291E-05	5.3057E-03	-2.4478E-04	1.9249E-02	-7.3228E-04	5.7069E-02
7/21/2016	25.0	1.034	-1.2436E-04	8.8327E-03	-4.1559E-04	3.1050E-02	-1.2769E-03	9.1288E-02
8/19/2016	25.0	0.9723	-8.7257E-05	8.6715E-03	-2.9372E-04	3.0680E-02	-9.0590E-04	9.3878E-02
8/29/2016	25.0	1.06	-1.1403E-04	8.8169E-03	-3.8468E-04	3.1189E-02	-1.3644E-03	9.6487E-02
8/4/2016	25.0	1.012	-1.4332E-04	8.4228E-03	-4.8567E-04	2.9914E-02	-1.4831E-03	8.8949E-02
8/22/2016	25.0	1.01198	-1.0599E-04	8.9632E-03	-3.5227E-04	3.1619E-02	-1.1816E-03	9.6710E-02
8/23/2016	25.0	1.01487	-1.1709E-04	9.1437E-03	-3.9919E-04	3.2212E-02	-1.4109E-03	9.9458E-02
8/17/2016	25.0	1.0066	-1.4727E-04	8.9405E-03	-4.9576E-04	3.1478E-02	-1.6664E-03	9.7338E-02
8/25/2016	25.0	2.0147	-2.2606E-04	1.7050E-02	-6.9336E-04	5.6989E-02	n/a	n/a
8/18/2016	25.0	2.0218	-4.9273E-04	1.7199E-02	-1.5516E-03	5.8003E-02	n/a	n/a
9/1/2016	25.0	2.0175	-3.4761E-04	1.7318E-02	-1.1260E-03	5.8562E-02	n/a	n/a
8/26/2016	25.0	4.0102	-1.0999E-03	3.0716E-02	-3.1651E-03	9.6951E-02	n/a	n/a
8/31/2016	25.0	4.0114	-7.9195E-04	3.1450E-02	-2.3307E-03	9.9669E-02	n/a	n/a
9/9/2016	10.0	4.0066	-7.0844E-04	3.7458E-02	-2.2100E-03	1.1232E-01	n/a	n/a
9/7/2016	40.0	4.0015	-6.2970E-04	2.2369E-02	-2.0896E-03	7.8593E-02	n/a	n/a

**Table 3.7** Decay constants  $\tau_1$  and  $\tau_2$  for double exponential decay fits of H<sub>2</sub>O decay curves (Appendices C and D).

Date	P(H <sub>2</sub> O) (Torr)	H <sub>2</sub> O 3837.8 cm <sup>-1</sup>		H <sub>2</sub> O 3816.1 cm <sup>-1</sup>		H <sub>2</sub> O 1717.4 cm <sup>-1</sup>		H <sub>2</sub> O 1695.9 cm <sup>-1</sup>	
		$\tau_1$	$\tau_2$	$\tau_1$	$\tau_2$	$\tau_1$	$\tau_2$	$\tau_1$	$\tau_2$
8/8/2016	0.9882	0.6468	4.7077	0.7053	5.4246	0.2738	3.0868	0.2845	3.0331
7/21/2016	0.9935	n/a	n/a	n/a	n/a	n/a	n/a	n/a	n/a
8/19/2016	0.9931	0.4984	4.6335	0.4876	4.9757	0.5688	3.8243	0.5661	3.6562
8/29/2016	1.0498	n/a	n/a	n/a	n/a	n/a	n/a	n/a	n/a
8/4/2016	2.4126	n/a	n/a	n/a	n/a	n/a	n/a	n/a	n/a
8/22/2016	2.4128	0.4254	5.1838	0.4564	5.6146	0.4553	5.3996	0.4725	5.4431
8/23/2016	2.4222	1.1482	7.0513	0.7351	6.3014	0.7112	5.3498	1.0142	6.6848
8/25/2016	2.4233	0.3271	2.5705	0.3395	2.5863	0.2667	2.2194	0.2912	2.2939
8/5/2016	2.4605	0.3790	2.7364	0.3735	2.6478	0.2509	1.9774	0.2769	1.9368
8/17/2016	3.9371	0.5632	7.8583	0.6417	8.1083	0.6256	7.4987	0.6163	7.6011
8/18/2016	3.9374	9.8212	0.4664	9.9270	0.4795	10.4260	0.4244	10.3200	0.4367
9/1/2016	3.9358	0.1071	3.5254	0.1019	3.4278	0.1118	3.3882	0.1015	3.3255
8/26/2016	3.9385	0.5188	7.8385	0.5074	7.9817	0.4450	8.0885	0.4654	8.1301
8/31/2016	3.9381	0.3128	9.0239	0.3021	8.9804	0.3186	9.5472	0.3252	9.5982
9/9/2016	3.9117	0.1574	7.5625	0.0468	6.1529	0.0470	6.0468	0.0545	6.0944
9/7/2016	3.9609	0.1667	1.8568	0.1690	1.5690	0.1291	1.3866	0.1589	1.4370

Most of the data sets were recorded with a time resolution of about 11 minutes. This was the time to co-add 256 interferograms and transform to a spectrum in wavenumber (cm<sup>-1</sup>) space. Therefore, the first spectrum was produced approximately 11 minutes after the gases were introduced into the cell. To determine if any dramatic changes to the HF and water vapor partial pressures were occurring in the first few minutes after the gases were introduced into the cell, we recorded spectra every 1.2 minutes (25 co-added interferograms) for the first 24 minutes of a data set. We would then switch over to 256 co-added scans at this point. **Figures 3.10** and **3.11** show the HF and water decay curves for a data set recorded on September 1, 2016 where we recorded spectra at 1.2 minute intervals at the beginning of the data set (black traces) and a data set recorded on August 18, 2016 where all the data points were recorded every 10.8 minutes. Both data sets were recorded with a nominal 2 Torr of HF, 4 Torr of water vapor and a total pressure of 760 Torr with dry nitrogen. In this example and other data sets with higher time resolution close to the start of the experiment, we did not notice any dramatic changes to the HF and water partial pressures immediately after the introduction of the gases into the cell.

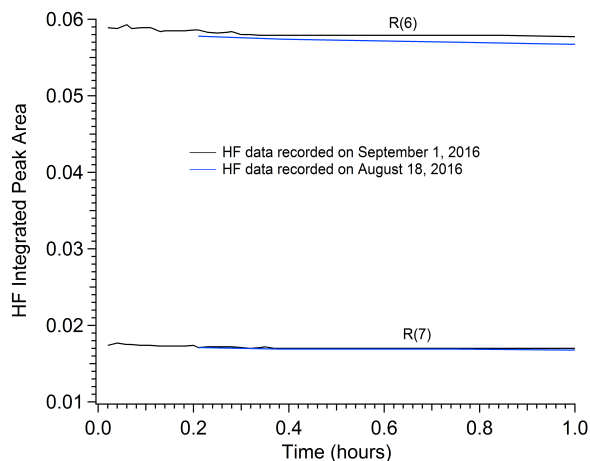


**Figure 3.10** HF decay curves for data recorded on September 1, 2016 (black traces) and August 18, 2016 (blue traces). Both experiments started with a nominal 2 Torr of HF, 4 Torr of water vapor and a total pressure of 760 Torr with dry nitrogen. For the September 1 measurement, a spectrum was recorded every 1.2 minutes until the 24<sup>th</sup> minute and then data collection resumed at the 48<sup>th</sup> minute, thereafter spectra were recorded every 10.8 minutes. For the August 18 measurement spectra were recorded every 10.8 minutes.

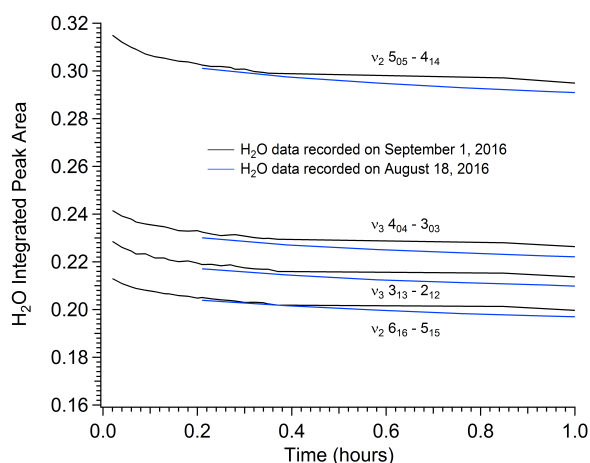


**Figure 3.11** H<sub>2</sub>O decay curves for data recorded on September 1, 2016 (black traces) and August 18, 2016 (blue traces). Both experiments started with a nominal 2 Torr of HF, 4 Torr of water vapor and a total pressure of 760 Torr with dry nitrogen. For the September 1 measurement, a spectrum was recorded every 1.2 minutes until the 24<sup>th</sup> minute and then data collection resumed at the 48<sup>th</sup> minute, thereafter spectra were recorded every 10.8 minutes. For the August 18 measurement spectra were recorded every 10.8 minutes.

**Figure 3.12** shows the  $\nu_1$  (H–F) stretch region of the H<sub>2</sub>O–HF complex. These data were measured on July 27, 2016 using 0.112 cm<sup>-1</sup> instrument resolution and a cell temperature of 25 °C. The gas cell contained 2.07 Torr of HF, 2.00 Torr of H<sub>2</sub>O, and enough dry nitrogen gas to bring the total pressure to approximately 760 Torr. The optical path was 20.0 cm. The three traces show that there is a slow decrease in the intensity of the band over time. This decline was also observed for the H<sub>2</sub>O–HF band data shown in **Figure 3.7** for the data recorded on August 31, 2016. We attempted to completely subtract the water and HF monomer transitions from the spectra shown in **Figure 3.12** to get a cleaner view of the  $\nu_1$  band of the complex, but this was not very successful. Bulychev and coworkers<sup>50, 51</sup> describe a more sophisticated

spectral subtraction procedure that accounts for the line broadening and shifts that take place with the mutual water and HF gas phase interactions. The results of their subtraction procedure are shown in **Figure 1.4**. Through a combination of experimental and *ab initio* calculations they have determined that the  $\nu_1$  band of the 1:1 complex is at  $3633.8\text{ cm}^{-1}$ , which is a shift of  $-331.8\text{ cm}^{-1}$  from the origin of the HF fundamental stretch, and that band is asymmetric with a strong low frequency head and an extended high frequency wing. The region is intermixed with hot bands originating from excited states of other intermolecular modes.

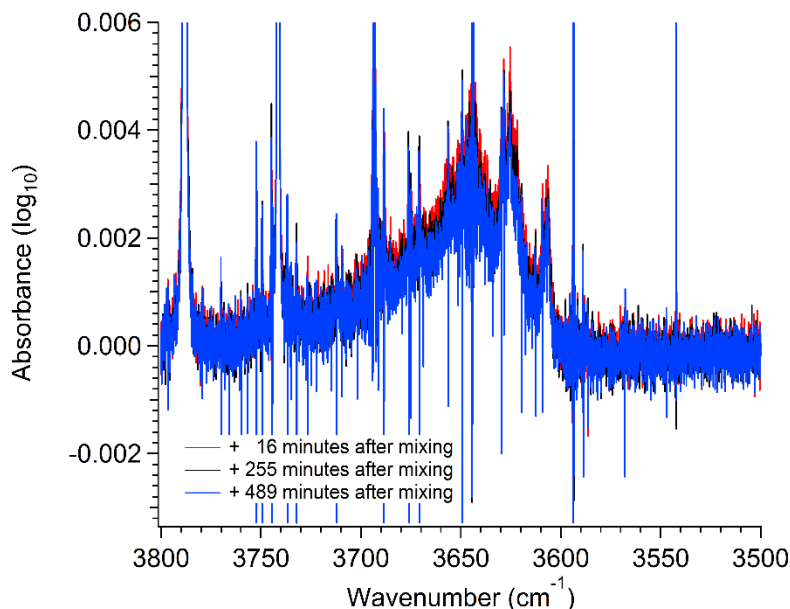


**Figure 3.12** The  $\nu_1(\text{H-F})$  stretch band of the  $\text{H}_2\text{O-HF}$  van der Waals complex at  $3608\text{ cm}^{-1}$ . The gas cell contained 2.07 Torr of HF, 2.00 Torr of  $\text{H}_2\text{O}$ , and dry nitrogen gas to bring the total pressure to approximately 760 Torr. The optical path is 20.0 cm and the temperature of the cell was 25.0 C. The data was recorded on July 27, 2016. Three traces are labeled with the total elapsed time since the mixing of the gases. Subtraction of water transitions was performed. Several positive-going HF P-branch transitions can be observed.

Finally, we recorded an overnight series of spectra for a nominal 4 Torr HF and 4 Torr water vapor mixture with a total pressure of 760 Torr at  $10\text{ }^\circ\text{C}$  and then another series for a mixture with the same pressure quantities at  $40\text{ }^\circ\text{C}$ . From the  $10\text{ }^\circ\text{C}$  series we found  $K_{\text{eq}} = 44(27)$  from the HF transitions and  $K_{\text{eq}} = 63(22)$  from the water transitions. From the  $40\text{ }^\circ\text{C}$  series, we found  $K_{\text{eq}} = 27(15)$  from the HF transitions and  $K_{\text{eq}} = 21(6)$  from the water transitions. For the  $10\text{ }^\circ\text{C}$  experiment, the initial vapor pressure of water was 4 Torr, which is below the saturation vapor pressure of 9 Torr at this temperature, so there should be no condensation on the cell walls and windows. The general trend is as we predicted in the Introduction: the  $10\text{ }^\circ\text{C}$  measurement should give a larger  $K_{\text{eq}}$  value than that of the  $40\text{ }^\circ\text{C}$ , but the measured  $10\text{ }^\circ\text{C}$   $K_{\text{eq}}$  value is nowhere close to the predicted value of 191. Our assumption that the  $\Delta H$  and  $\Delta S$  values for the formation of the  $\text{H}_2\text{O-HF}$  cluster are not strongly dependent on temperature appears to be incorrect. The  $40\text{ }^\circ\text{C}$   $K_{\text{eq}}$  measured values are closer to the predicted values with a smaller standard deviation.

## 4.0 Discussion

Adebayo and coworkers'  $K_{\text{eq}}$  value for the equilibrium shown in Eq. 1 at 25 °C was calculated to be 84(18).<sup>46</sup> This value is based on  $\Delta H$  and  $\Delta S$  values that were calculated, using several assumptions, from spectroscopic data. The  $1\sigma$  uncertainty for their value is dominated by the uncertainty in the dissociation energy<sup>45</sup> for H<sub>2</sub>O–HF propagated through their statistical mechanical calculations. Our experimental values for  $K_{\text{eq}}$  at 25 °C based on the diminution of the water vapor and HF transitions, respectively, are 77(46) and 51(24) averaged between one and ten hours after the vapors were mixed in the gas cell. The percent differences between the Legon et al. value and our water vapor and HF measurements are 8.7% and 49%, respectively. We see our  $K_{\text{eq}}$  values, as measured from the HF transitions, to be systematically lower than those measured from the water vapor transitions. It was also interesting to note that in all the measurement series, the ratios of the slopes of the decay curves for the three HF transitions remained approximately constant. Is there a rotational dependence to the adsorption of the HF to the cell wall and windows? Beyond these observations, there seems to be no pattern to the decay of the HF and water vapor: either the decay of the HF transition intensities keeps up with the decay of the water vapor transitions, or it lags behind. Consequently, we calculated the  $K_{\text{eq}}$  values at each time step for each of the transitions monitored and averaged these from hour one to hour ten after the gases were introduced into the cell, and then averaged these 25 °C values over those measurement series that did not show a rapid rise of water vapor during the course of the measurement (Appendix C). This is the procedure that produced the  $K_{\text{eq}}$  values given above.

The decay of the transition intensities continued over the extended period of the measurements (>10 hours). It is possible that the formation of H<sub>2</sub>O–HF reaches equilibrium soon after mixing with a small decrease in the intensities of the tracked transitions and a resulting smaller  $K_{\text{eq}}$  value. In this case, what we are averaging over are other equilibrium processes. But lacking a definitive and physically meaningful point in the decay curves, we decided that taking the average of the  $K_{\text{eq}}$  values over the extended period was the only unbiased way of representing the results. Monitoring the integrated signal of the H<sub>2</sub>O–HF cluster may help with interpreting the data, but neatly subtracting off the HF and water vapor absorptions is problematic and time consuming, and even for the one case where we did this (see **Figure 3.7**), the absorption signal for this species also declined as the HF and water vapor partial pressures continued to decline.

There are clearly other reactions competing with the equilibrium reaction given in Eq. 1. Hydrogen fluoride and water vapor may be adsorbing to the wall and windows of the cell, creating a film of hydrofluoric acid. Also, (HF)<sub>n</sub> clusters may be in equilibrium with the vapor. We tried to be consistent when preparing the gold-coated gas cell for each measurement. We evacuated the cell at 25 °C for several hours while preparing for the next measurement. Even when this was done, we could see HF and water vapor transitions grow in – very weakly – while recording the background spectra. The use of the Teflon-coated cell seemed to make things worse. Perhaps a cell made from Monel that has been properly pretreated with hydrogen fluoride might make a less “sticky” surface for HF, but once water vapor is introduced and it sticks to the cell wall, the HF vapor would begin to dissolve into the water film. Despite working at partial pressures in Helms and Deal's<sup>75</sup> “No Condensation” regime, it was still apparent that the buildup of a film on the wall and windows was evident. In his book *Reaction Kinetics: Homogeneous Gas Reactions (Volume 1)*, Laidler<sup>79</sup> recommends conducting these kinds of experiments in cells with widely different surface area to volume ratios and extrapolating out any adsorption effects from the equilibrium measurements. Working with smaller partial pressures and higher cell temperatures (40 °C) might produce more tractable results. Viton was not the best choice for O-ring material for the gas cell. In the future, an alternate material should be used.

Conducting the measurements in a flow system<sup>80, 81</sup> rather than in a static cell may produce better results, assuming that there is thorough mixing of the two vapors and the reaction goes to completion before they enter into a region of the flow system where they are measured spectroscopically. Using different concentrations of HF and water vapor mixed in streams of nitrogen,  $K_{eq}$  could be determined. Using a flow system could possibly minimize adsorption of the reactants to the walls of the system. If the nitrogen vapor mixtures flow into a White cell for spectroscopic measurement with the FTIR, much smaller partial pressures of HF and water vapor could be used, further reducing the accumulation of the reactants on the tubing and White cell walls. Setting up such a flow system would provide engineering challenges, but these would not be insurmountable.

When we placed a carefully measured amount of water vapor in the gas cell in the spectrometer and then added enough nitrogen gas to the cell to bring the total pressure to 760 Torr, we measured, using the FTIR, integrated band intensities that were consistent with the NWIR database. This was a nice check of our experimental technique. Similar quantitative measurements were made with mixtures of HF and nitrogen, and we obtained good quantitative agreement between our measured HF band intensities and those taken from the NWIR database. However, when we made mixtures of water vapor and nitrogen in the gas manifold and then expanded these into the gas cell and recorded spectra of these mixtures, we observed a much smaller quantity of water vapor in the cell than we expected from the starting partial pressure. The amount we expected to see in the cell accounted for the expansion ratio between the gas manifold and the cell. If we waited only ten minutes after introducing the water vapor and nitrogen into the manifold, we saw very little water vapor when the mixture was expanded into the gas cell in the spectrometer. If we waited an hour for the nitrogen and water vapor to mix, we measured about 73% of what we expected. Clearly this is a diffusion issue, though we were surprised by the amount of time required to obtain just partial mixing of the vapor and gas.<sup>71-74</sup> First, approximately one Torr of water vapor is measured into the manifold and then about an atmosphere of nitrogen is introduced into the manifold. Because of the location of the port on the manifold where the nitrogen is introduced, much of the water vapor is pushed down to one end of the manifold when the nitrogen is added. The manifold was kept at a temperature of about 60 °C and has a volume of about 2 L. Using Fick's law,<sup>68</sup> we calculate that we should get complete mixing about two hours after the gases are introduced into the manifold. After twelve hours of mixing in the manifold, however, we observed only about 85% of the anticipated water vapor partial pressure in the gas cell. To avoid waiting extended periods of time for the nitrogen and water vapor to mix, we determined the amount of water vapor we needed to put into the manifold to get a specific partial pressure of the vapor in the gas cell with just one hour of mixing in the manifold. This method was vetted by experiment. Nonetheless, our observations raise the issue of how much time is required for the HF vapor and water/nitrogen to mix. A small amount of HF vapor is introduced into the cell, and then roughly an atmosphere of water vapor and nitrogen mixture is introduced through a valve at one end of the cell. The HF is pushed to one end of the cell and then must counter diffuse through the water vapor/nitrogen mixture in a volume of 350 mL at a temperature of 25 °C. We have not modeled this diffusion problem, and an understanding of this issue will be necessary to better understand the equilibrium data we have recorded.

Other issues also need to be addressed to better understand the HF/water system. We observed a large difference between the  $K_{eq}$  value measured at 10 °C and that calculated using Adebayo's et al. thermodynamic values.<sup>46</sup> Either there was a large systematic experimental error, or the temperature dependence of the thermodynamic values for the formation reaction was not properly accounted for. The measurement of the thermodynamic properties of the H<sub>2</sub>O–HF system, to better determine  $\Delta H$  and  $\Delta S$  and their temperature dependence, would be helpful. This could be done through gas-phase calorimetry methods,<sup>82</sup> for example, as well as spectroscopic methods. Estimates of these values could also be achieved using *ab initio* methods. Chaban and Gerber<sup>49</sup> have calculated MP2/TZP level of theory potential energy surfaces for (HF)<sub>n</sub> and (HF)<sub>n</sub>(H<sub>2</sub>O)<sub>n</sub> (n = 1, 2, 4) mixed clusters. Do other clusters affect our results? The strong (HF)<sub>n</sub> vibrational absorptions were below the passband of our calcium fluoride

windows, so we do not know to what extent these clusters formed under the conditions of our experiments.<sup>49, 83-87</sup> Other researchers<sup>88-93</sup> have published semi-empirical potential energy surfaces for HF vapor and HF/water vapor with the aim of determining the bulk vapor phase properties of these systems. It may be possible to use these simulations to determine the equilibrium partial pressures of HF, water vapor and H<sub>2</sub>O–HF.

Using a static gas cell and mixtures of different partial pressures of water vapor and HF, we have made measurements of the equilibrium constant for the gas phase reaction  $\text{HF} + \text{H}_2\text{O} \leftrightarrow \text{H}_2\text{O-HF}$  at 25 °C. Though the values we obtained for  $K_{\text{eq}}$  were comparable to a value determined from statistical mechanical methods, there were several problems with the experimental technique that contributed to large uncertainties in the results. The continuous decay of the HF and water vapor spectroscopic signals suggests that there is substantial adsorption of the reactants on the wall and windows of the cell, and there is concern about how well the reactants are mixed in the time immediately after they are introduced into the cell. Future measurements for this system using static cells with different volume-to-wall surface area ratios, and/or a flow system may improve the results and reduce the systematic experimental errors.

## 5.0 References

1. Boscak, V. "Evaluation of Control Technology for the Phosphate Fertilizer Industry." Environmental Protection Agency, 1979.
2. Barnard, William R., and D. Kirk Nordstrom. "Fluoride in Precipitation – II. Implications for the Geochemical Cycling of Fluorine." *Atmos. Environ.* 16 (1982): 105-11.
3. Murphy, C. E., and J. Ares. "The Uptake of Hydrogen Fluoride by a Forest." *Ecol. Model.* 15, no. 3 (1982): 265-85.
4. Mankin, W. G., M. T. Coffey, K. V. Chance, W. A. Traub, B. Carli, F. Mencaraglia, S. Piccioli, *et al.* "Intercomparison of Measurements of Stratospheric Hydrogen Fluoride." *J. Atmos. Chem.* 10, no. 2 (Feb 1990): 219-36.
5. "Hydrogen Fluoride Study: Final Report to Congress, Section 112(N)(6), Clean Air Act as Amended." Environmental Protection Agency, 1993.
6. Beck, D. E., W. D. Bostick, and D. P. Armstrong. "Potential Detection Systems for Monitoring UF<sub>6</sub> Releases." Report K/TCD-1105, Martin Marietta, Oak Ridge, Tennessee, USA, 1994.
7. Bourgeau, M., D. Chapin, K. Foster, R. Jones, M. Prior, M. Shepherd, and P. Walsh. "National Ambient Air Quality Objectives for Hydrogen Fluoride (HF)." Report by Environment Canada, Toronto, Canada, 1996.
8. Russell, J. M., L. E. Deaver, M. Z. Luo, R. J. Cicerone, J. H. Park, L. L. Gordley, G. C. Toon, *et al.* "Validation of Hydrogen Fluoride Measurements made by the Halogen Occultation Experiment from the UARS Platform." *J Geophys Res-Atmos* 101, no. D6 (Apr 30 1996): 10163-74.
9. Hance, C. D., P. A. Solomon, L. G. Salmon, T. Fall, and G. R. Cass. "Hydrofluoric Acid in the Southern California Atmosphere." *J. Geophys. Res.* 101(D6) (1997): 10163-74.
10. Hoke, S. H., M. L. Clay, K. L. McNesby, C. S. Miser, M. K. Leonnig, Polyanski, C. Herud, and W. Bolt. "Comparison of Methods for Measuring Hydrogen Fluoride Gas as a Fire Suppression By-product." Paper presented at the Halon Options Technical Working Conference, May 1997 1997.
11. McNesby, K. L., R. R. Skaggs, A. W. Miziolek, M. Clay, S. H. Hoke, and C. S. Miser. "Diode Laser-Based Measurements of Hydrogen Fluoride Gas During Chemical Suppression of Fires." Report No. ARL-TR-1785, Army Research Laboratory, 1998.
12. Gillespie, A. R., M. M. Hyland, and J. B. Metson. "Irreversible HF Adsorption in the Dry-Scrubbing Process." *JOM* 51, no. 5 (May 1999): 30-32.
13. Textor, C., H.-F. Graf, C. Timmreck, and A. Robock. "Emissions from Volcanoes." In *Emissions of Chemical Compounds and Aerosols in the Atmosphere*. Dordrecht, the Netherlands: Kluwer Academic Publishers, 2004.
14. Coleman, P., R. Mascarenhas, and P. Rumsby. "A Review of the Toxicity and Environmental Behaviour of Hydrogen Fluoride in Air." United Kingdom Environmental Agency, 2005.
15. Rampersadh, Pradish. "Removal of Hydrogen Fluoride from Gas Streams." University of Witwatersrand, Johannesburg, South Africa, 2005.
16. Mezghani, Imed, Nada Elloumi, Ferjani Ben Abdallah, Mohamed Chaieb, and Makki Boukhris. "Fluoride Accumulation by Vegetation in the Vicinity of a Phosphate Fertilizer Plant in Tunisia." *Fluoride* 38, no. 1 (2005): 69-75.
17. Guigard, Selma, Warren Kindziarski, Colleen Putrill, Jason Schultz, and John Vidmar. "Assessment Report on Hydrogen Fluoride for Developing Ambient Air Quality Objectives." Toxic-Logic Consulting, Inc. for Alberta Environment, Edmonton, Alberta, Canada, 2006.
18. Dando, Neal, Weizong Xu, and Jon Nathaniel Peace. "Continuous Measurement of Peak Hydrogen Fluoride Exposures in Aluminum Smelter Potrooms: Instrument Development and In-plant Evaluation." *J Occup Environ Hyg* 5, no. 2 (Feb 2008): 67-74.

19. Duchatelet, P., P. Demoulin, F. Hase, R. Ruhnke, W. Feng, M. P. Chipperfield, P. F. Bernath, *et al.* "Hydrogen Fluoride Total and Partial Column Time Series Above the Jungfrauoch from Long-Term FTIR Measurements: Impact of the Line-Shape Model, Characterization of the Error Budget and Seasonal Cycle, and Comparison With Satellite and Model Data." *J. Geophys. Res.* 115 (2010): D22306.
20. Duchatelet, P. "Fluorine in the Atmosphere: Inorganic Fluorine Budget and Long-term Trends Based on FTIR Measurements at Jungfrauoch." University of Liège, 2011.
21. Kohlhepp, R., S. Barthlott, T. Blumenstock, F. Hase, I. Kaiser, U. Raffalski, and R. Ruhnke. "Trends of HCl, ClONO<sub>2</sub>, and HF Column Abundances from Ground-Based FTIR Measurements in Kiruna (Sweden) in Comparison With KASIMA Model Calculations." *Atmos. Chem. Phys.* 11, no. 10 (2011): 4669-77.
22. Fujita, Eric M. , and David E. Campbell. "Review of Current Air Monitoring Capabilities near Refineries in the San Francisco Bay Area." Desert Research Institute, Reno, NV, 2013.
23. Arellano, S. R. "Studies of Volcanic Plumes with Spectroscopic Remote Sensing Techniques." Chalmers University of Technology, 2013.
24. Alvarez, Manuel S., and David B. Spry. "Humidity and Temperature Corrections to Improve Accuracy of HF Ambient Air Monitors Based on Tunable Diode Laser IR Absorption Measurements." United States: US 8,614,096 B2, 13/223,756, Exxon Mobile Research and Engineering Company, 2013.
25. Polyakov, A. V., Y. M. Timofeev, Y. A. Virolainen, and A. V. Poberovskii. "Ground-Based Measurements of HF Total Column Abundances in the Stratosphere Near St. Petersburg (2009-2013)." *Izvestiya Atmospheric and Oceanic Physics* 50, no. 6 (Nov 2014): 595-601.
26. Ariti, J. "2011–12 Midland Background Air Quality Study." Department of Environmental Regulation, Perth, Western Australia, 2015.
27. Choubisa, S. L., and D. Choubisa. "Status of Industrial Fluoride Pollution and its Diverse Adverse Health Effects in man and Domestic Animals in India." *Environ Sci Pollut Res Int* 23, no. 8 (Apr 2016): 7244-54.
28. Butz, A., A. S. Dinger, N. Bobrowski, J. Kostinek, L. Fieber, C. Fischerkeller, G. B. Giuffrida, *et al.* "Remote Sensing of Volcanic CO<sub>2</sub>, HF, HCl, SO<sub>2</sub>, and BrO in the Downwind Plume of Mt. Etna." *Atmospheric Measurement Techniques* 10, no. 1 (Jan 2 2017): 1-14.
29. Czarnowski, W., B. Wielgomas, and J. Krechniak. "A Passive Dosimeter for Evaluation Exposure to Hydrogen Fluoride." *Fluoride* 35 (2002): 22-27.
30. Johansson, Ilsa. "Hydrogen Fluoride Method Development for the Ogawa Passive Sampling Device." University of South Florida, 2005.
31. Senten, C., M. De Maziere, B. Dils, C. Hermans, M. Kruglanski, E. Neefs, F. Scolas, *et al.* "Technical Note: New Ground-Based FTIR Measurements at ile de la Réunion: Observations, Error Analysis, and Comparisons With Independent Data." *Atmos. Chem. Phys.* 8, no. 13 (2008): 3483-508.
32. Hoff, Raymond M., and Sundar A. Christopher. "Remote Sensing of Particulate Pollution from Space: Have We Reached the Promised Land?" *J. Air Waste Manage. Assoc.* 59 (2009): 645-75.
33. "Monitoring Emissions of Hydrogen Fluoride (HF)." Application Bulletin No. 150, Unisearch Associates, Inc., 2014.
34. Subramaniam, T. K. "Quantum Cascade Laser in Atmospheric Trace Gas Analysis." *AASCIT J. Environ* 1 (2015): 1-4.
35. Harrison, Jeremy J., Martyn P. Chipperfield, Christopher D. Boone, Sandip S. Dhomse, Peter F. Bernath, Lucien Froidevaux, John Anderson, and James Russell III. "Satellite Observations of Stratospheric Hydrogen Fluoride and Comparisons With SLIMCAT Calculations." *Atmos. Chem. Phys.* 16, no. 16 (Aug 22 2016): 10501-19.
36. Dugheri, Stefano, Alessandro Bonari, Ilenia Pompilio, Alessandro Monti, Nicola Mucci, and Giulio Arcangeli. "Innovative Monitoring of Atmospheric Gaseous Hydrogen Fluoride." *Int J Anal Chem* 2016 (2016): 2129053.

37. Thomas, R. K. "Hydrogen Bonding in the Vapour Phase Between Water and Hydrogen Fluoride: The Infrared Spectrum of the 1:1 Complex." *Proc. R. Soc. Lond. A* 344, no. 1639 (1975): 579-92.
38. Bevan, John W., Anthony C. Legon, D. James Millen, and Stephen C. Rogers. "Existence and Molecular Properties of a Gas-Phase, Hydrogen-Bonded Complex Between Hydrogen Fluoride and Water Established from Microwave Spectroscopy." *J. C. S. Chem. Comm.* 1975 (1975): 341-43.
39. Giguere, Paul A., and Sylvia Turrell. "The Nature of Hydrofluoric Acid. A Spectroscopic Study of the Proton-Transfer Complex  $\text{H}_3\text{O}^+\text{F}$ ." *J Am Chem Soc* 102, no. 17 (1980): 5473-77.
40. Legon, Anthony C., and L. C. Willoughby. "D-Nuclear Quadrupole and H(D),  $^{19}\text{F}$  Nuclear-Spin – Nuclear-Spin Hyperfine Coupling Constants from Rotational Spectra of  $\text{H}_2\text{O}\text{-DF}$  and  $\text{H}_2\text{O}\text{-HF}$ ." *Chem. Phys. Lett.* 92, no. 4: 333-38.
41. Kisiel, Z., A. C. Legon, and D. J. Millen. "Stark Effects in the Rotational Spectrum of the Dimer  $\text{H}_2\text{O}\cdots\text{HF}$  and the Variation of the Electric Dipole Moment With Excitation of the Low-Frequency, Hydrogen-Bond Modes." *J. Chem. Phys.* 78, no. 6 (1983): 2910-14.
42. ———. "Potential Constants for the Hydrogen-bonded Dimer  $\text{H}_2\text{O}\text{-HF}$ : Directional Character of the Hydrogen Bond." *Journal of Molecular Structure* 112, no. 1-2 (1984): 1-8.
43. Szczesniak, M. M., Steve Scheiner, and Y. Bouteiller. "Theoretical Study of  $\text{H}_2\text{O}\text{-HF}$  and  $\text{H}_2\text{O}\text{-HCl}$ : Comparison with Experiment." *J. Chem. Phys.* 81, no. 11 (1984): 5024-30.
44. Cazzoli, G., P. G. Favero, D. G. Lister, A. C. Legon, D. J. Millen, and Z. Kisiel. "The Rotational Spectrum of the Hydrogen-bonded Heterodimer  $\text{H}_2\text{O}\text{-HF}$  in the Frequency Range 40-80 GHz." *Chemical Physics Letters* 117, no. 6 (1985): 543-49.
45. Legon, A. C., D. J. Millen, and Hazel M. North. "Experimental Determination of the Dissociation Energies  $D_0$  and  $D_e$  of  $\text{H}_2\text{O}\text{-HF}$ ." *Chemical Physics Letters* 135, no. 3 (Apr 3 1987): 303-06.
46. Adebayo, S. L. A., A.C. Legon, and D.J. Millen. "Thermodynamic Properties of Hydrogen-bonded Dimers B-HF from Spectroscopy: B=HCN,  $\text{CH}_3\text{CN}$ ,  $\text{HC}_2\text{CN}$ ,  $(\text{CH}_3)_3\text{CCN}$ , and  $\text{H}_2\text{O}$ ." *J Chem. Soc. Faraday Trans.* 87, no. 3 (1991): 443-47.
47. Hernandez, Norge Cruz, and Javier Fdez. Sanz. "Ab Initio Group Model Potentials Including Electron Correlation Effects." *J. Chem. Phys.* 113, no. 15 (Oct 15 2000): 6082-87.
48. Li, Zhi-Ru, Di Wu, Ze-Sheng Li, Xu-Ri Huang, Fu-Ming Tao, and Chia-Chung Sun. "Long Range  $\pi$ -type Hydrogen Bond in the Dimers." *J. Phys. Chem. A* 105 (2001): 1163-68.
49. Chaban, G. M., and R. B. Gerber. "Ab initio Calculations of Anharmonic Vibrational Spectroscopy for Hydrogen Fluoride  $(\text{HF})_n$  ( $n = 3, 4$ ) and Mixed Hydrogen Fluoride/Water  $(\text{HF})_n(\text{H}_2\text{O})_n$  ( $n = 1, 2, 4$ ) Clusters." *Spectrochim Acta A Mol Biomol Spectrosc* 58, no. 4 (Mar 01 2002): 887-98.
50. Bulychev, V. P., E. I. Gromova, and K. G. Tokhadze. "Experimental and Theoretical Study of the  $\nu(\text{HF})$  Absorption Band Structure in the  $\text{H}_2\text{O}\text{-HF}$  Complex." *Optics Spectrosc.* 96, no. 5 (May 2004): 774-88.
51. Bulychev, V. P., I. M. Grigoriev, E. I. Gromova, and K. G. Tokhadze. "Study of the  $\nu_1$  Band Shape of the  $\text{H}_2\text{O}\cdots\text{HF}$ ,  $\text{H}_2\text{O}\cdots\text{DF}$ , and  $\text{H}_2\text{O}\cdots\text{HCl}$  Complexes in the Gas Phase." *Phys. Chem. Chem. Phys.* 7, no. 11 (2005): 2266-78.
52. Belov, S. P., V. M. Demkin, N. F. Zobov, E. N. Karyakin, A. F. Krupnov, I. N. Kozin, O. L. Polyansky, and M. Yu Tretyakov. "Microwave Study of the Submillimeter Spectrum of the  $\text{H}_2\text{O}\cdots\text{HF}$  Dimer." *J. Mol. Spectrosc.* 241, no. 2 (2007): 124-35.
53. Oxtoby D. W., H. P. Gillis, and N. H. Nachtrieb. *Principles of Modern Chemistry*. New York: Harcourt Brace College Publishing, 1999. Chap. 9.
54. Atkins, P. *Physical Chemistry*. Sixth ed. New York: WH Freeman and Co, 1998. Chap. 9.
55. Schotte, William. "Fog Formation of Hydrogen Fluoride in Air." *Ind. Eng. Chem. Res.* 26 (1987): 300-06.
56. Hanna, Steven R., David G. Strimaitis, and Joseph C. Chang. "Evaluation of Fourteen Hazardous Gas Models With Ammonia and Hydrogen Fluoride Field Data." *J. Haz. Mat.* 26 (1991): 127-58.

57. Hall, D. J., and S. Walker. "Scaling Rules for Reduced-Scale Field Releases of Hydrogen Fluoride." *J. Haz. Mat.* 54 (1997): 89-111.
58. Mandellos, Nicholas A., Zoe S. Nivolianitou, and Nicholas C. Markatos. "A Newly Developed Algorithm Describing the Fog Formation of Hydrogen Fluoride (HF) in Air." *Ind. Eng. Chem. Res.* 37, no. 12 (1998): 4844-53.
59. Tickle, G. A. "Thermodynamic Modelling of Anhydrous HF/Moist Air/Imiscible Component Mixtures and Validation Against Experimental Data." AEA Technology Report No. AEAT/NOIL/27328006/002(R), 2001.
60. Ott, S. "An Integral Model for Continuous HF Releases." Riso National University Report No. Riso-R-1293(EN), 2001.
61. Wittcoff, H. A. , and B. G. Reuben. *Industrial Organic Chemicals*. New York: John Wiley and Sons, Inc., 1996. Chap. 2.
62. Meyers, R. A. *Handbook of Petroleum Refining Processes*. Second ed. New York: McGraw-Hill, 1997.
63. Sharpe, Steven W., Timothy J. Johnson, Robert L. Sams, Pamela M. Chu, George C. Rhoderick, and Patricia A. Johnson. "Gas-Phase Databases for Quantitative Infrared Spectroscopy." *Appl. Spectrosc.* 58, no. 12 (Dec 2004): 1452-61.
64. Braker, W., and A. L. Mossman. *Matheson Gas Data Book*. Sixth ed. Lyndhurst, NJ: Matheson, 1980.
65. Administration, Occupational Safety and Health. "Fluoride (F<sup>-</sup> and HF) in Workplace Atmospheres." US Department of Labor OSHA Method ID-110, 1991.
66. Muttenthaler, Markus, Fernando Albericio, and Philip E. Dawson. "Methods, Setup and Safe Handling for Anhydrous Hydrogen Fluoride Cleavage in Boc Solid-Phase Peptide Synthesis." *Nat Protoc* 10, no. 7 (Jul 2015): 1067-83.
67. Rothman, L. S., D. Jacquemart, A. Barbe, D. Chris Benner, M. Birk, L. R. Brown, M. R. Carleer, et al. "The HITRAN 2004 Molecular Spectroscopic Database." *J. Quant. Spectrosc. Rad. Transfer.* 96, no. 2 (2005): 139-204.
68. Moore, W. J. *Physical Chemistry*. Fourth ed. Englewood Cliffs, New Jersey: Prentice-Hall, 1972. Chap. 4.
69. Marrero, T. R., and E. A. Mason. "Gaseous Diffusion Coefficients." *J. Phys. Chem. Ref. Data* 1 (1972): 3-118.
70. Browkaw, Richard S. "Predicting Transport Properties of Dilute Gases." *Indus. Eng. Chem. Process Design. Devel.* 8, no. 2 (1969): 240-53.
71. Krishna, R., and J. A. Wesselingh. "The Maxwell-Stefan Approach to Mass Transfer." *Chem. Eng. Sci.* 52, no. 6 (Mar 1997): 861-911.
72. Mills, A. F. "On Steady One-Dimensional Diffusion in Binary Ideal gas Mixtures." *Int. J. Heat Mass Tran.* 46, no. 13 (Jun 2003): 2495-97.
73. Sanchez, A. L., M. Vera, and A. Linan. "Exact Solutions for Transient Mixing of Two Gases of Different Densities." *Physics of Fluids* 18, no. 7 (Jul 2006): 078102.
74. Dil'man, V. V., O. A. Kashirskaya, and V. A. Lotkhov. "Specific Features of Multicomponent Diffusion." *Theor. Found. Chem. Eng.* 44, no. 4 (Aug 2010): 379-83.
75. Helms, C. R., and B. E. Deal. "Mechanisms of the HF/H<sub>2</sub>O Vapor Phase Etching of SiO<sub>2</sub>." *J. Vac. Sci. Technol. A* 10, no. 4 (1992): 806-11.
76. Munter, P. A., O. T. Aepli, and R. A. Kossatz. "Hydrofluoric Acid-Water and Hydrofluoric Acid-Hydrofluorosilic Acid-Water." *Ind. Eng. Chem.* 39 (1947): 427-31.
77. ———. "Partial Pressure Measurements on the System Hydrogen Fluoride-Water." *Ind. Eng. Chem.* 41, no. 7 (1949): 1504-08.
78. Miki, N., M. Maeno, K. Maruhashi, and T. Ohmi. "Vapor-Liquid Equilibrium of the Binary System HF-H<sub>2</sub>O Extending to Extremely Anhydrous Hydrogen Fluoride." *J. Electrochem. Soc.* 137, no. 3 (Mar 1990): 787-90.

79. Laidler, Keith J. *Reaction Kinetics: Homogeneous Gas Reactions*. Vol. 1, New York: Pergamon, 2013.
80. Johnson, Timothy J., Steven W. Sharpe, and Matthew A. Covert. "Disseminator for Rapid, Selectable, and Quantitative Delivery of low and Semivolatile Liquid Species to the Vapor Phase." *Rev. Sci. Instrum.* 77, no. 9 (2006): 094103.
81. ———. "Erratum: "Disseminator for Rapid, Selectable, and Quantitative Delivery of Low- and Semi-volatile Liquid Species to the Vapor Phase." *Rev. Sci. Instrum.* 78 (2007): 019902-1.
82. Wormald, C. J. "A New Gas Phase Flow Mixing Calorimeter: Test Measurements on (Nitrogen + Cyclohexane)." *J. Chem. Thermodyn.* 29, no. 6 (Jun 1997): 701-14.
83. Redington, Richard L. "Nonideal-Associated Vapor Analysis of Hydrogen Fluoride." *J. Phys. Chem.* 86 (1982): 552-60.
84. ———. "Infrared Absorbance of Hydrogen Fluoride Oligomers." *J. Phys. Chem.* 86 (1982): 561-63.
85. Sun, Huai, Robert O. Watts, and U. Buck. "The Infrared Spectrum and Structure of Hydrogen Fluoride Clusters and the Liquid: Semiclassical and Classical Studies." *J. Chem. Phys.* 96, no. 3 (Feb 1 1992): 1810-21.
86. Quack, Martin, Ulrich Schmitt, and Martin A. Suhm. "FTIR Spectroscopy of Hydrogen Fluoride Clusters in Synchronously Pulsed Supersonic Jets. Isotopic Isolation, Substitution and 3-d Condensation." *Chemical Physics Letters* 269, no. 1-2 (Apr 25 1997): 29-38.
87. Blake, Thomas A., Steven W. Sharpe, and Sotiris S. Xantheas. "Rotationally Resolved Spectroscopy of a Librational Fundamental Band of Hydrogen Fluoride Tetramer." *J. Chem. Phys.* 113, no. 2 (2000): 707-18.
88. Twu, Chong H., John E. Coon, and John R. Cunningham. "An Equation of State for Hydrogen Fluoride." *Fluid Phase Equilibria* 86 (1993): 47-62.
89. Economou, Ioannis G., and Cor J. Peters. "Phase Equilibria Prediction of Hydrogen Fluoride Systems from an Associating Model." *Ind. Eng. Chem. Res.* 34, no. 5 (May 1995): 1868-72.
90. Visco, Jr. Donald P. , and David A. Kofke. "Improved Thermodynamic Equation of State for Hydrogen Fluoride." *Ind. Eng. Chem. Res.* 38 (1999): 4125-29.
91. ———. "Erratum : "Improved Thermodynamic Equation of State for Hydrogen Fluoride"." *Ind. Eng. Chem. Res.* 39 (1999): 242.
92. Wierzchowski, Scott J., and David A. Kofke. "Fugacity Coefficients of Saturated Water from Molecular Simulation." *Ind. Eng. Chem. Res.* (2003): 12808-13.
93. ———. "Liquid-Phase Activity Coefficients for Saturated HF/H<sub>2</sub>O Mixtures with Vapor-Phase Nonidealities Described by Molecular Simulation." *Ind. Eng. Chem. Res.* 43, no. 1 (Jan 7 2004): 218-27.

## Appendix A

### Pacific Northwest National Laboratory Hydrogen Fluoride First Aid, Handling, and Monitoring Procedures

#### Hydrofluoric Acid (HF)

##### First aid for EYE contact with HF:

1. **Do not apply calcium gluconate gel to the affected EYE.**
2. Flush the affected EYE with copious quantities of water or dilute saline solution for at least 15 minutes while holding eyelids open.
3. Obtain immediate medical attention and treatment.

Hydrofluoric acid (HF) is very corrosive and presents a special hazard because of its unique health hazard properties. Hydrofluoric acid solution can produce serious health effects by any route of exposure. These effects are due to the fluoride ion's aggressive and destructive penetration of tissues. HF readily penetrates the skin and can cause both local cellular destruction of deep tissue layers (including the bone) as well as systemic toxicity by hypocalcemia. Unlike other acids which neutralize rapidly, this process may continue for days if untreated. Both liquid and vapor can cause severe burns to all parts of the body and quickly destroy the corneas of the eyes. Do not breathe HF acid vapor even for a very short time; the fumes can cause severe damage to the respiratory system. Therefore, all work with HF, including opening new packages, must be performed inside a fume hood and away from worker's breathing zone to minimize inhalation. Wear Chemical Goggles and Flexible Laminate Silver Shield gloves for maximum protection (Neoprene or Nitrile Gloves as minimum personal protective equipment (PPE) to reduce skin exposure).

If you are exposed to HF, regardless of the concentration, rinse the affected area with copious quantities of water for at least 15 minutes. Exposure to even a dilute concentration of HF may result in serious and delayed symptoms and **REQUIRES IMMEDIATE TREATMENT WITH CALCIUM GLUCONATE GEL/CREAM** and prompt medical attention from a health provider for advanced treatment (e.g., intravenous injection with 10% solution of sodium gluconate or its administration using a nebulizer). Dilute solution of HF allows deeper penetration of the non-dissociated HF acid, more severe burn, and delayed injuries and symptoms. Calcium gluconate gel/cream is an antidote that helps neutralize the HF acid burns on the skin. All lab users must read and thoroughly understand this information and the hazards associated with HF as well as discuss the hazards with the cognizant space manager (CSM) before working in this space. Please contact the CSM for location of container of calcium gluconate gel.

Note: Establish a designated work area (e.g., fume hood, section of the lab, or the entire lab) and post a "Danger" sign for [Hydrofluoric Acid](#).

**Additional severity and extent of risk information:**

\*\*\*\*\*  
FIRST AID STEPS AND ADDITIONAL MEDICAL INSTRUCTIONS FOR HF EXPOSURE  
\*\*\*\*\*

**SKIN CONTACT**

1. Move victim immediately under safety shower or other water source and flush affected area thoroughly with large amounts of running water.
2. Call 375-2400 ASAP. Communicate the following information to 375-2400:
  - a. Report a potential life-threatening HF skin exposure
  - b. Request an immediate 911/ambulance response
3. Remove all contaminated clothing while continuing to flush with water.
4. After five minutes stop rinsing the affected area. Don surgical gloves, then apply calcium gluconate gel to affected skin area. Massage gel into the skin continuously until emergency medical assistance arrives.

**INHALATION**

1. Immediately move victim to fresh air
2. Call 375-2400 ASAP. Communicate the following information to 375-2400:
  - a. Report a potential life-threatening HF inhalation exposure
  - b. Request an immediate 911/ambulance response
3. Keep victim warm, quiet and comfortable until medical assistance arrives.
4. The Hanford/Richland Fire Departments carry calcium gluconate nebulizers.

**EYE CONTACT**

1. Immediately flush the eyes for at least 15 minutes with large amounts of gently flowing water. Hold the eyelids open and away from the eye during irrigation to allow thorough flushing of the eyes.
2. Call 375-2400 ASAP. Communicate the following information to 375-2400:
  - a. Report an HF eye exposure
  - b. Request an immediate 911/ambulance response

Anhydrous hydrogen fluoride (corrosive and toxic) will be used for spectroscopic experiments in this lab space. The hydrogen fluoride is stored in a cylinder located in a ventilated and sprinklered cabinet located in the RTL/520 West Service Corridor directly behind the laboratory. Hydrogen fluoride gas runs from the cylinder through a cross purge regulator manifold, through 1/4" diameter stainless steel tubing with welded joints into the laboratory. This tubing line terminates at a valve located in a ventilated cabinet that is attached to a manifold stand. From the cabinet, another 1/4" stainless steel line brings the hydrogen fluoride gas into a gas manifold where it is used for experiments. For most experiments, less than a Torr-liter will be used. Once used the gas will be exhausted through a vacuum manifold and out through a small diffusion pump and mechanical pump. There is an alumina bead trap in line in front of the

mechanical pump. The pump exhaust goes out through the lab's exhaust ventilation system.

There is no affordable, reliable, continuous air monitoring system for hydrogen fluoride. The odor threshold for hydrogen fluoride is 0.04 ppm. The odor is described as strong, pungent and irritating. Symptoms of HF exposure include irritation of the eyes, skin, nose, and throat, eye and skin burns, rhinitis, bronchitis, pulmonary edema (fluid buildup in the lungs), and bone damage. The ACGIH Threshold Limit Value-Time Weighted Average (TLV-TWA) for HF is 0.5 ppm. The ACGIH Threshold Limit Values-Ceiling. (TLV-C) is 2.0 ppm. Personnel shall not be exposed to concentrations above this ceiling under any circumstance.

Real-time exposure monitoring for HF gas is REQUIRED during the initial startup of the HF gas and IR spectrophotometer system. Modification or repair of the system with the potential to release more than trace quantities of HF gas is not allowed unless real-time HF monitoring is being performed.

During normal operations and in the absence of real-time HF monitoring, HF odor detection or the presence of a white fog (caused by HF aerosols in the air) will alert personnel to a hydrogen fluoride leak. The presence of HF odor or a white HF aerosol cloud is NOT expected and is NOT within the work scope of this permit

Upon sensing the odor or seeing the cloud the lab space should be immediately evacuated and 375-2400 should be called. If possible and if it is safe to do so, the valve on the hydrogen fluoride cylinder in the cabinet in the Service Corridor should be closed.

Tubes of calcium gluconate are at the hydrogen fluoride gas handling manifold in room 336, near the gas cabinet in the service corridor behind room 336, and in the chemical cabinet on the west wall in room 336. The gluconate is for skin contact. A sheet with HF first aid measures shall be placed near the work area and in the vicinity of the calcium gluconate supplies.

## Appendix B

### MATLAB Codes for Data Handling and Processing

The MATLAB code given in this Appendix was used to process the water-hydrogen fluoride decay spectra.

```
% PROCESS_HFH2O_SPECTRA3.M
% This script automates the processing of HF-H2O spectra
% The spectra are baseline corrected, and peak areas are computed so
that
% the change in HF and H2O lines can be computed.
%
% Chris Thompson
% 10/8/16

% Prompt the user for data
%hf_press=input('Enter the HF pressure (Torr):');
%h2o_init_press=input('Enter the H2O pressure (Torr):');
%man_init_press=input('Enter the H2O/N2 pressure (Torr) before
expansion into the cell:');
%final_press=input('Enter the final pressure (Torr) after adding
H2O/N2 to the cell:');

%spec_num=input('Enter the spectrum index (column of spec):');

% Load std HF and H2O spectra
%load 'C:\Chris\DATA\FTIR\2016\HF and H2O Subtraction
Spectra\hf_h2o_std_spectra.mat'

% Prompt user for which std spectra & pressures to use for comparison
%hf_stdspec=input('Enter the std HF spectrum (baseline corrected):');
%hf_stdpress=input('Enter the std HF pressure:');
%h2o_stdspec=input('Enter the std H2O spectrum (baseline
corrected):');
%h2o_stdpress=input('Enter the std H2O pressure:');

% Baseline correct mixture spectra
```

```

%mixb=ir_slope_corr2(real(spec(:,spec_num)),wav,3400,3410,4290,4300);
%mixb2=ir_slope_corr2(mixb,wav,1200,1250,2150,2200);
specb=ir_slope_corr2(real(spec),wav,3400,3410,4290,4300);
specb2=ir_slope_corr2(specb,wav,1200,1250,2150,2200);

% Scale std HF spectrum
%hf_stdspec_scaled=hf_stdspec*hf_press/hf_stdpress;

% Calculate the H2O partial pressure
% Transfer percentage of 0.6925 is based on experiments where H2O/N2
% was added to the H2O manifold, allowed to mix for 1 hr, and then
% expanded into the cell. Resulting spectral peak areas were compared
to
% those from measurements where H2O was added directly to the cell and
then
% pressurized with N2.
%h2o_press=h2o_init_press*final_press/man_init_press*.6925;

% Scale std H2O spectrum
%h2o_stdspec_scaled=h2o_stdspec*h2o_press/h2o_stdpress;

% Loop through the matrix of spectra & integrate HF and H2O lines
% Preallocate variable to hold peak areas and max absorbances for HF
[r,num]=size(spec);
area_4230=zeros(num,1);
max_abs_4230=zeros(num,1);
area_4203=zeros(num,1);
max_abs_4203=zeros(num,1);
area_4174=zeros(num,1);
max_abs_4174=zeros(num,1);
area_3837=zeros(num,1);
area_3816=zeros(num,1);
area_1717=zeros(num,1);
area_1695=zeros(num,1);

for i=1:num
    % Peak area for HF line at 4230.7
    i1=62544;
    i2=62548;
    area_4230(i)=trapz(flipud(wav(i1:i2)),flipud(specb2(i1:i2,i)));
    max_abs_4230(i)=max(real(specb2(i1:i2,i)));

    % Peak area for HF line at 4203.3
    i1=62998;
    i2=63005;
    area_4203(i)=trapz(flipud(wav(i1:i2)),flipud(specb2(i1:i2,i)));
    max_abs_4203(i)=max(real(specb2(i1:i2,i)));

    % Peak area for HF line at 4174.0
    i1=63480;
    i2=63495;
    area_4174(i)=trapz(flipud(wav(i1:i2)),flipud(specb2(i1:i2,i)));

```

```

max_abs_4174(i)=max(real(specb2(i1:i2,i)));

% Peak area for H2O line at 3837.9
i1=69050;
i2=69080;
area_3837(i)=trapz(flipud(wav(i1:i2)),flipud(specb2(i1:i2,i)));

% Peak area for H2O line at 3816.1
i1=69410;
i2=69445;
area_3816(i)=trapz(flipud(wav(i1:i2)),flipud(specb2(i1:i2,i)));

% Peak area for H2O line at 1717.4
i1=104240;
i2=104260;
area_1717(i)=trapz(flipud(wav(i1:i2)),flipud(specb2(i1:i2,i)));

% Peak area for H2O line at 1695.9
i1=104595;
i2=104620;
area_1695(i)=trapz(flipud(wav(i1:i2)),flipud(specb2(i1:i2,i)));
end

% Calculate changes in peak areas using 2 approaches:
%   a) change relative to the 1st spectrum
%   b) change relative to the spectrum with the max peak area
% Preallocate variables for storing percent changes of peak areas
pchange_4230_1=zeros(num,1);
pchange_4230_max=zeros(num,1);
pchange_4203_1=zeros(num,1);
pchange_4203_max=zeros(num,1);
pchange_4174_1=zeros(num,1);
pchange_4174_max=zeros(num,1);
pchange_3837_1=zeros(num,1);
pchange_3837_max=zeros(num,1);
pchange_3816_1=zeros(num,1);
pchange_3816_max=zeros(num,1);
pchange_1717_1=zeros(num,1);
pchange_1717_max=zeros(num,1);
pchange_1695_1=zeros(num,1);
pchange_1695_max=zeros(num,1);
for i=1:num
    pchange_4230_1(i)=(area_4230(i)-area_4230(1))/area_4230(1)*100;
    pchange_4230_max(i)=(area_4230(i)-
max(area_4230))/max(area_4230)*100;
    pchange_4203_1(i)=(area_4203(i)-area_4203(1))/area_4203(1)*100;
    pchange_4203_max(i)=(area_4203(i)-
max(area_4203))/max(area_4203)*100;
    pchange_4174_1(i)=(area_4174(i)-area_4174(1))/area_4174(1)*100;
    pchange_4174_max(i)=(area_4174(i)-
max(area_4174))/max(area_4174)*100;

```

```

    pchange_3837_1(i)=(area_3837(i)-area_3837(1))/area_3837(1)*100;
    pchange_3837_max(i)=(area_3837(i)-
max(area_3837))/max(area_3837)*100;
    pchange_3816_1(i)=(area_3816(i)-area_3816(1))/area_3816(1)*100;
    pchange_3816_max(i)=(area_3816(i)-
max(area_3816))/max(area_3816)*100;
    pchange_1717_1(i)=(area_1717(i)-area_1717(1))/area_1717(1)*100;
    pchange_1717_max(i)=(area_1717(i)-
max(area_1717))/max(area_1717)*100;
    pchange_1695_1(i)=(area_1695(i)-area_1695(1))/area_1695(1)*100;
    pchange_1695_max(i)=(area_1695(i)-
max(area_1695))/max(area_1695)*100;
end
spectrum_count = (1:num)';

% % Calculate changes in peak areas
% pchange_4230=(mix_area_4230-hf_area_4230)/hf_area_4230*100;
% pchange_4203=(mix_area_4203-hf_area_4203)/hf_area_4203*100;
% pchange_4174=(mix_area_4174-hf_area_4174)/hf_area_4174*100;
% pchange_3837=(mix_area_3837-h2o_area_3837)/h2o_area_3837*100;
% pchange_3816=(mix_area_3816-h2o_area_3816)/h2o_area_3816*100;
% pchange_1717=(mix_area_1717-h2o_area_1717)/h2o_area_1717*100;
% pchange_1695=(mix_area_1695-h2o_area_1695)/h2o_area_1695*100;
%
% Setup variable for copying data to Excel
excel=[spectrum_count (t/60)' area_4230 pchange_4230_1
pchange_4230_max max_abs_4230 ...
    area_4203 pchange_4203_1 pchange_4203_max max_abs_4203 ...
    area_4174 pchange_4174_1 pchange_4174_max max_abs_4174 ...
    area_3837 pchange_3837_1 pchange_3837_max ...
    area_3816 pchange_3816_1 pchange_3816_max ...
    area_1717 pchange_1717_1 pchange_1717_max...
    area_1695 pchange_1695_1 pchange_1695_max];

% Plot decay curves for visual confirmation
figure(1)
subplot(221)
plot(t/60,area_4230,'.')
grid
xlabel('Time (hr)')
ylabel('Peak Area')
title('HF 4230.7 cm-1')

subplot(222)
plot(t/60,area_4203,'.')
grid
xlabel('Time (hr)')
ylabel('Peak Area')
title('HF 4203.3 cm-1')

subplot(223)
plot(t/60,area_4174,'.')

```

```

grid
xlabel('Time (hr)')
ylabel('Peak Area')
title('HF 4174.0 cm-1')

figure(2)
subplot(221)
plot(t/60,area_3837,'.')
grid
xlabel('Time (hr)')
ylabel('Peak Area')
title('H2O 3837.9 cm-1')

subplot(222)
plot(t/60,area_3816,'.')
grid
xlabel('Time (hr)')
ylabel('Peak Area')
title('H2O 3816.1 cm-1')

subplot(223)
plot(t/60,area_1717,'.')
grid
xlabel('Time (hr)')
ylabel('Peak Area')
title('H2O 1717.4 cm-1')

subplot(224)
plot(t/60,area_1695,'.')
grid
xlabel('Time (hr)')
ylabel('Peak Area')
title('H2O 1695.9 cm-1')

disp('Done! Results are stored in the variable 'excel'')
% h2o_press
% disp(' ')
% disp('Percent change in 3 HF & 4 H2O lines:')
%
% [pchange_4230 pchange_4203 pchange_4174 pchange_3837 pchange_3816
pchange_1717 pchange_1695]
%
% %clear hf_press spec_num mixb mixb2 hf_stdspec_scaled i1 i2
% %clear h2o_stdspec_scaled h2o_press h2o_init_press man_init_press
final_press
% %clear hf_stdspec hf_stdpress h2o_stdspec h2o_stdpress

```

```

function corr_spec = ir_slope_corr2(spec,wav,w1,w2,w3,w4)
% IR_SLOPE_CORR Linear slope baseline correction for FTIR spectra.
% This function performs a sloped, linear baseline correction of
% FTIR spectra. The line to be subtracted from each spectrum is
% calculated using a least squares fit of the absorbances from
% 2 specified regions of the input spectra. The regions are
specified
% in terms of wavenumbers (e.g., 2600-2620 and 3870-3924 cm-1).
% Note: The subtraction is performed over the specified wavenumber
% region only. Data outside this region is not altered.
%
% Usage: corr_spec = ir_slope_corr(spec,wav,w1,w2,w3,w4)
%         spec = matrix of spectra (in columns) to be corrected
%         wav = vector of wavenumbers for the spectra
%         w1 - w4 = wavenumbers bounding the regions for the
%                 calculated least-squares fit
% Chris Thompson
% 3/22/11
% Last modified 5/3/16

% Add several checks to make sure input arguments are valid
% Check for proper number of arguments
% Verify that wav and spec have the same number of rows
% Verify that w1 - w4 are unique and are in ascending order

% Determine the ordering of the wavenumber vector (descending or
ascending)
numwavs = length(wav);
low2high = wav(1) < wav(numwavs);
% This function was originally designed to work with spectra in
descending
% order. If the spectra are in ascending order, rearrange the data
if low2high
    wav = flipud(wav);
    spec = flipud(spec);
end

% Begin by getting the indices of the wavenumber boundaries
i1 = min(find(wav<w4));
i2 = min(find(wav<w3));
i3 = min(find(wav<w2));
i4 = min(find(wav<w1));
% Verify that i1 - i4 are populated (i.e., each wavenumber specified
% exists in the wavenumber vector. Later, logic could be used to
% locate the closest wavenumber
if isempty(i1)
    error('wavenumber vector does not contain an exact match for w4
argument (%d)', w4);
end
if isempty(i2)
    error('wavenumber vector does not contain an exact match for w3
argument (%d)', w3);

```

```

end
if isempty(i3)
    error('wavenumber vector does not contain an exact match for w2
argument (%d)', w2);
end
if isempty(i4)
    error('wavenumber vector does not contain an exact match for w1
argument (%d)', w1);
end

% Set up truncated vector of wavenumbers for the least-squares fit
w=[wav(i1:i2)' wav(i3:i4)']';

% Set up a matrix of absorbance data (a) to use for the least-squares
fit
[r,c]=size(spec);
a=zeros(length(w),c);
for i=1:c
    a(:,i)=[spec(i1:i2,i)' spec(i3:i4,i)']';
end

% Calculate least squares fit for each spectrum in spec
% Store in a new matrix (p)
p=zeros(2,c);
for i=1:c
    p(:,i)=polyfit(w,a(:,i),1);
end

% Calculate the values to subtract from each spectrum
% Store in a new matrix
offset = zeros(size(spec));
for i=1:c
    offset(i1:i4,i) = polyval(p(:,i),wav(i1:i4));
end

% Finally, calculate the corrected spectra
corr_spec=zeros(size(spec));
corr_spec = spec - offset;
% Rearrange the wavenumber ordering if necessary
if low2high
    corr_spec = flipud(corr_spec);
end
end

```

## **Appendix C**

### **HF and Water Vapor Decay Curve Plots**

The decay curves and experimental conditions for the hydrogen fluoride-water experiments summarized in Table 3.5 are presented in this Appendix.

**Table C.1** Experimental conditions for measurements recorded at 25 °C on August 8, 2016.<sup>1</sup>

Partial Pressures (Torr)				
HF	H <sub>2</sub> O (Corrected) <sup>2</sup>	H <sub>2</sub> O (Initial)	H <sub>2</sub> O/N <sub>2</sub> (before release)	Final Pressure
0.4833	0.9882	1.64	874.28	760.76

<sup>1</sup> Original spectrum 28 was omitted due to unusual wavy shape (possible interferometer glitch).

<sup>2</sup> Transfer factor is 0.6925 (see text for details).

**Figure C.1** Decay curves for measurements recorded at 25 °C on August 8, 2016.

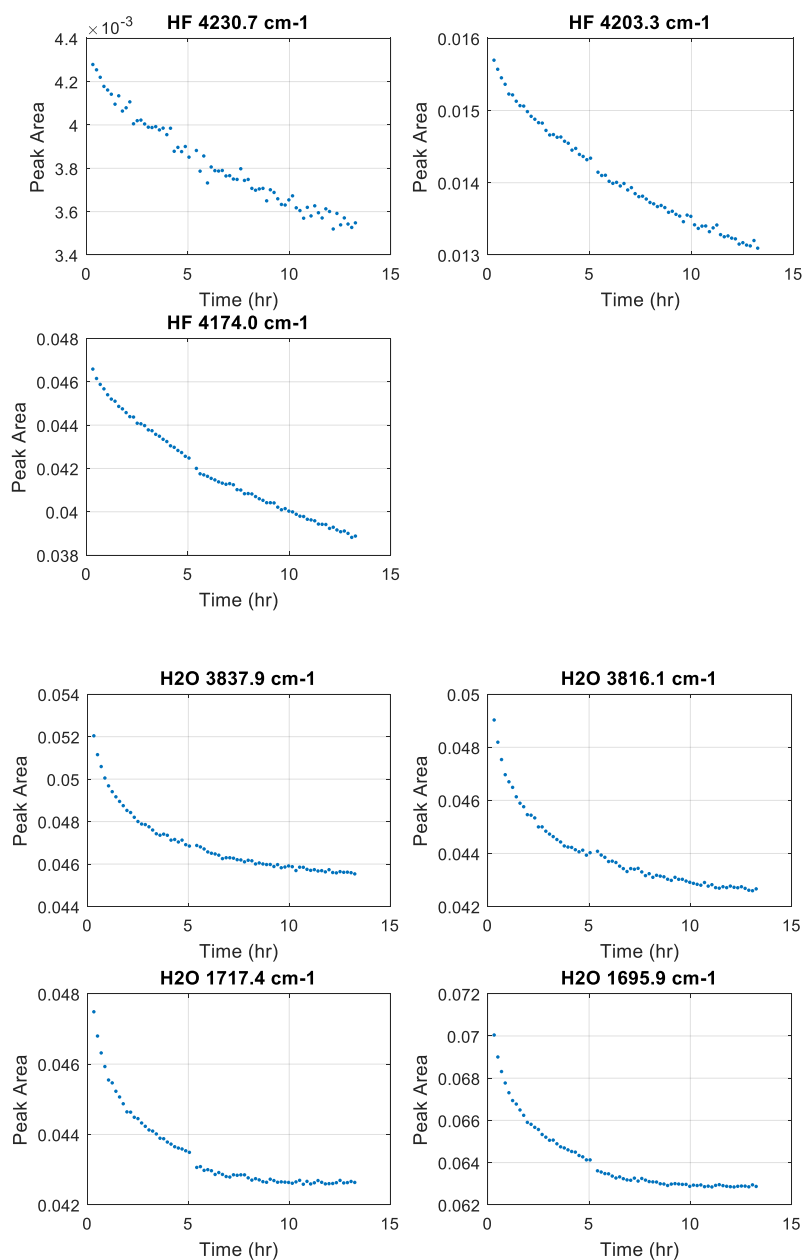


**Table C.2** Experimental conditions for measurements recorded at 25 °C on August 5, 2016.

Partial Pressures (Torr)				
HF	H <sub>2</sub> O (Corrected) <sup>1</sup>	H <sub>2</sub> O (Initial)	H <sub>2</sub> O/N <sub>2</sub> (before release)	Final Pressure
0.57748	2.4605	4.08	873.97	761.11

<sup>1</sup> Transfer factor is 0.6925 (see text for details).

**Figure C.2** Decay curves for measurements recorded at 25 °C on August 5, 2016.

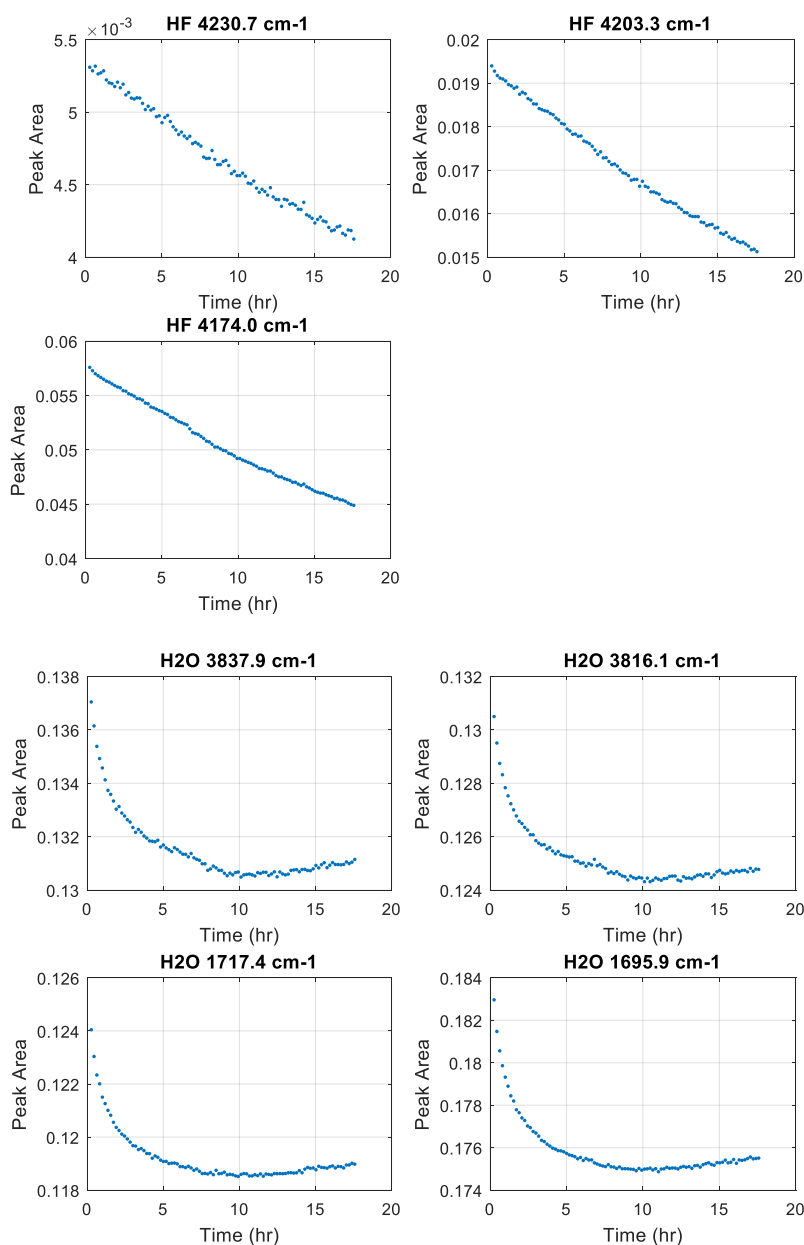


**Table C.3** Experimental conditions for measurements recorded at 25 °C on July 21, 2016.<sup>1</sup>

Partial Pressures (Torr)				
HF	H <sub>2</sub> O (Corrected) <sup>2</sup>	H <sub>2</sub> O (Initial)	H <sub>2</sub> O/N <sub>2</sub> (before release)	Final Pressure
1.034	0.9935	1.64	865.17	756.82

<sup>1</sup>Water concentrations increases for the duration of this experiment. The water concentrations were not used to estimate K.

<sup>2</sup>Transfer factor is 0.6925 (see text for details).

**Figure C.3** Decay curves for measurements recorded at 25 °C on July 21, 2016.

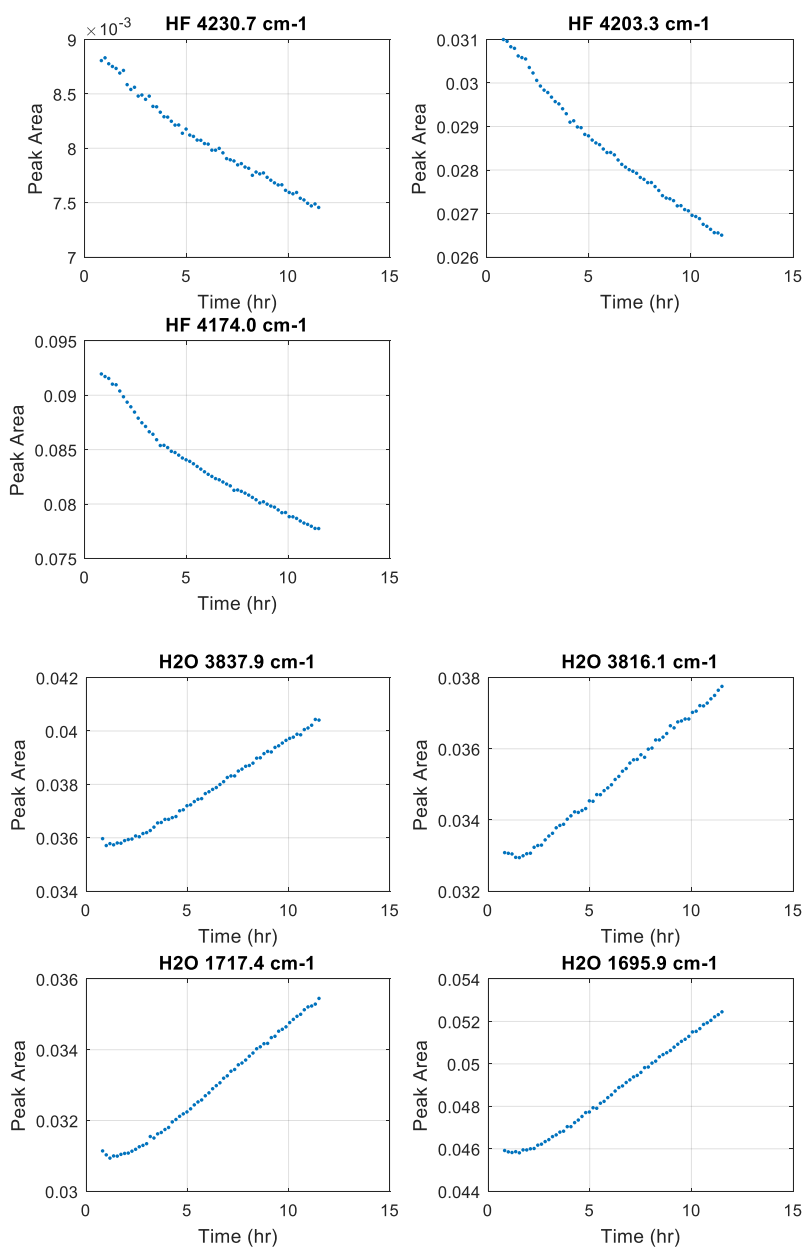


**Table C.4** Experimental conditions for measurements recorded at 25 °C on August 19, 2016.

Partial Pressures (Torr)				
HF	H <sub>2</sub> O (Corrected) <sup>1</sup>	H <sub>2</sub> O (Initial)	H <sub>2</sub> O/N <sub>2</sub> (before release)	Final Pressure
0.9723	0.9931	1.64	869.32	760.16

<sup>1</sup> Transfer factor is 0.6925 (see text for details).

**Figure C.4** Decay curves for measurements recorded at 25 °C on August 19, 2016.

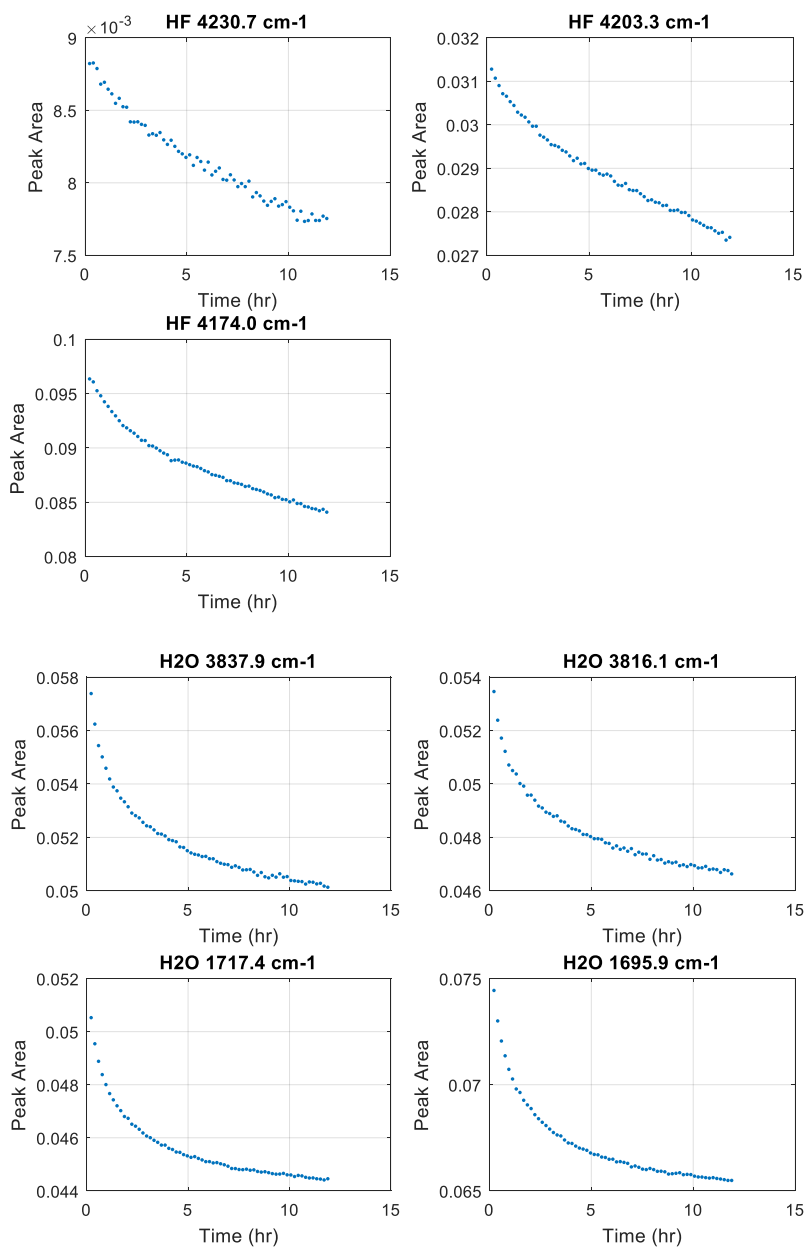


**Table C.5** Experimental conditions for measurements recorded at 25 °C on August 29, 2016.<sup>1</sup>

Partial Pressures (Torr)				
HF	H <sub>2</sub> O (Corrected) <sup>2</sup>	H <sub>2</sub> O (Initial)	H <sub>2</sub> O/N <sub>2</sub> (before release)	Final Pressure
1.06	1.0498	1.74	874.13	761.61

<sup>1</sup> H<sub>2</sub>O decay curves are oddly shaped--initial decrease for about 1 hr followed by steady increase.

The water concentration data was not used to calculate K values.

<sup>2</sup> Transfer factor is 0.6925 (see text for details).

**Figure C.5** Decay curves for measurements recorded at 25 °C on August 29, 2016.

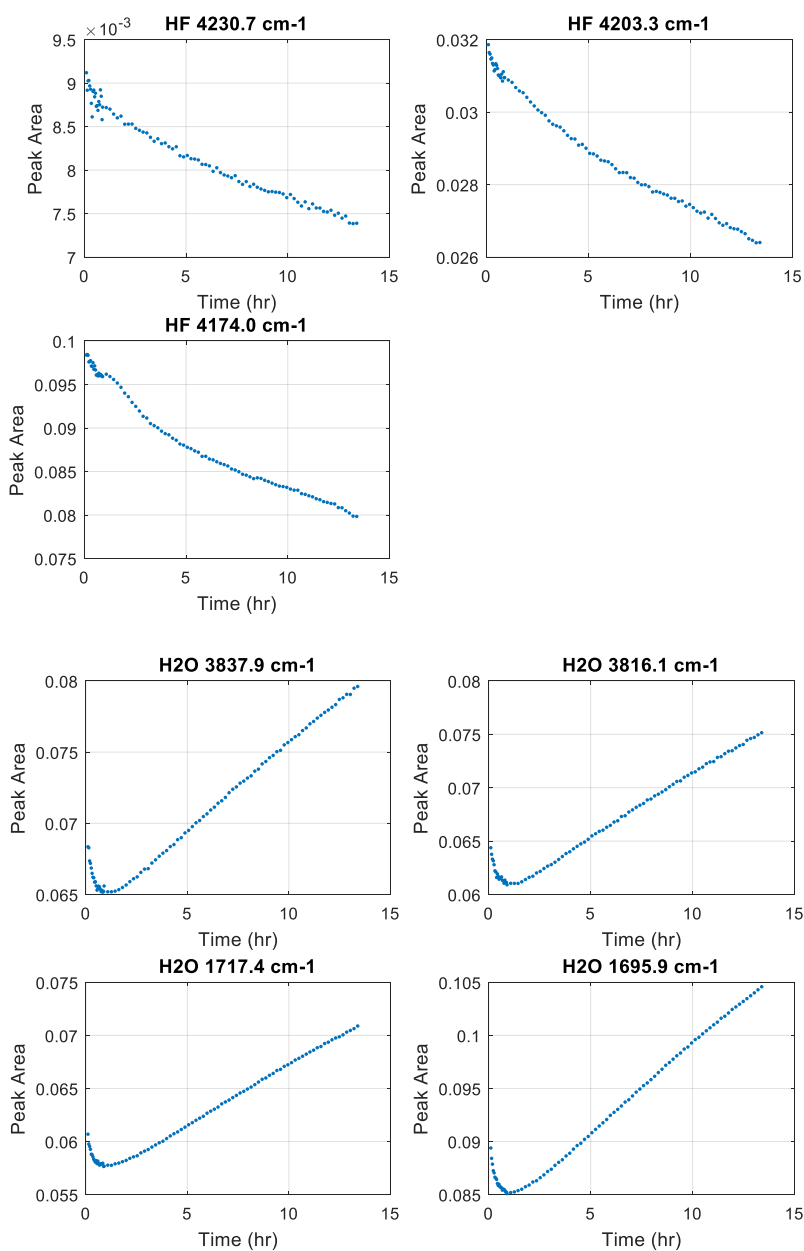


**Table C.6** Experimental conditions for measurements recorded at 25 °C on August 4, 2016.

Partial Pressures (Torr)				
HF	H <sub>2</sub> O (Corrected) <sup>1</sup>	H <sub>2</sub> O (Initial)	H <sub>2</sub> O/N <sub>2</sub> (before release)	Final Pressure
1.012	2.4126	4	873.3	760.62

<sup>1</sup> Transfer factor is 0.6925 (see text for details).

**Figure C.6** Decay curves for measurements recorded at 25 °C on August 4, 2016.

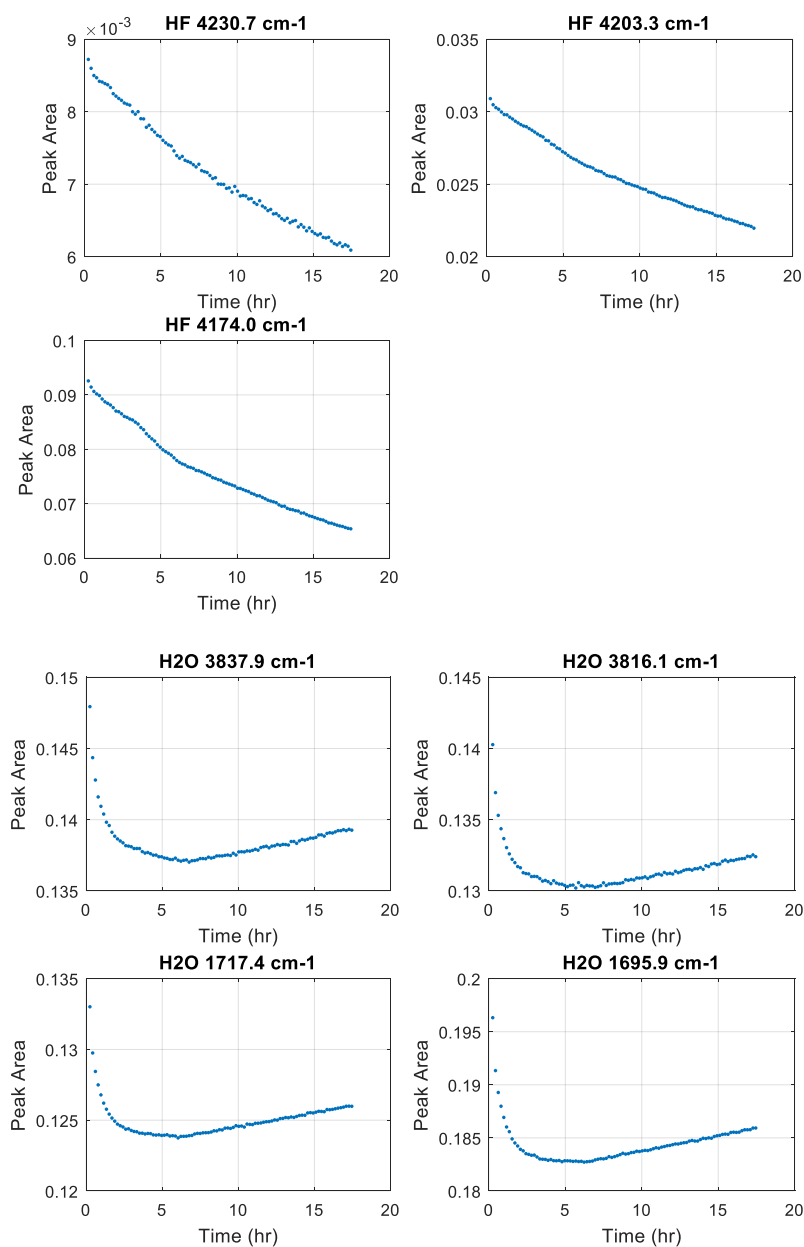


**Table C.7** Experimental conditions for measurements recorded at 25 °C on August 22, 2016.

Partial Pressures (Torr)				
HF	H <sub>2</sub> O (Corrected) <sup>1</sup>	H <sub>2</sub> O (Initial)	H <sub>2</sub> O/N <sub>2</sub> (before release)	Final Pressure
1.01198	2.4128	4	870.54	758.29

<sup>1</sup> Transfer factor is 0.6925 (see text for details).

**Figure C.7** Decay curves for measurements recorded at 25 °C on August 22, 2016.

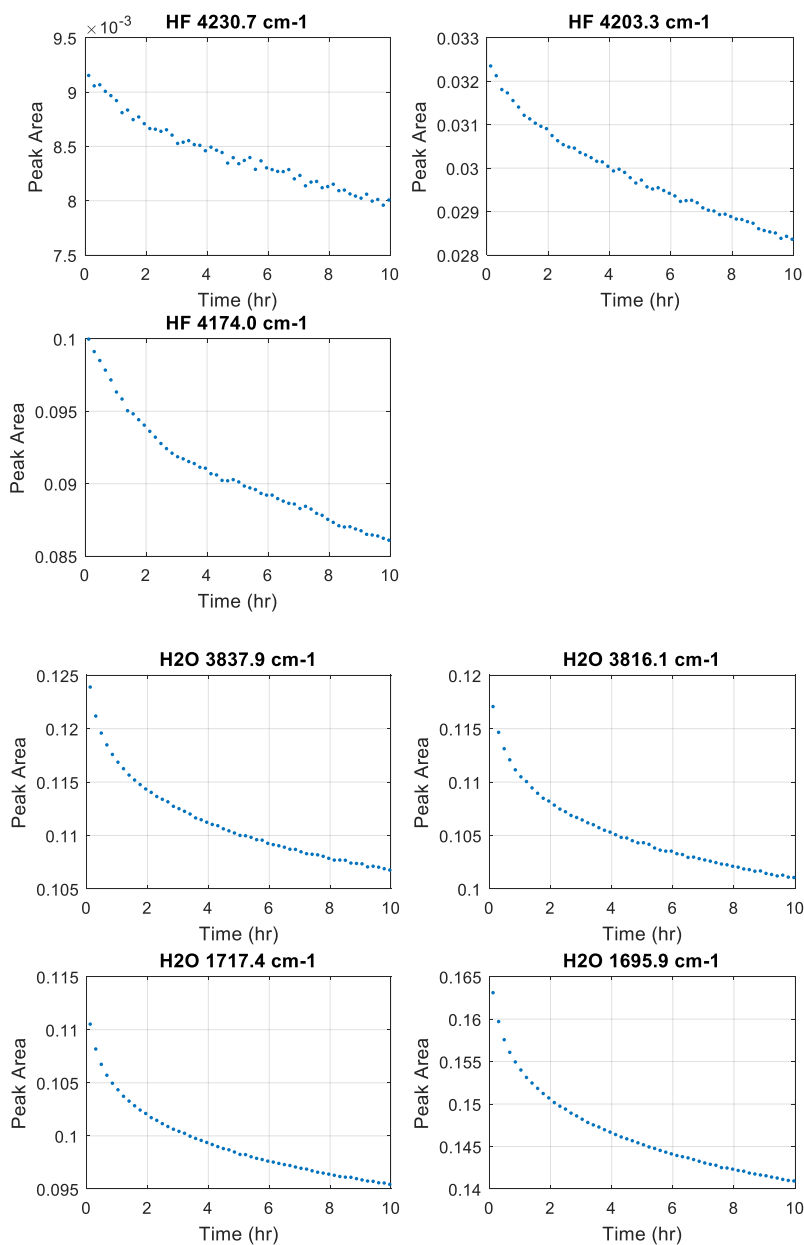


**Table C.8** Experimental conditions for measurements recorded at 25 °C on August 23, 2016.<sup>1</sup>

Partial Pressures (Torr)				
HF	H <sub>2</sub> O (Corrected) <sup>2</sup>	H <sub>2</sub> O (Initial)	H <sub>2</sub> O/N <sub>2</sub> (before release)	Final Pressure
1.01487	2.4222	4	868.36	759.32

<sup>1</sup>Delay collecting first spectrum due to interferometer malfunction.

<sup>2</sup>Transfer factor is 0.6925 (see text for details).

**Figure C.8** Decay curves for measurements recorded at 25 °C on August 23, 2016.

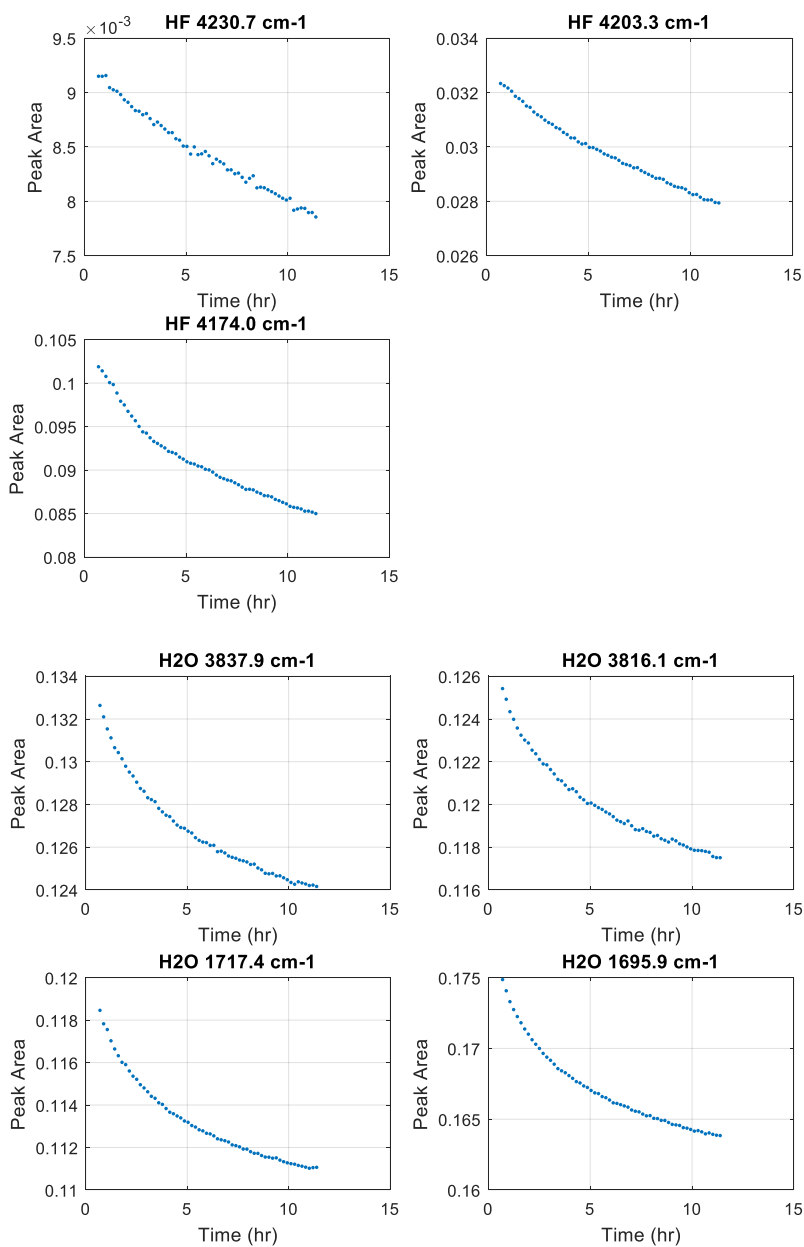


**Table C.9** Experimental conditions for measurements recorded at 25 °C on August 17, 2016.

Partial Pressures (Torr)				
HF	H <sub>2</sub> O (Corrected) <sup>1</sup>	H <sub>2</sub> O (Initial)	H <sub>2</sub> O/N <sub>2</sub> (before release)	Final Pressure
1.0066	3.9371	6.5	870.84	761.69

<sup>1</sup> Transfer factor is 0.6925 (see text for details).

**Figure C.9** Decay curves for measurements recorded at 25 °C on August 17, 2016.

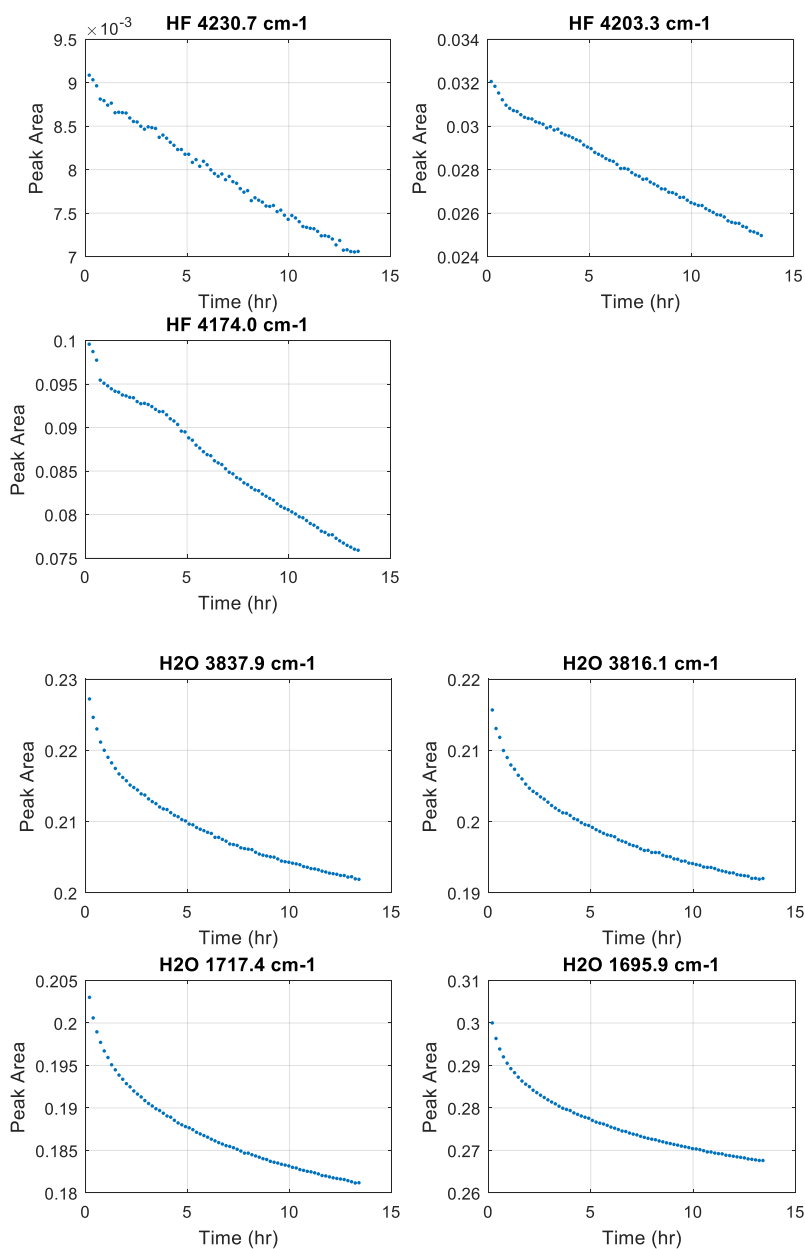


**Table C.10** Experimental conditions for measurements recorded at 25 °C on August 25, 2016.

Partial Pressures (Torr)				
HF	H <sub>2</sub> O (Corrected) <sup>1</sup>	H <sub>2</sub> O (Initial)	H <sub>2</sub> O/N <sub>2</sub> (before release)	Final Pressure
2.0147	2.4233	4	869.78	760.91

<sup>1</sup> Transfer factor is 0.6925 (see text for details).

**Figure C.10** Decay curves for measurements recorded at 25 °C on August 25, 2016.

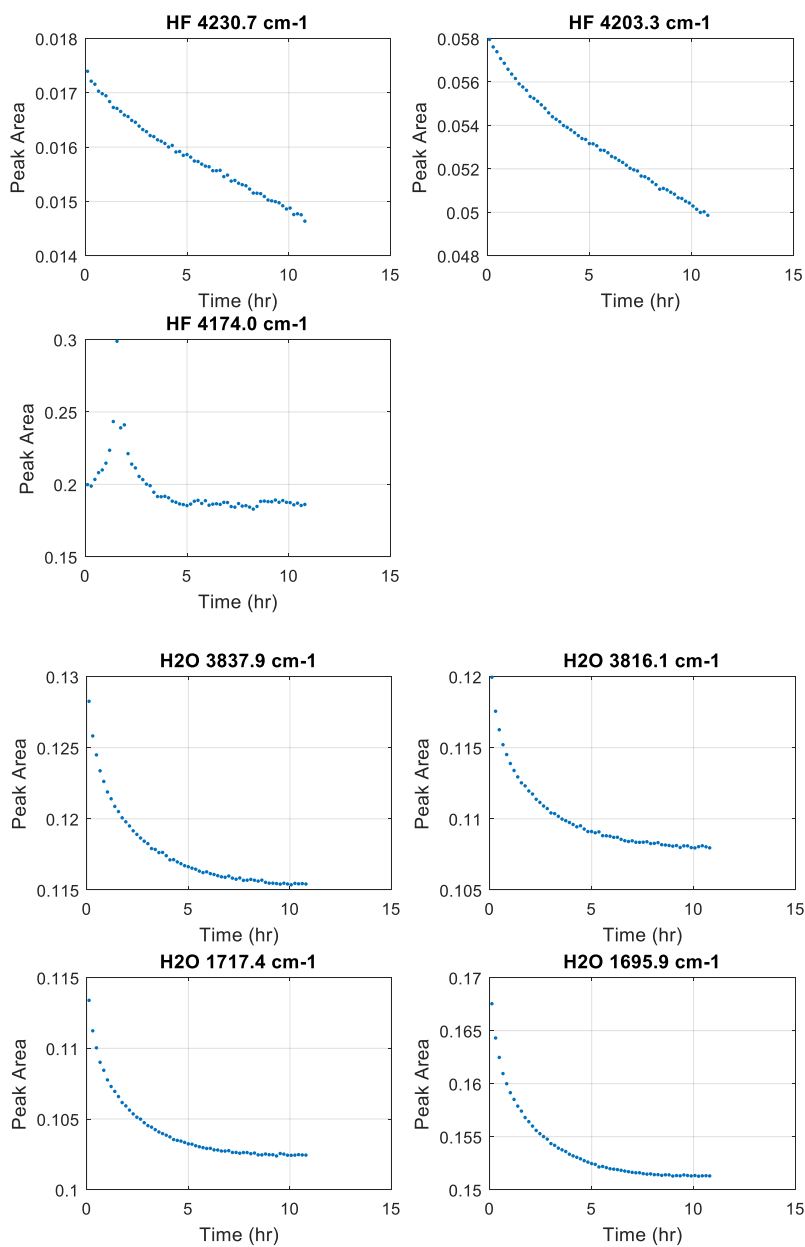


**Table C.11** Experimental conditions for measurements recorded at 25 °C on August 18, 2016.

Partial Pressures (Torr)				
HF	H <sub>2</sub> O (Corrected) <sup>1</sup>	H <sub>2</sub> O (Initial)	H <sub>2</sub> O/N <sub>2</sub> (before release)	Final Pressure
2.0218	3.9374	6.5	872.46	763.18

<sup>1</sup> Transfer factor is 0.6925 (see text for details).

**Figure C.11** Decay curves for measurements recorded at 25 °C on August 18, 2016.

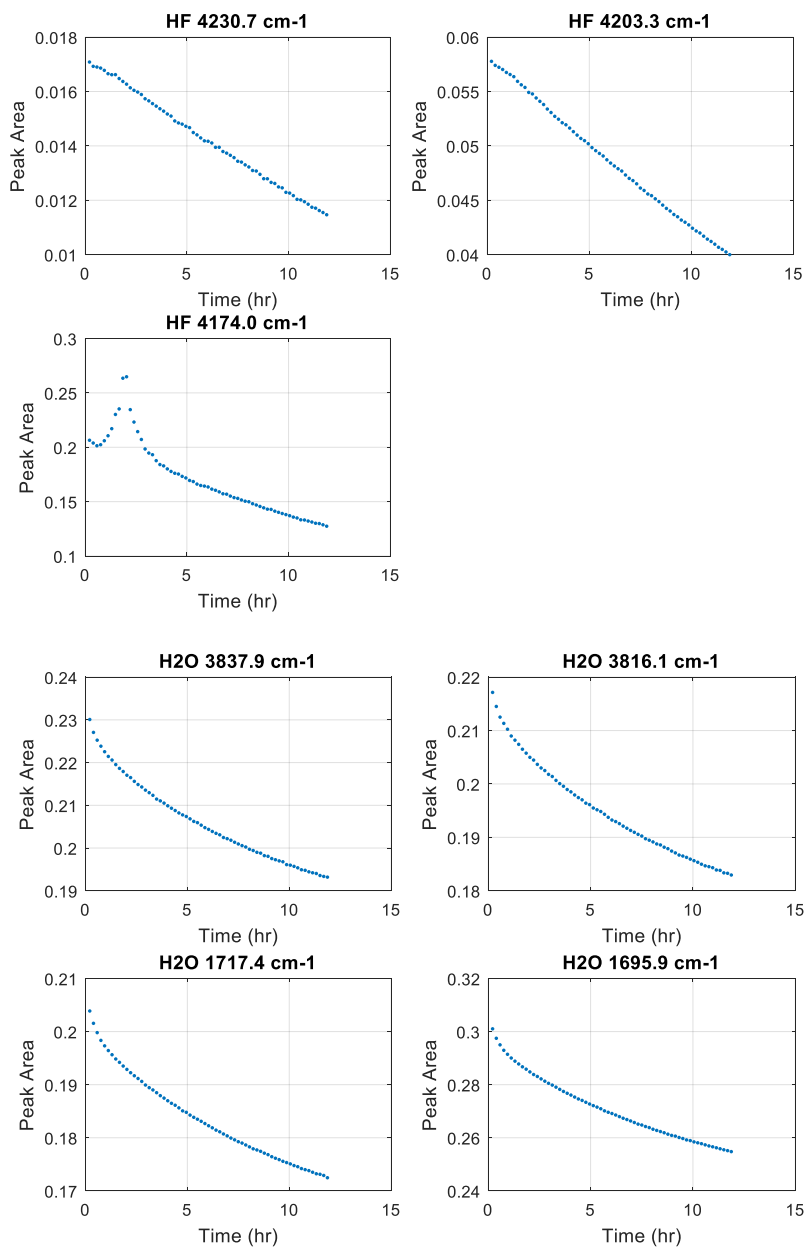


**Table C.12** Experimental conditions for measurements recorded at 25 °C on September 1, 2016.

Partial Pressures (Torr)				
HF	H <sub>2</sub> O (Corrected) <sup>1</sup>	H <sub>2</sub> O (Initial)	H <sub>2</sub> O/N <sub>2</sub> (before release)	Final Pressure
2.0175	3.9358	6.5	871.42	761.95

<sup>1</sup> Transfer factor is 0.6925 (see text for details).

**Figure C.12** Decay curves for measurements recorded at 25 °C on September 1, 2016.

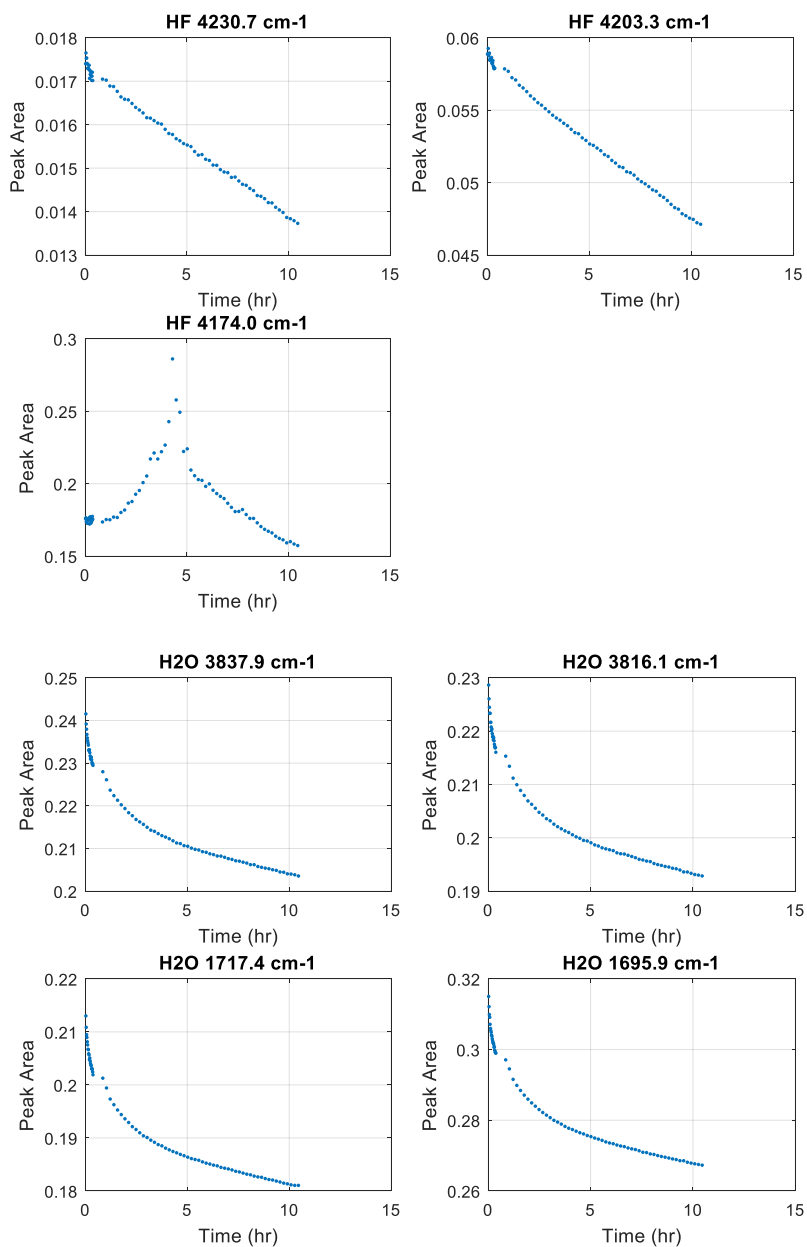


**Table C.13** Experimental conditions for measurements recorded at 25 °C on August 26, 2016.

Partial Pressures (Torr)				
HF	H <sub>2</sub> O (Corrected) <sup>1</sup>	H <sub>2</sub> O (Initial)	H <sub>2</sub> O/N <sub>2</sub> (before release)	Final Pressure
4.0102	3.9385	6.5	868.46	759.89

<sup>1</sup> Transfer factor is 0.6925 (see text for details).

**Figure C.13** Decay curves for measurements recorded at 25 °C on August 26, 2016.

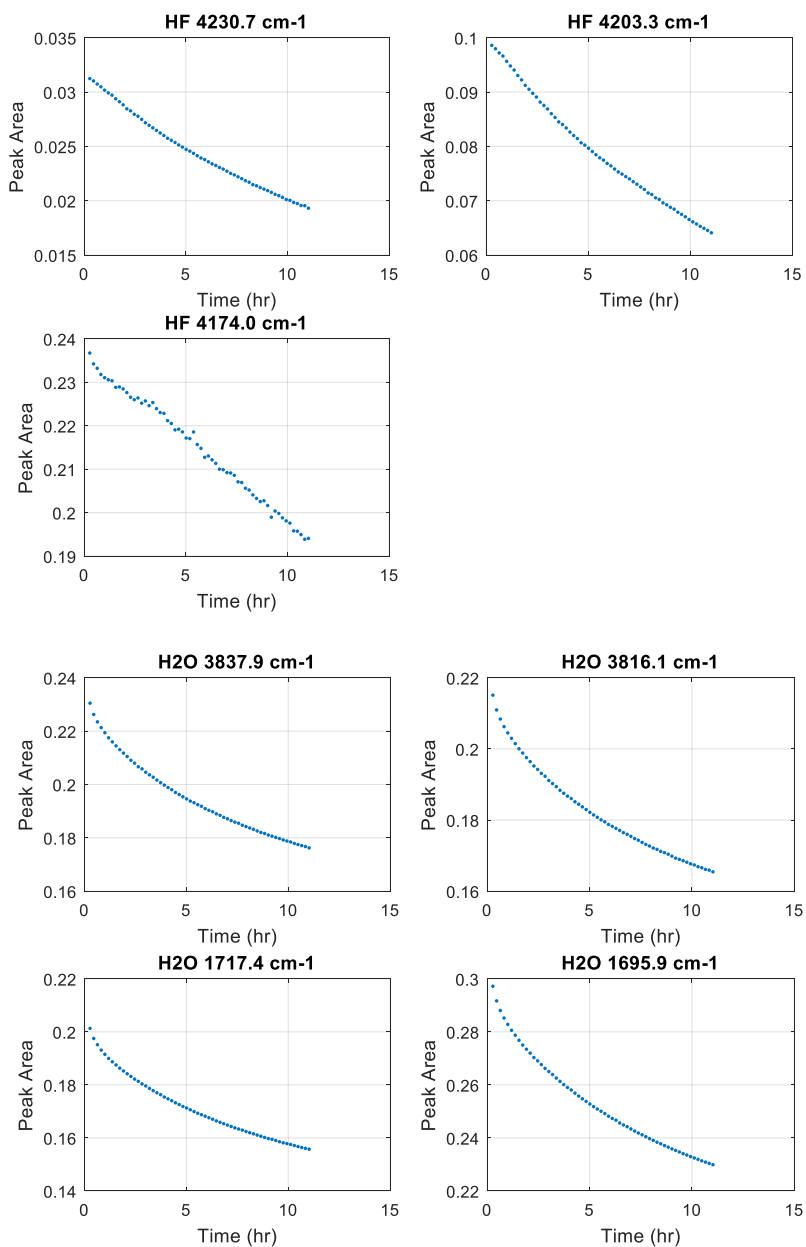


**Table C.14** Experimental conditions for measurements recorded at 25 °C on August 31, 2016.

Partial Pressures (Torr)				
HF	H <sub>2</sub> O (Corrected) <sup>1</sup>	H <sub>2</sub> O (Initial)	H <sub>2</sub> O/N <sub>2</sub> (before release)	Final Pressure
4.0114	3.9381	6.5	868.82	760.12

<sup>1</sup> Transfer factor is 0.6925 (see text for details).

**Figure C.14** Decay curves for measurements recorded at 25 °C on August 31, 2016.

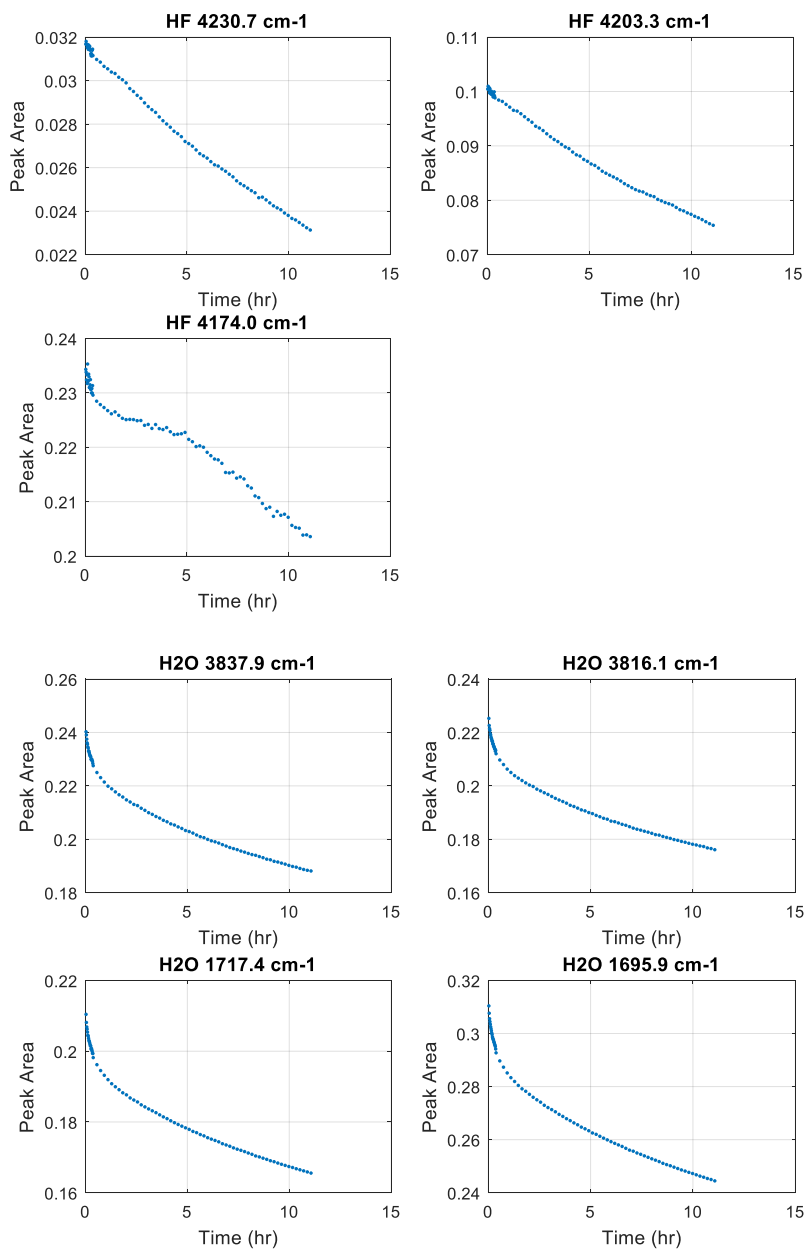


**Table C.15** Experimental conditions for measurements recorded at 10 °C on September 9, 2016.<sup>1</sup>

Partial Pressures (Torr)				
HF	H <sub>2</sub> O (Corrected) <sup>2</sup>	H <sub>2</sub> O (Initial)	H <sub>2</sub> O/N <sub>2</sub> (before release)	Final Pressure
4.0066	3.9117	6.5	873.08	758.72

<sup>1</sup>Intensities of H<sub>2</sub>O lines were about 30% lower than those in 25 and 40 °C experiments (condensation or unknown systematic error?)

<sup>2</sup>Transfer factor is 0.6925 (see text for details).

**Figure C.15** Decay curves for measurements recorded at 10 °C on September 9, 2016.

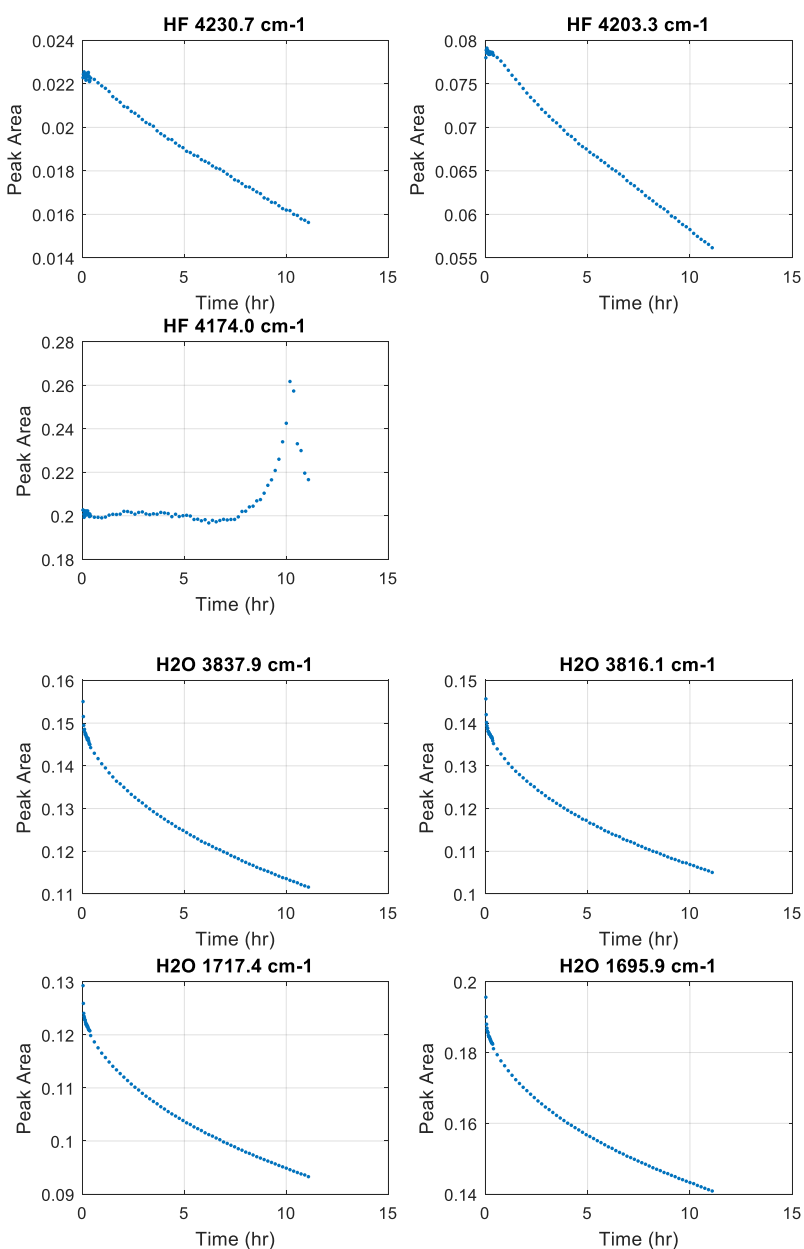
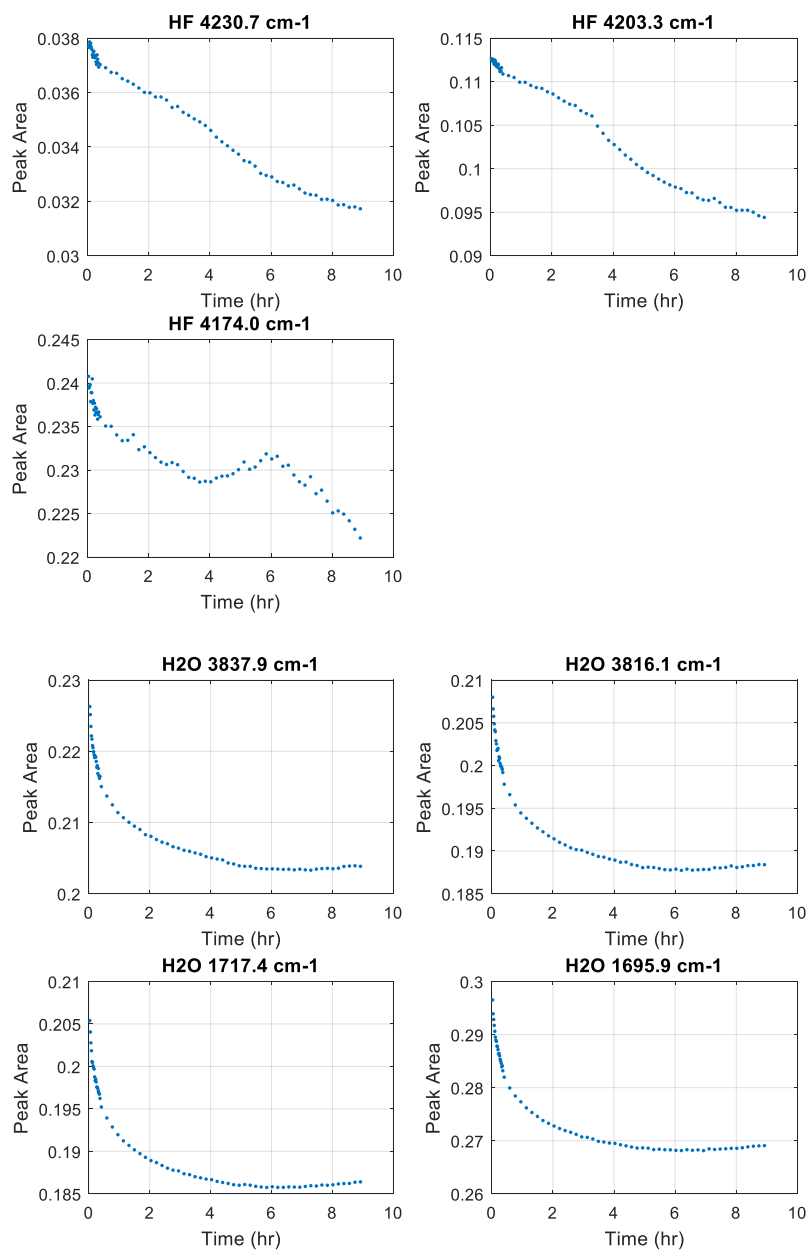


**Table C.16** Experimental conditions for measurements recorded at 40 °C on September 7, 2016.

Partial Pressures (Torr)				
HF	H <sub>2</sub> O (Corrected) <sup>1</sup>	H <sub>2</sub> O (Initial)	H <sub>2</sub> O/N <sub>2</sub> (before release)	Final Pressure
4.0015	3.9609	6.5	871.39	766.79

<sup>1</sup> Transfer factor is 0.6925 (see text for details).

**Figure C.16** Decay curves for measurements recorded at 40 °C on September 7, 2016.



## Appendix D

### Fit Parameters for HF and Water Vapor Decay Curves

Because the water decay curves shown in Appendix C show an initial fast decline followed by a slower decay, the water decay curves were fit using the double exponential decay equation given by Eq. 8. The coefficients of these fits are given in tables below. The  $\tau_1$  constant gives the slow decay time constant in hours and the  $\tau_2$  constant gives the faster decay constant, also in hours. The  $1\sigma$  uncertainty in the coefficients is also given. The hydrogen fluoride decay curves were fit to a straight line and the slope and intercept values are also given in the tables along with their  $1\sigma$  uncertainties. The slopes are in units of absorption peak area per hour. Some of the hydrogen fluoride decay curves showed some initial, rapid downward curvature, so all of these were also fit using the double exponential equation, though the uncertainties of the coefficients were typically quite large.

**Table D.1a** Experimental conditions for measurements recorded at 25 °C on August 8, 2016.<sup>1</sup>

HF	Partial Pressures (Torr)				Final Pressure
	H <sub>2</sub> O (Corrected) <sup>2</sup>	H <sub>2</sub> O (Initial)	H <sub>2</sub> O/N <sub>2</sub> (before release)		
0.4833	0.9882	1.64	874.28	760.76	

<sup>1</sup> Original spectrum 28 was omitted due to unusual wavy shape (possible interferometer glitch).<sup>2</sup> Transfer factor is 0.6925 (see text for details).**Table D.1b** Parameters from the double exponential fit of 71 data points, recorded on August 8, 2016.

		y <sub>0</sub>	A <sub>1</sub>	τ <sub>1</sub>	A <sub>2</sub>	τ <sub>2</sub>	x <sub>0</sub>	χ <sup>2</sup>
HF 4230.7 cm <sup>-1</sup>	Coeff.	0.0032342	0.000977627	11.0512	7.59E-05	0.383985	0.31	4.72E-08
	1σ	8.50E-05	6.89E-05	1.7851	3.00E-05	0.319118		
HF 4203.3 cm <sup>-1</sup>	Coeff.	0.0121564	0.00331144	10.4525	0.000259496	0.383108	0.31	1.35E-07
	1σ	0.000128831	0.000101707	0.780501	5.09E-05	0.15804		
HF 4174.0 cm <sup>-1</sup>	Coeff.	0.0341426	0.00835695	20.3942	0.00383286	5.38147	0.31	7.51E-07
	1σ	2.71E-02	0.00314976	1.67E+02	0.0285182	1.48E+01		
H <sub>2</sub> O 3837.8 cm <sup>-1</sup>	Coeff.	0.0452913	0.00235314	0.646747	0.0043179	4.7077	0.31	2.81E-07
	1σ	5.23E-05	0.000133568	0.0561456	9.94E-05	0.250362		
H <sub>2</sub> O 3816.1 cm <sup>-1</sup>	Coeff.	0.0422383	0.00263698	0.705309	0.00405821	5.42457	0.31	4.10E-07
	1σ	8.52E-05	0.000160998	0.0655065	1.05E-04	0.431523		
H <sub>2</sub> O 1717.4 cm <sup>-1</sup>	Coeff.	0.0424875	0.00112797	0.273801	0.00390851	3.08679	0.31	5.43E-07
	1σ	2.92E-05	0.000131071	0.064384	9.43E-05	0.131491		
H <sub>2</sub> O 1695.9 cm <sup>-1</sup>	Coeff.	0.0627053	0.00153454	0.284461	0.0057846	3.03308	0.31	8.35E-07
	1σ	3.57E-05	0.000166509	0.0614209	1.23E-04	0.109903		

**Table D.1c** Parameters from the linear fit of 71 data points, recorded on August 8, 2016.

		Intercept	Slope	χ <sup>2</sup>
HF 4230.7 cm <sup>-1</sup>	Coeff.	0.00416878	-5.23E-05	1.40E-07
	1σ	1.10E-05	1.41E-06	
HF 4203.3 cm <sup>-1</sup>	Coeff.	0.0153021	-0.000181675	1.35E-06
	1σ	3.40E-05	4.37E-06	
HF 4174.0 cm <sup>-1</sup>	Coeff.	0.0455242	-0.000549709	1.11E-05
	1σ	9.74E-05	1.25E-05	

**Table D.2a** Experimental conditions for measurements recorded at 25 °C on August 5, 2016.

Partial Pressures (Torr)				
HF	H <sub>2</sub> O (Corrected) <sup>1</sup>	H <sub>2</sub> O (Initial)	H <sub>2</sub> O/N <sub>2</sub> (before release)	Final Pressure
0.57748	2.4605	4.08	873.97	761.11

<sup>1</sup> Transfer factor is 0.6925 (see text for details).

**Table D.2b** Parameters from the double exponential fit of 96 data points, recorded on August 5, 2016.

		y <sub>0</sub>	A <sub>1</sub>	τ <sub>1</sub>	A <sub>2</sub>	τ <sub>2</sub>	x <sub>0</sub>	χ <sup>2</sup>
HF	Coeff.	0.00261492	0.00136837	29.3058	1.36E-03	30.2074	0.27	1.30E-07
4230.7 cm <sup>-1</sup>	1σ	6.44E-03	2.09E+02	66255.1	2.09E+02	72177.1		
HF	Coeff.	0.00907437	0.00518389	32.9483	0.00512004	31.9868	0.27	2.92E-07
4203.3 cm <sup>-1</sup>	1σ	0.0121906	303.492	29370.8	3.03E+02	27415.4		
HF	Coeff.	0.0309938	0.0134119	26.2443	0.0131902	26.7596	0.27	2.33E-06
4174.0 cm <sup>-1</sup>	1σ	1.84E-02	1174.44	2.20E+04	1174.43	2.36E+04		
H <sub>2</sub> O	Coeff.	0.13071	0.00178659	0.378959	0.00453834	2.7364	0.27	2.96E-06
3837.8 cm <sup>-1</sup>	1σ	3.31E-05	0.000314727	0.116812	2.84E-04	0.188847		
H <sub>2</sub> O	Coeff.	0.124514	0.00204992	0.373511	0.00394955	2.64781	0.27	1.76E-06
3816.1 cm <sup>-1</sup>	1σ	2.49E-05	0.000248719	0.0785498	2.26E-04	0.163535		
H <sub>2</sub> O	Coeff.	0.118684	0.00128276	0.250907	0.0040328	1.97735	0.27	1.49E-06
1717.4 cm <sup>-1</sup>	1σ	1.87E-05	0.000233975	0.0835587	2.08E-04	0.106069		
H <sub>2</sub> O	Coeff.	0.175141	0.00199621	0.276912	0.00586315	1.93675	0.27	2.43E-06
1695.9 cm <sup>-1</sup>	1σ	2.38E-05	0.000327773	0.077899	3.02E-04	0.0978324		

**Table D.2c** Parameters from the linear fit of 96 data points, recorded on August 5, 2016.

		Intercept	Slope	χ <sup>2</sup>
HF	Coeff.	0.00530565	-6.93E-05	1.93E-07
4230.7 cm <sup>-1</sup>	1σ	9.38E-06	9.15E-07	
HF	Coeff.	0.0192493	-0.000244777	9.95E-07
4203.3 cm <sup>-1</sup>	1σ	2.13E-05	2.08E-06	
HF	Coeff.	0.0570693	-0.000732284	1.18E-05
4174.0 cm <sup>-1</sup>	1σ	7.35E-05	7.17E-06	

**Table D.3a** Experimental conditions for measurements recorded at 25 °C on July 21, 2016.<sup>1</sup>

Partial Pressures (Torr)				
HF	H <sub>2</sub> O (Corrected) <sup>2</sup>	H <sub>2</sub> O (Initial)	H <sub>2</sub> O/N <sub>2</sub> (before release)	Final Pressure
1.034	0.9935	1.64	865.17	756.82

<sup>1</sup>Water concentrations increases for the duration of this experiment. The water concentrations were not used to estimate K.

<sup>2</sup>Transfer factor is 0.6925 (see text for details).

**Table D.3b** Parameters from the double exponential fit of 60 data points, recorded on July 21, 2016.

		y <sub>0</sub>	A <sub>1</sub>	τ <sub>1</sub>	A <sub>2</sub>	τ <sub>2</sub>	x <sub>0</sub>	χ <sup>2</sup>
HF	Coeff.	0.00664725	0.00111505	11.9222	1.08E-03	10.5943	0.82	9.16E-08
4230.7 cm <sup>-1</sup>	1σ	3.09E-02	5.92E+01	41184.3	5.93E+01	31423.6		
HF	Coeff.	0.0236015	0.00378938	12.3092	0.00368281	10.9109	0.82	2.12E-07
4203.3 cm <sup>-1</sup>	1σ	0.0530644	94.1226	20361.7	9.42E+01	15374		
HF	Coeff.	0.0657272	0.0221712	17.422	0.0046393	2.40258	0.82	2.44E-06
4174.0 cm <sup>-1</sup>	1σ	1.63E-03	0.00123878	4.71E-07	0.000563143	7.38E-07		

**Table D.3c** Parameters from the linear fit of 96 data points, recorded on July 21, 2016.

		Intercept	Slope	χ <sup>2</sup>
HF	Coeff.	0.00883269	-1.24E-04	2.25E-07
4230.7 cm <sup>-1</sup>	1σ	1.77E-05	2.56E-06	
HF	Coeff.	0.0310498	-0.000415587	1.65E-06
4203.3 cm <sup>-1</sup>	1σ	4.81E-05	6.95E-06	
HF	Coeff.	0.0912881	-0.00127685	3.99E-05
4174.0 cm <sup>-1</sup>	1σ	2.36E-04	3.42E-05	

**Table D.4a** Experimental conditions for measurements recorded at 25 °C on August 19, 2016.

Partial Pressures (Torr)				
HF	H <sub>2</sub> O (Corrected) <sup>1</sup>	H <sub>2</sub> O (Initial)	H <sub>2</sub> O/N <sub>2</sub> (before release)	Final Pressure
0.9723	0.9931	1.64	869.32	760.16

<sup>1</sup> Transfer factor is 0.6925 (see text for details).

**Table D.4b** Parameters from the double exponential fit of 65 data points, recorded on August 19, 2016.

		y <sub>0</sub>	A <sub>1</sub>	τ <sub>1</sub>	A <sub>2</sub>	τ <sub>2</sub>	x <sub>0</sub>	χ <sup>2</sup>
HF	Coeff.	0.00733033	0.000730662	8.40243	7.12E-04	9.80435	0.22	1.43E-07
4230.7 cm <sup>-1</sup>	1σ	1.08E-02	1.08E+01	8669.13	1.08E+01	12904.3		
HF	Coeff.	0.0110591	0.0191378	73.7325	0.0010638	1.48971	0.22	1.60E-07
4203.3 cm <sup>-1</sup>	1σ	0.0283683	0.0281532	123.172	2.08E-04	0.32634		
HF	Coeff.	0.0614546	0.00489761	1.59307	0.0302093	40.4296	0.22	7.06E-07
4174.0 cm <sup>-1</sup>	1σ	1.97E-02	0.000550295	1.81E-01	0.0191256	3.29E+01		
H <sub>2</sub> O	Coeff.	0.0498517	0.00275075	0.49844	0.0047297	4.63352	0.22	1.92E-07
3837.8 cm <sup>-1</sup>	1σ	5.12E-05	0.0000962	0.0302939	6.09E-05	0.187884		
H <sub>2</sub> O	Coeff.	0.046284	0.00261334	0.487557	0.00455802	4.97571	0.22	2.75E-07
3816.1 cm <sup>-1</sup>	1σ	6.88E-05	0.000108	0.0362531	6.30E-05	0.258245		
H <sub>2</sub> O	Coeff.	0.0442945	0.00251312	0.568762	0.00364719	3.8243	0.22	1.05E-07
1717.4 cm <sup>-1</sup>	1σ	2.89E-05	0.0000954	0.0317739	7.71E-05	0.151099		
H <sub>2</sub> O	Coeff.	0.065332	0.00359191	0.56605	0.00543401	3.65616	0.22	1.74E-07
1695.9 cm <sup>-1</sup>	1σ	3.44E-05	0.000127664	0.0290321	1.06E-04	0.12295		

**Table D.4b** Parameters from the linear fit of 65 data points, recorded on August 19, 2016.

		Intercept	Slope	χ <sup>2</sup>
HF	Coeff.	0.00867147	-8.73E-05	2.95E-07
4230.7 cm <sup>-1</sup>	1σ	1.73E-05	2.48E-06	
HF	Coeff.	0.0306802	-0.000293723	2.17E-06
4203.3 cm <sup>-1</sup>	1σ	4.68E-05	6.73E-06	
HF	Coeff.	0.093878	-0.000905896	4.30E-05
4174.0 cm <sup>-1</sup>	1σ	2.08E-04	3.00E-05	

**Table D.5a** Experimental conditions for measurements recorded at 25 °C on August 29, 2016.<sup>1</sup>

Partial Pressures (Torr)				
HF	H <sub>2</sub> O (Corrected) <sup>2</sup>	H <sub>2</sub> O (Initial)	H <sub>2</sub> O/N <sub>2</sub> (before release)	Final Pressure
1.06	1.0498	1.74	874.13	761.61

<sup>1</sup> H<sub>2</sub>O decay curves are oddly shaped--initial decrease for about 1 hr followed by steady increase.

The water concentration data was not used to calculate K values.

<sup>2</sup> Transfer factor is 0.6925 (see text for details).

**Table D.5b** Parameters from the double exponential fit of 90 data points, recorded on August 29, 2016.

		y <sub>0</sub>	A <sub>1</sub>	τ <sub>1</sub>	A <sub>2</sub>	τ <sub>2</sub>	x <sub>0</sub>	χ <sup>2</sup>
HF	Coeff.	0.00641467	0.00242991	15.0278	2.18E-04	0.177438	0.1	2.65E-07
4230.7 cm <sup>-1</sup>	1σ	2.35E-04	2.19E-04	2.22262	4.52E-05	0.0767952		
HF	Coeff.	0.0233355	0.00401357	8.8955	0.00412973	22.5263	0.1	7.02E-07
4203.3 cm <sup>-1</sup>	1σ	0.0614005	0.191319	116.234	1.30E-01	1214.95		
HF	Coeff.	0.065035	0.0092938	4.28837	0.023898	28.4078	0.1	1.05E-05
4174.0 cm <sup>-1</sup>	1σ	9.25E-02	0.0246283	5.28E+00	0.0680686	1.91E+02		

**Table D.5c** Parameters from the linear fit of 90 data points, recorded on August 29, 2016.

		Intercept	Slope	χ <sup>2</sup>
HF	Coeff.	0.00881688	-1.14E-04	7.38E-07
4230.7 cm <sup>-1</sup>	1σ	1.61E-05	2.27E-06	
HF	Coeff.	0.0311886	-0.00038468	5.37E-06
4203.3 cm <sup>-1</sup>	1σ	4.34E-05	6.12E-06	
HF	Coeff.	0.0964872	-0.00136442	1.37E-04
4174.0 cm <sup>-1</sup>	1σ	2.19E-04	3.09E-05	

**Table D.5d** Parameters from the polynomial fit of 90 data points, recorded on August 29, 2016.

	H <sub>2</sub> O 3837.8 cm <sup>-1</sup>		H <sub>2</sub> O 3816.1 cm <sup>-1</sup>		H <sub>2</sub> O 1717.4 cm <sup>-1</sup>		H <sub>2</sub> O 1695.9 cm <sup>-1</sup>	
	Coeff.	1σ	Coeff.	1σ	Coeff.	1σ	Coeff.	1σ
K <sub>0</sub>	0.067573	9.70E-05	0.0634347	9.17E-05	0.0595666	8.47E-05	0.0879543	1.09E-04
K <sub>1</sub>	-0.00496423	2.68E-04	-0.00503738	2.53E-04	-0.00381893	2.34E-04	-0.00568262	3.02E-04
K <sub>2</sub>	0.00311823	1.93E-04	0.00320308	1.82E-04	0.00243438	1.68E-04	0.00359382	2.18E-04
K <sub>3</sub>	-0.00072705	5.74E-05	-0.00075612	5.42E-05	-0.00056600	5.01E-05	-0.00083316	6.47E-05
K <sub>4</sub>	0.000086	8.11E-06	0.0000904	7.66E-06	0.0000673	7.07E-06	0.000099	9.15E-06
K <sub>5</sub>	-0.00000501	5.41E-07	-0.00000531	5.11E-07	-0.00000394	4.72E-07	-0.0000058	6.10E-07
K <sub>6</sub>	0.000000114	1.37E-08	0.000000122	1.30E-08	8.99E-08	1.20E-08	0.000000133	1.55E-08
x <sub>0</sub>	0.1		0.1		0.1		0.1	
χ <sup>2</sup>	0.00000448		0.00000399		0.00000341		0.0000057	

**Table D.6a** Experimental conditions for measurements recorded at 25 °C on August 4, 2016.

Partial Pressures (Torr)				
HF	H <sub>2</sub> O (Corrected) <sup>1</sup>	H <sub>2</sub> O (Initial)	H <sub>2</sub> O/N <sub>2</sub> (before release)	Final Pressure
1.012	2.4126	4	873.3	760.62

<sup>1</sup> Transfer factor is 0.6925 (see text for details).**Table D.6b** Parameters from the double exponential fit of 55 data points, recorded on August 4, 2016.

		y <sub>0</sub>	A <sub>1</sub>	τ <sub>1</sub>	A <sub>2</sub>	τ <sub>2</sub>	x <sub>0</sub>	χ <sup>2</sup>
HF	Coeff.	0.0049554	0.001878	15.231	1.81E-03	14.784	0.25	1.53E-07
4230.7 cm <sup>-1</sup>	1σ	2.07E-03	2.48E+02	0.000306	2.48E+02	29400		
HF	Coeff.	0.016474	0.0093564	25.6	0.0048551	9.9344	0.25	6.31E-07
4203.3 cm <sup>-1</sup>	1σ	0.0311	0.0682	315	9.91E-02	57.9		
HF	Coeff.	0.050218	0.024368	28.374	0.017599	8.1186	0.12	1.17E-06
4174.0 cm <sup>-1</sup>	1σ	3.60E-03	0.00274	6.98E-07	0.000175	2.38E-06		
H <sub>2</sub> O	Coeff.	0.13797	0.0018495	0.070947	0.0080766	0.71043	0.25	3.61E-05
3837.8 cm <sup>-1</sup>	1σ	7.14E-05	0.00174	0.218	1.62E-03	0.135		
H <sub>2</sub> O	Coeff.	0.13112	0.0011853	0.015871	0.0079994	0.60138	0.25	3.66E-05
3816.1 cm <sup>-1</sup>	1σ	7.07E-05	0.00184	116	1.72E-03	0.123		
H <sub>2</sub> O	Coeff.	0.12472	0.0011274	0.67882	0.0067029	0.0075408	0.25	7.52E-05
1717.4 cm <sup>-1</sup>	1σ	1.02E-04	0.00209	127	2.30E-03	1700000		
H <sub>2</sub> O	Coeff.	0.18396	0.011793	0.48112	0.00056611	0.045767	0.25	8.59E-05
1695.9 cm <sup>-1</sup>	1σ	1.07E-04	0.00387	0.133	4.01E-03	2.24		

**Table D.6c** Parameters from the linear fit of 55 data points, recorded on August 4, 2016

		Intercept	Slope	χ <sup>2</sup>
HF	Coeff.	0.0084228	-1.43E-04	1.25E-06
4230.7 cm <sup>-1</sup>	1σ	2.39E-05	2.35E-06	
HF	Coeff.	0.029914	-0.00048567	1.29E-05
4203.3 cm <sup>-1</sup>	1σ	7.66E-05	7.53E-06	
HF	Coeff.	0.088949	-0.0014831	1.97E-04
4174.0 cm <sup>-1</sup>	1σ	3.00E-04	2.95E-05	

**Table D.7a** Experimental conditions for measurements recorded at 25 °C on August 22, 2016.

HF	Partial Pressures (Torr)				Final Pressure
	H <sub>2</sub> O (Corrected) <sup>1</sup>	H <sub>2</sub> O (Initial)	H <sub>2</sub> O/N <sub>2</sub> (before release)		
1.01198	2.4128	4	870.54	758.29	

<sup>1</sup> Transfer factor is 0.6925 (see text for details).**Table D.7b** Parameters from the double exponential fit of 55 data points, recorded on August 22, 2016.

		y <sub>0</sub>	A <sub>1</sub>	τ <sub>1</sub>	A <sub>2</sub>	τ <sub>2</sub>	x <sub>0</sub>	χ <sup>2</sup>
HF	Coeff.	0.00679906	0.000331738	0.891665	2.08E-03	17.5822	0.12	1.21E-07
4230.7 cm <sup>-1</sup>	1σ	1.53E-03	1.28E-04	0.480007	1.40E-03	18.91		
HF	Coeff.	0.0243844	0.00704279	17.2843	0.000940333	0.823969	0.12	1.25E-07
4203.3 cm <sup>-1</sup>	1σ	0.00138831	0.00127496	4.96188	1.14E-04	0.149213		
HF	Coeff.	0.0689695	0.00603	1.27741	0.0252171	25.731	0.12	1.17E-06
4174.0 cm <sup>-1</sup>	1σ	1.14E-03	0.000307836	9.58E-07	0.000950606	1.86E-07		
H <sub>2</sub> O	Coeff.	0.104915	0.00547643	0.425366	0.0133685	5.18384	0.12	4.32E-07
3837.8 cm <sup>-1</sup>	1σ	1.53E-04	0.000149	0.0213271	8.61E-05	0.166283		
H <sub>2</sub> O	Coeff.	0.0989366	0.00540237	0.456363	0.0126507	5.61458	0.12	3.99E-07
3816.1 cm <sup>-1</sup>	1σ	1.77E-04	0.000146	0.0223933	9.46E-05	0.207298		
H <sub>2</sub> O	Coeff.	0.0936479	0.00505693	0.455293	0.011675	5.39958	0.12	2.56E-07
1717.4 cm <sup>-1</sup>	1σ	1.32E-04	0.000119	0.0192735	7.07E-05	0.166345		
H <sub>2</sub> O	Coeff.	0.138208	0.00748796	0.472445	0.0172026	5.44312	0.12	4.83E-07
1695.9 cm <sup>-1</sup>	1σ	1.87E-04	0.000167976	0.0187536	9.88E-05	0.161755		

**Table D.7c** Parameters from the linear fit of 55 data points, recorded on August 22, 2016.

		Intercept	Slope	χ <sup>2</sup>
HF	Coeff.	0.00896318	-1.06E-04	3.63E-07
4230.7 cm <sup>-1</sup>	1σ	2.24E-05	3.86E-06	
HF	Coeff.	0.0316187	-0.00035227	2.44E-06
4203.3 cm <sup>-1</sup>	1σ	5.82E-05	1.00E-05	
HF	Coeff.	0.0967103	-0.0011816	5.87E-05
4174.0 cm <sup>-1</sup>	1σ	2.85E-04	4.90E-05	

**Table D.8a** Experimental conditions for measurements recorded at 25 °C on August 23, 2016.<sup>1</sup>

HF	Partial Pressures (Torr)			
	H <sub>2</sub> O (Corrected) <sup>2</sup>	H <sub>2</sub> O (Initial)	H <sub>2</sub> O/N <sub>2</sub> (before release)	Final Pressure
1.01487	2.4222	4	868.36	759.32

<sup>1</sup>Delay collecting first spectrum due to interferometer malfunction.<sup>2</sup>Transfer factor is 0.6925 (see text for details).**Table D.8b** Parameters from the double exponential fit of 60 data points, recorded on August 23, 2016.

		y <sub>0</sub>	A <sub>1</sub>	τ <sub>1</sub>	A <sub>2</sub>	τ <sub>2</sub>	x <sub>0</sub>	χ <sup>2</sup>
HF 4230.7 cm <sup>-1</sup>	Coeff.	0.0063386	0.00139596	17.5186	1.39E-03	18.1082	0.7	1.21E-07
	1σ	6.02E-03	und	und	und	und		
HF 4203.3 cm <sup>-1</sup>	Coeff.	0.024463	0.00382919	7.97639	0.00403483	22.4035	0.7	1.95E-07
	1σ	0.000460647	0.000272971	6.74E-08	3.70E-04	1.61E-08		
HF 4174.0 cm <sup>-1</sup>	Coeff.	-4.55318	0.00881616	1.93873	4.64686	5660.5	0.7	2.09E-06
	1σ	1.51E+03	0.00203187	3.72E-01	1510.66	1.84E+06		
H <sub>2</sub> O 3837.8 cm <sup>-1</sup>	Coeff.	0.122382	0.00225754	1.1482	0.00793519	7.05126	0.7	2.19E-07
	1σ	3.20E-04	0.000363	0.170498	1.29E-04	0.827381		
H <sub>2</sub> O 3816.1 cm <sup>-1</sup>	Coeff.	0.116158	0.00147171	0.735052	0.00775451	6.30143	0.7	3.44E-07
	1σ	2.07E-04	0.000196	0.137082	9.26E-05	0.471083		
H <sub>2</sub> O 1717.4 cm <sup>-1</sup>	Coeff.	0.110064	0.00143498	0.711207	0.00696489	5.34975	0.7	1.54E-07
	1σ	9.87E-05	0.000139	0.0937502	7.45E-05	0.250094		
H <sub>2</sub> O 1695.9 cm <sup>-1</sup>	Coeff.	0.161789	0.0030262	1.01421	0.0100202	6.68477	0.7	1.48E-07
	1σ	2.06E-04	0.000231389	0.0803288	8.93E-05	0.402417		

**Table D.8c** Parameters from the linear fit of 60 data points, recorded on August 23, 2016.

		Intercept	Slope	χ <sup>2</sup>
HF 4230.7 cm <sup>-1</sup>	Coeff.	0.00914372	-1.17E-04	1.47E-07
	1σ	1.41E-05	2.08E-06	
HF 4203.3 cm <sup>-1</sup>	Coeff.	0.0322122	-0.000399188	1.76E-06
	1σ	4.88E-05	7.17E-06	
HF 4174.0 cm <sup>-1</sup>	Coeff.	0.0994583	-0.00141094	9.15E-05
	1σ	3.52E-04	5.17E-05	

**Table D.9a** Experimental conditions for measurements recorded at 25 °C on August 17, 2016.

HF	Partial Pressures (Torr)				Final Pressure
	H <sub>2</sub> O (Corrected) <sup>1</sup>	H <sub>2</sub> O (Initial)	H <sub>2</sub> O/N <sub>2</sub> (before release)		
1.0066	3.9371	6.5	870.84	761.69	

<sup>1</sup> Transfer factor is 0.6925 (see text for details).**Table D.9b** Parameters from the double exponential fit of 74 data points, recorded on August 17, 2016.

		y <sub>0</sub>	A <sub>1</sub>	τ <sub>1</sub>	A <sub>2</sub>	τ <sub>2</sub>	x <sub>0</sub>	χ <sup>2</sup>
HF	Coeff.	0.00499481	0.00202307	21.6787	2.00E-03	17.9951	0.19	2.07E-07
4230.7 cm <sup>-1</sup>	1σ	1.58E-01	6.67E+01	78889.7	6.69E+01	48500		
HF	Coeff.	0.0126298	0.00954576	29.5124	0.00943695	32.8225	0.19	1.05E-06
4203.3 cm <sup>-1</sup>	1σ	0.00105975	0.000861697	6.39E-08	8.79E-04	5.28E-08		
HF	Coeff.	0.036961	0.0306499	30.5958	0.0302359	28.1012	0.19	2.27E-05
4174.0 cm <sup>-1</sup>	1σ	4.93E-03	0.00403495	8.99E-07	0.0039699	1.02E-06		
H <sub>2</sub> O	Coeff.	0.197882	0.00723274	0.563205	0.022077	7.85834	0.19	6.16E-07
3837.8 cm <sup>-1</sup>	1σ	1.69E-04	0.000125	0.0187445	9.54E-05	0.150305		
H <sub>2</sub> O	Coeff.	0.187917	0.00712757	0.641667	0.0205119	8.10828	0.19	8.16E-07
3816.1 cm <sup>-1</sup>	1σ	2.20E-04	0.000155	0.0257766	1.19E-04	0.217136		
H <sub>2</sub> O	Coeff.	0.178114	0.00642765	0.625593	0.0182633	7.49868	0.19	4.48E-07
1717.4 cm <sup>-1</sup>	1σ	1.39E-04	0.000116	0.0208093	7.31E-05	0.151465		
H <sub>2</sub> O	Coeff.	0.262889	0.00972	0.616326	0.0271034	7.60112	0.19	8.90E-07
1695.9 cm <sup>-1</sup>	1σ	1.99E-04	0.000161352	0.0189578	1.06E-04	0.146219		

**Table D.9c** Parameters from the linear fit of 74 data points, recorded on August 17, 2016.

		Intercept	Slope	χ <sup>2</sup>
HF	Coeff.	0.00894054	-1.47E-04	2.56E-07
4230.7 cm <sup>-1</sup>	1σ	1.40E-05	1.79E-06	
HF	Coeff.	0.0314776	-0.000495758	1.46E-06
4203.3 cm <sup>-1</sup>	1σ	3.35E-05	4.28E-06	
HF	Coeff.	0.0973376	-0.00166643	2.97E-05
4174.0 cm <sup>-1</sup>	1σ	1.51E-04	1.93E-05	

**Table D.10a** Experimental conditions for measurements recorded at 25 °C on August 25, 2016.

Partial Pressures (Torr)				
HF	H <sub>2</sub> O (Corrected) <sup>1</sup>	H <sub>2</sub> O (Initial)	H <sub>2</sub> O/N <sub>2</sub> (before release)	Final Pressure
2.0147	2.4233	4	869.78	760.91

<sup>1</sup> Transfer factor is 0.6925 (see text for details).**Table D.10b** Parameters from the double exponential fit of 60 data points, recorded on August 25, 2016.

		y <sub>0</sub>	A <sub>1</sub>	τ <sub>1</sub>	A <sub>2</sub>	τ <sub>2</sub>	x <sub>0</sub>	χ <sup>2</sup>
HF	Coeff.	0.0119579	0.00510378	17.7091	3.19E-04	0.685138	0.1	1.23E-07
4230.7 cm <sup>-1</sup>	1σ	3.67E-04	2.80E-04	2.38E-08	7.34E-05	2.15E-08		
HF	Coeff.	0.0382632	0.0184101	23.5209	0.00136053	1.11361	0.1	2.02E-07
4203.3 cm <sup>-1</sup>	1σ	0.000469285	0.000380515	6.92E-08	1.14E-04	9.18E-08		
HF	<b>Transition is saturated. It was not included in the fit.</b>							
4174.0 cm <sup>-1</sup>								
H <sub>2</sub> O	Coeff.	0.115245	0.00384421	0.327144	0.00917505	2.57049	0.1	1.91E-07
3837.8 cm <sup>-1</sup>	1σ	2.25E-05	0.000114	0.016572	9.51E-05	0.0397421		
H <sub>2</sub> O	Coeff.	0.107875	0.00385153	0.339496	0.0081584	2.58631	0.1	1.97E-07
3816.1 cm <sup>-1</sup>	1σ	2.32E-05	0.000118	0.0175383	1.00E-04	0.0466937		
H <sub>2</sub> O	Coeff.	0.102342	0.00294479	0.266727	0.00810842	2.21937	0.1	1.41E-07
1717.4 cm <sup>-1</sup>	1σ	1.55E-05	0.000095	0.0154291	7.97E-05	0.029926		
H <sub>2</sub> O	Coeff.	0.151106	0.00471312	0.291172	0.0116869	2.29392	0.1	2.07E-07
1695.9 cm <sup>-1</sup>	1σ	1.98E-05	0.000119282	0.0127894	1.02E-04	0.0272135		

**Table D.10c** Parameters from the linear fit of 60 data points, recorded on August 25, 2016.

		Intercept	Slope	χ <sup>2</sup>
HF	Coeff.	0.0170497	-2.26E-04	6.06E-07
4230.7 cm <sup>-1</sup>	1σ	2.64E-05	4.21E-06	
HF	Coeff.	0.0569886	-0.000693356	5.93E-06
4203.3 cm <sup>-1</sup>	1σ	8.28E-05	1.32E-05	
HF	Coeff.	<b>Transition is saturated. It was not included in the fit.</b>		
4174.0 cm <sup>-1</sup>	1σ			

**Table D.11a** Experimental conditions for measurements recorded at 25 °C on August 18, 2016.

Partial Pressures (Torr)				
HF	H <sub>2</sub> O (Corrected) <sup>1</sup>	H <sub>2</sub> O (Initial)	H <sub>2</sub> O/N <sub>2</sub> (before release)	Final Pressure
2.0218	3.9374	6.5	872.46	763.18

<sup>1</sup> Transfer factor is 0.6925 (see text for details).

**Table D.11b** Parameters from the double exponential fit of 65 data points, recorded on August 18, 2016.

		y <sub>0</sub>	A <sub>1</sub>	τ <sub>1</sub>	A <sub>2</sub>	τ <sub>2</sub>	x <sub>0</sub>	χ <sup>2</sup>
HF	Coeff.	0.00149429	0.00792869	26.9054	7.88E-03	24.8497	0.21	4.53E-07
4230.7 cm <sup>-1</sup>	1σ	7.01E-04	5.73E-04	3.77E-08	5.65E-04	4.28E-08		
HF	Coeff.	-0.0002387	0.02931	27.8813	0.0291484	34.9782	0.21	1.57E-06
4203.3 cm <sup>-1</sup>	1σ	0.00130255	0.00107256	2.44E-07	1.11E-03	1.64E-07		
HF		<b>Transition is saturated. It was not included in the fit.</b>						
4174.0 cm <sup>-1</sup>								
H <sub>2</sub> O	Coeff.	0.179384	0.0452215	9.82115	0.00529807	0.466364	0.21	7.74E-07
3837.8 cm <sup>-1</sup>	1σ	4.10E-04	0.000314	0.171593	1.42E-04	0.0251765		
H <sub>2</sub> O	Coeff.	0.170061	0.0419091	9.92704	0.00498724	0.479461	0.21	5.60E-07
3816.1 cm <sup>-1</sup>	1σ	3.61E-04	0.000277	0.163914	1.21E-04	0.0234586		
H <sub>2</sub> O	Coeff.	0.159709	0.0394201	10.4256	0.00477705	0.424433	0.21	1.41E-07
1717.4 cm <sup>-1</sup>	1σ	2.12E-04	0.000171	0.103287	6.51E-05	0.0119419		
H <sub>2</sub> O	Coeff.	0.236125	0.0579479	10.3204	0.00693198	0.436703	0.21	3.17E-07
1695.9 cm <sup>-1</sup>	1σ	2.81E-04	0.000224217	0.0930098	8.79E-05	0.0113665		

**Table D.11c** Parameters from the linear fit of 65 data points, recorded on August 18, 2016.

		Intercept	Slope	χ <sup>2</sup>
HF	Coeff.	0.0171992	-4.93E-04	3.00E-07
4230.7 cm <sup>-1</sup>	1σ	1.74E-05	2.51E-06	
HF	Coeff.	0.0580026	-0.00155156	2.18E-06
4203.3 cm <sup>-1</sup>	1σ	4.69E-05	6.75E-06	
HF	Coeff.	<b>Transition is saturated. It was not included in the fit.</b>		
4174.0 cm <sup>-1</sup>	1σ			

**Table D.12a** Experimental conditions for measurements recorded at 25 °C on September 1, 2016.

Partial Pressures (Torr)				
HF	H <sub>2</sub> O (Corrected) <sup>1</sup>	H <sub>2</sub> O (Initial)	H <sub>2</sub> O/N <sub>2</sub> (before release)	Final Pressure
2.0175	3.9358	6.5	871.42	761.95

<sup>1</sup> Transfer factor is 0.6925 (see text for details).

**Table D.12b** Parameters from the double exponential fit of 75 data points, recorded on September 1, 2016.

		y <sub>0</sub>	A <sub>1</sub>	τ <sub>1</sub>	A <sub>2</sub>	τ <sub>2</sub>	x <sub>0</sub>	χ <sup>2</sup>
HF	Coeff.	0.00780142	0.00480057	23.6626	4.78E-03	21.786	0.02	5.69E-07
4230.7 cm <sup>-1</sup>	1σ	7.81E-04	6.70E-04	2.58E-08	6.62E-04	2.95E-08		
HF	Coeff.	0.02926	0.0147977	22.0041	0.0147182	20.6735	0.02	2.53E-06
4203.3 cm <sup>-1</sup>	1σ	0.00164595	0.00139805	0.00000019	1.39E-03	2.09E-07		
HF		<b>Transition is saturated. It was not included in the fit.</b>						
4174.0 cm <sup>-1</sup>								
H <sub>2</sub> O	Coeff.	0.203089	0.00883307	0.107133	0.029099	3.5254	0.02	1.91E-05
3837.8 cm <sup>-1</sup>	1σ	2.72E-04	0.000434	0.0123789	2.96E-04	0.111795		
H <sub>2</sub> O	Coeff.	0.192499	0.00888384	0.101932	0.0266073	3.42781	0.02	1.93E-05
3816.1 cm <sup>-1</sup>	1σ	2.59E-04	0.000436	0.0117724	2.92E-04	0.114925		
H <sub>2</sub> O	Coeff.	0.180624	0.00800145	0.111824	0.0238875	3.38817	0.02	1.54E-05
1717.4 cm <sup>-1</sup>	1σ	2.31E-04	0.000395	0.0129316	2.74E-04	0.116434		
H <sub>2</sub> O	Coeff.	0.26692	0.0120001	0.101451	0.0355605	3.32553	0.02	2.97E-05
1695.9 cm <sup>-1</sup>	1σ	3.06E-04	0.000541913	0.0108014	3.63E-04	0.101236		

**Table D.12c** Parameters from the linear fit of 75 data points, recorded on September 1, 2016.

		Intercept	Slope	χ <sup>2</sup>
HF	Coeff.	0.0173176	-3.48E-04	5.59E-07
4230.7 cm <sup>-1</sup>	1σ	1.58E-05	2.95E-06	
HF	Coeff.	0.0585623	-0.00112598	3.60E-06
4203.3 cm <sup>-1</sup>	1σ	4.01E-05	7.48E-06	
HF	Coeff.	<b>Transition is saturated. It was not included in the fit.</b>		
4174.0 cm <sup>-1</sup>	1σ			

**Table D.13a** Experimental conditions for measurements recorded at 25 °C on August 26, 2016.

Partial Pressures (Torr)				
HF	H <sub>2</sub> O (Corrected) <sup>1</sup>	H <sub>2</sub> O (Initial)	H <sub>2</sub> O/N <sub>2</sub> (before release)	Final Pressure
4.0102	3.9385	6.5	868.46	759.89

<sup>1</sup> Transfer factor is 0.6925 (see text for details).

**Table D.13b** Parameters from the double exponential fit of 60 data points, recorded on August 26, 2016.

		y <sub>0</sub>	A <sub>1</sub>	τ <sub>1</sub>	A <sub>2</sub>	τ <sub>2</sub>	x <sub>0</sub>	χ <sup>2</sup>
HF	Coeff.	0.0108311	0.01039	11.8423	1.01E-02	12.7231	0.27	1.97E-07
4230.7 cm <sup>-1</sup>	1σ	1.09E-01	9.01E+02	34900	9.01E+02	43100		
HF	Coeff.	0.0418359	0.0289245	12.0208	0.0281571	11.167	0.27	2.09E-06
4203.3 cm <sup>-1</sup>	1σ	0.156852	1227.69	19900	1.23E+03	17000		
HF		<b>Transition is saturated. It was not included in the fit.</b>						
4174.0 cm <sup>-1</sup>								
H <sub>2</sub> O	Coeff.	0.160562	0.00707295	0.518771	0.0625838	7.83845	0.27	9.49E-07
3837.8 cm <sup>-1</sup>	1σ	4.17E-04	0.000199	0.0272891	2.71E-04	0.113685		
H <sub>2</sub> O	Coeff.	0.150744	0.00703997	0.507366	0.0570624	7.98172	0.27	9.33E-07
3816.1 cm <sup>-1</sup>	1σ	4.13E-04	0.000189	0.0257073	2.75E-04	0.123751		
H <sub>2</sub> O	Coeff.	0.141822	0.0064002	0.445039	0.0529406	8.08845	0.27	3.25E-07
1717.4 cm <sup>-1</sup>	1σ	2.35E-04	0.000103	0.0141491	1.65E-04	0.0747724		
H <sub>2</sub> O	Coeff.	0.209156	0.00952791	0.465385	0.0783049	8.1301	0.27	6.70E-07
1695.9 cm <sup>-1</sup>	1σ	3.48E-04	0.000151399	0.0143937	2.42E-04	0.0753638		

**Table D.13c** Parameters from the linear fit of 60 data points, recorded on August 26, 2016.

		Intercept	Slope	χ <sup>2</sup>
HF	Coeff.	0.0307158	-1.10E-03	9.66E-06
4230.7 cm <sup>-1</sup>	1σ	1.08E-04	1.67E-05	
HF	Coeff.	0.096951	-0.00316508	8.89E-05
4203.3 cm <sup>-1</sup>	1σ	3.28E-04	5.06E-05	
HF	Coeff.	<b>Transition is saturated. It was not included in the fit.</b>		
4174.0 cm <sup>-1</sup>	1σ			

**Table D.14a** Experimental conditions for measurements recorded at 25 °C on August 31, 2016.

Partial Pressures (Torr)				
HF	H <sub>2</sub> O (Corrected) <sup>1</sup>	H <sub>2</sub> O (Initial)	H <sub>2</sub> O/N <sub>2</sub> (before release)	Final Pressure
4.0114	3.9381	6.5	868.82	760.12

<sup>1</sup> Transfer factor is 0.6925 (see text for details).

**Table D.14b** Parameters from the double exponential fit of 80 data points, recorded on August 31, 2016.

		y <sub>0</sub>	A <sub>1</sub>	τ <sub>1</sub>	A <sub>2</sub>	τ <sub>2</sub>	x <sub>0</sub>	χ <sup>2</sup>
HF	Coeff.	0.0121645	0.00977476	19.2295	9.70E-03	19.3385	0.03	5.70E-07
4230.7 cm <sup>-1</sup>	1σ	1.58E-02	5.24E+02	4580	5.24E+02	4700		
HF	Coeff.	0.0523328	0.0241552	14.9417	0.0239278	15.4565	0.03	4.36E-06
4203.3 cm <sup>-1</sup>	1σ	0.0148002	und	und	und	und		
HF		<b>Transition is saturated. It was not included in the fit.</b>						
4174.0 cm <sup>-1</sup>								
H <sub>2</sub> O	Coeff.	0.172919	0.0138951	0.312751	0.0523666	9.02386	0.03	7.90E-06
3837.8 cm <sup>-1</sup>	1σ	9.74E-04	0.000273	0.0120167	7.86E-04	0.316661		
H <sub>2</sub> O	Coeff.	0.162642	0.0137004	0.302094	0.0471716	8.98038	0.03	7.35E-06
3816.1 cm <sup>-1</sup>	1σ	9.22E-04	0.00026	0.0112566	7.45E-04	0.331393		
H <sub>2</sub> O	Coeff.	0.151953	0.0127901	0.318614	0.0440173	9.54721	0.03	6.68E-06
1717.4 cm <sup>-1</sup>	1σ	1.00E-03	0.000249	0.0122236	8.28E-04	0.39828		
H <sub>2</sub> O	Coeff.	0.224207	0.0190624	0.325231	0.0651058	9.59824	0.03	1.16E-05
1695.9 cm <sup>-1</sup>	1σ	1.34E-03	0.000330327	0.0110872	1.11E-03	0.361758		

**Table D.14c** Parameters from the linear fit of 80 data points, recorded on August 31, 2016.

		Intercept	Slope	χ <sup>2</sup>
HF	Coeff.	0.0314495	-7.92E-04	3.96E-06
4230.7 cm <sup>-1</sup>	1σ	3.93E-05	6.95E-06	
HF	Coeff.	0.0996686	-0.00233067	5.11E-05
4203.3 cm <sup>-1</sup>	1σ	1.41E-04	2.50E-05	
HF	Coeff.	<b>Transition is saturated. It was not included in the fit.</b>		
4174.0 cm <sup>-1</sup>	1σ			

**Table C.15** Experimental conditions for measurements recorded at 10 °C on September 9, 2016.<sup>1</sup>

Partial Pressures (Torr)				
HF	H <sub>2</sub> O (Corrected) <sup>2</sup>	H <sub>2</sub> O (Initial)	H <sub>2</sub> O/N <sub>2</sub> (before release)	Final Pressure
4.0066	3.9117	6.5	873.08	758.72

<sup>1</sup>Intensities of H<sub>2</sub>O lines were about 30% lower than those in 25 and 40 °C experiments (condensation or unknown systematic error?)

<sup>2</sup>Transfer factor is 0.6925 (see text for details).

**Table D.15b** Parameters from the double exponential fit of 80 data points, recorded on September 9, 2016.

		y <sub>0</sub>	A <sub>1</sub>	τ <sub>1</sub>	A <sub>2</sub>	τ <sub>2</sub>	x <sub>0</sub>	χ <sup>2</sup>
HF	Coeff.	0.00516627	0.00869189	20.3247	8.64E-03	24.1559	0.03	6.15E-07
4230.7 cm <sup>-1</sup>	1σ	8.10E-04	6.74E-04	6.45E-08	6.92E-04	4.83E-08		
HF	Coeff.	0.0245801	0.0273473	21.4142	0.0271329	20.0357	0.03	5.03E-06
4203.3 cm <sup>-1</sup>	1σ	0.00231572	0.00194437	5.34E-07	1.92E-03	5.90E-07		
HF	<b>Transition is saturated. It was not included in the fit.</b>							
4174.0 cm <sup>-1</sup>								
H <sub>2</sub> O	Coeff.	0.102102	0.00682832	0.157415	0.0433276	7.56246	0.03	2.25E-05
3837.8 cm <sup>-1</sup>	1σ	1.01E-03	0.000419	0.0202573	8.14E-04	0.356019		
H <sub>2</sub> O	Coeff.	0.0996251	0.00733081	0.0468298	0.03816	6.15286	0.03	2.01E-05
3816.1 cm <sup>-1</sup>	1σ	5.38E-04	0.000476	0.00585985	4.79E-04	0.18154		
H <sub>2</sub> O	Coeff.	0.0887339	0.00658307	0.0469756	0.0333894	6.04683	0.03	1.72E-05
1717.4 cm <sup>-1</sup>	1σ	4.28E-03	0.000646	0.0000553	2.78E-03	0.00000646		
H <sub>2</sub> O	Coeff.	0.133807	0.0099359	0.0545425	0.0505843	6.09441	0.03	3.84E-05
1695.9 cm <sup>-1</sup>	1σ	7.42E-04	0.000638235	0.00687458	6.52E-04	0.189673		

**Table D.15c** Parameters from the linear fit of 80 data points, recorded on September 9, 2016.

		Intercept	Slope	χ <sup>2</sup>
HF	Coeff.	0.0223686	-6.30E-04	1.88E-06
4230.7 cm <sup>-1</sup>	1σ	2.71E-05	4.79E-06	
HF	Coeff.	0.0785934	-0.00208955	2.36E-05
4203.3 cm <sup>-1</sup>	1σ	9.61E-05	1.69E-05	
HF	Coeff.	<b>Transition is saturated. It was not included in the fit.</b>		
4174.0 cm <sup>-1</sup>	1σ			

**Table C.16** Experimental conditions for measurements recorded at 40 °C on September 7, 2016.

Partial Pressures (Torr)				
HF	H <sub>2</sub> O (Corrected) <sup>1</sup>	H <sub>2</sub> O (Initial)	H <sub>2</sub> O/N <sub>2</sub> (before release)	Final Pressure
4.0015	3.9609	6.5	871.39	766.79

<sup>1</sup> Transfer factor is 0.6925 (see text for details).

**Table D.16b** Parameters from the double exponential fit of 68 data points, recorded on September 7, 2016.

		y <sub>0</sub>	A <sub>1</sub>	τ <sub>1</sub>	A <sub>2</sub>	τ <sub>2</sub>	x <sub>0</sub>	χ <sup>2</sup>
HF	Coeff.	0.0239095	0.00685396	8.37205	6.81E-03	20.7527	0.03	2.24E-06
4230.7 cm <sup>-1</sup>	1σ	1.55E-03	1.16E-03	0.000000316	1.35E-03	7.93E-08		
HF	Coeff.	0.071966	0.0204555	14.0439	0.0202988	14.4353	0.03	3.49E-05
4203.3 cm <sup>-1</sup>	1σ	0.00613652	0.00504452	1.77E-06	5.07E-03	1.69E-06		
HF	<b>Transition is saturated. It was not included in the fit.</b>							
4174.0 cm <sup>-1</sup>								
H <sub>2</sub> O	Coeff.	0.203239	0.00841773	0.166647	0.0139756	1.85677	0.03	8.50E-06
3837.8 cm <sup>-1</sup>	1σ	1.16E-04	0.00046	0.0168734	4.28E-04	0.0941092		
H <sub>2</sub> O	Coeff.	0.187867	0.0072372	0.168974	0.0124134	1.56897	0.03	5.89E-06
3816.1 cm <sup>-1</sup>	1σ	8.20E-05	0.000445	0.0179648	4.37E-04	0.0767176		
H <sub>2</sub> O	Coeff.	0.185889	0.00656995	0.129062	0.0124407	1.38659	0.03	4.99E-06
1717.4 cm <sup>-1</sup>	1σ	6.66E-05	0.000344	0.0136	3.37E-04	0.0553		
H <sub>2</sub> O	Coeff.	0.268325	0.00978912	0.158911	0.0173558	1.43704	0.03	8.50E-06
1695.9 cm <sup>-1</sup>	1σ	9.11E-05	0.000542607	0.0154204	5.42E-04	0.0597728		

**Table D.16c** Parameters from the linear fit of 68 data points, recorded on September 7, 2016.

		Intercept	Slope	χ <sup>2</sup>
HF	Coeff.	0.0374578	-7.08E-04	3.50E-06
4230.7 cm <sup>-1</sup>	1σ	4.24E-05	9.53E-06	
HF	Coeff.	0.112316	-0.00221004	4.21E-05
4203.3 cm <sup>-1</sup>	1σ	1.47E-04	3.30E-05	
HF	Coeff.	<b>Transition is saturated. It was not included in the fit.</b>		
4174.0 cm <sup>-1</sup>	1σ			



**Pacific Northwest**  
NATIONAL LABORATORY

*Proudly Operated by **Battelle** Since 1965*

902 Battelle Boulevard  
P.O. Box 999  
Richland, WA 99352  
**1-888-375-PNNL (7665)**

U.S. DEPARTMENT OF  
**ENERGY**

---

**[www.pnnl.gov](http://www.pnnl.gov)**